Electronic Supplementary Material (ESI) for Photochemical & Photobiological Science

Supporting information

for

Photosolvolysis of bulky (4-hydroxyphenyl)naphthalene derivatives

By

Đani Škalamera,[a] Kata Mlinarić-Majerski,[a] Lidija Uzelac,[b] Marijeta Kralj,[b] Peter Wan,[c] Nikola Basarić[a]*

[a] Department of Organic Chemistry and Biochemistry, Ruđer Bošković Institute, Bijenička cesta 54, 10 000 Zagreb, Croatia.
Fax: + 385 1 4680 195; Tel: +385 1 4561 141; E-mail: nbasaric@irb.hr

[b] Department of Molecular Medicine, Ruđer Bošković Institute, Bijenička cesta 54, 10000 Zagreb, Croatia

[c] Department of Chemistry, University of Victoria, Box 3065 Stn CSC, Victoria BC, V8W3V6, Canada.

Electronic Supplementary Material (ESI) for Photochemical & Photobiological Science

Table of contents:

1. Experimental procedures and characterization of compounds

1-Bromo-5-nitronaphthalene

1-Nitronaphthalene (6.92 g, 40 mmol) was placed in a two-necked reaction flask and bromine (2.5 mL, 45 mmol) was added dropwise. The reaction mixture was mixed overnight at rt. The crude product was dissolved in chloroform (100 mL) and washed with a saturated Na_2SO_3 solution and water. The organic phase was dried over anhydrous $MgSO_4$. After filtration and removal of the solvent by a rotary evaporation, the crude product was obtained. After purification by a column chromatography on silica gel using ether-hexane (1:9) as eluent 5.42 g (54%) of the pure product was obtained in the form of dark red solid.

Dark red solid; ^{1}H NMR (300MHz, $CDCl_3$) δ (ppm) 8.61 (d, 1H), 8.47 (d, 1H), 8.23 (d, 1H), 7.94 (d, 1H), 7.67 (t, 1H),7.54 (t, 1H).

1-Amino-5-bromonaphthalene

1-Bromo-5-nitronaphthalene (5.30 g, 37.6 mmol) was placed in a two-necked flask equipped with a reflux condenser. Acetone (160 mL) and an aqueous solution of NH_4Cl (4.02 g in 24 mL of water) were added. The resulting suspension was heated until reflux was obtained. Heating was stopped and Zn-powder (9.34 g, 142.8 mmol) was gradually added in the clear solution. After addition of the entire quantitiy of Zn, the resulting suspension was refluxed 1.5 h and filtered while hot. The precipitate on funnel was washed with hot acetone (20 mL). After removal of the solvent by rotary evaporation, the crude product was dissolved in chloroform (100 mL), the solution was washed with water and dried over anhydrous $MgSO_4$. After filtration and removal of the solvent by rotary evaporation, the crude product was obtained. The product was purified by a chromatography on silica gel using CH_2Cl_2 as eluent. 2.33 g (50%) of the pure product were obtained in the form of dark red crystalline solid.

Red crystalline solid; mp 49-51 °C; IR (KBr) ν/cm^{-1}: 3383 (N-H), 3074 (C-H), 3043 (C-H), 3017 (C-H); ^{1}H NMR (300 MHz, $CDCl_3$) δ (ppm) 7.78-7.69 (m, 2H), 7.69 (d, 1H), 7.35 (t, 1H), 7.22 (t, 1H), 6.78 (d, 1H), 4.11 (br. s, 2H).

1-Bromo-5-iodonaphthalene

1-Amino-5-bromonaphthalene (504 mg, 2.27 mmol), conc. HCl (1 mL), water (1 mL) and finely crushed ice (2.5 g) were placed in a round-bottomed flask and well mixed to form a suspension. With external cooling (ice bath), a solution of $NaNO_2$ (161 mg, 2.32 mmol) in cold water (1 mL) was added. The resulting mixture was stirred for 10 min. A cold solution of KI (404 mg, 2.43 mmol, in 1 mL of water) was added dropwise accompained with an extensive foaming of the reaction mixture. The reaction mixture was mixed 1 h at 0 °C and at rt overnight. The next day, the reaction mixture was heated under reflux for 30 min. After cooling, the product was extracted with CH_2Cl_2 (3 × 15 mL). The combined organic extracts were dried over anhydrous $MgSO_4$. After filtration and removal of the solvent by rotary evaporation, the crude product was obtained. The product was purified by a chromatography on silica gel using hexane as eluent. 520 mg (69 %) of the product were obtained in the form of white crystalline solid.

White crystaline solid; mp 105-106 °C; IR (KBr) ν/cm^{-1}: 3039 (C-H), 3007 (C-H); ^{1}H NMR (300 MHz, $CDCl_3$) δ (ppm) 8.28 (d, 1H, J = 8.4 Hz), 8.13 (*quasi*-t, 2H), 7.84 (d, 1H, J = 7.3 Hz), 7.41 (t, 1H, J = 8.0 Hz), 7.28 (d, 1H, J = 8.0 Hz).

2. Irradiations of compounds 7, 9, 11 and 12 under different conditions

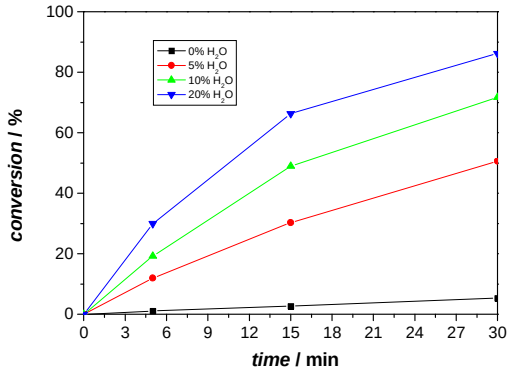

Fig S1. Conversion of **7** to **22** on photolysis (8 lamps, 300 nm) in CH_3OH-H_2O with different H_2O content.

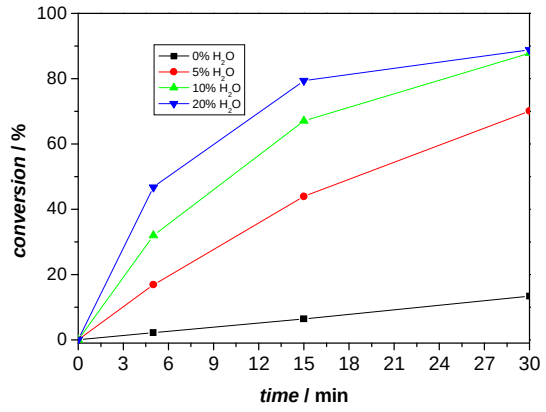

Fig S2. Conversion of **9** to **23** on photolysis (8 lamps, 300 nm) in CH_3OH-H_2O with different H_2O content.

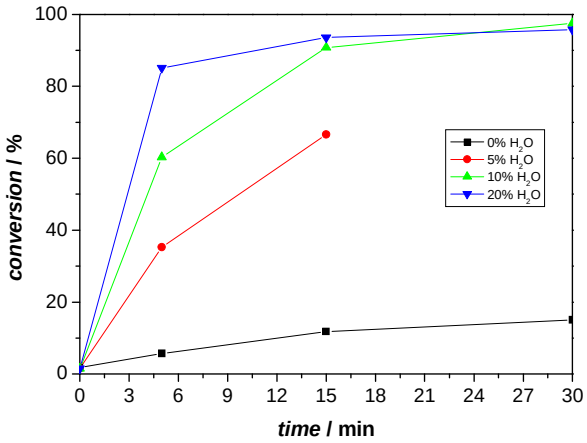

Fig S3. Conversion of **11** to **24** on photolysis (8 lamps, 300 nm) in CH_3OH-H_2O with different H_2O content.

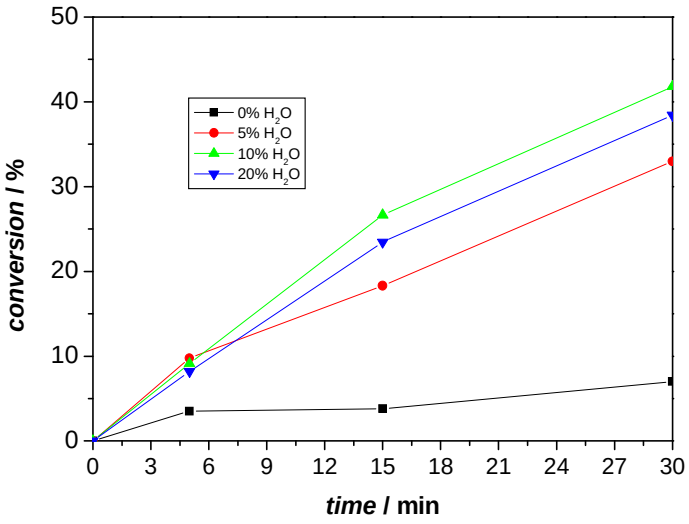

Fig S4. Conversion of **12** to **25** on photolysis (8 lamps, 300 nm) in CH_3OH-H_2O with different H_2O content.

3. UV-vis and Fluorescence spectra of 7-12

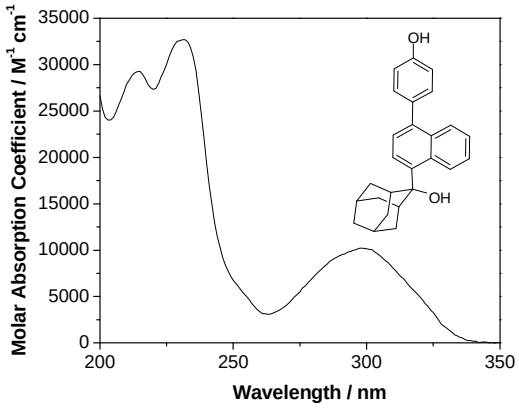

Fig S5. Absorption spectrum of **7** in CH_3CN.

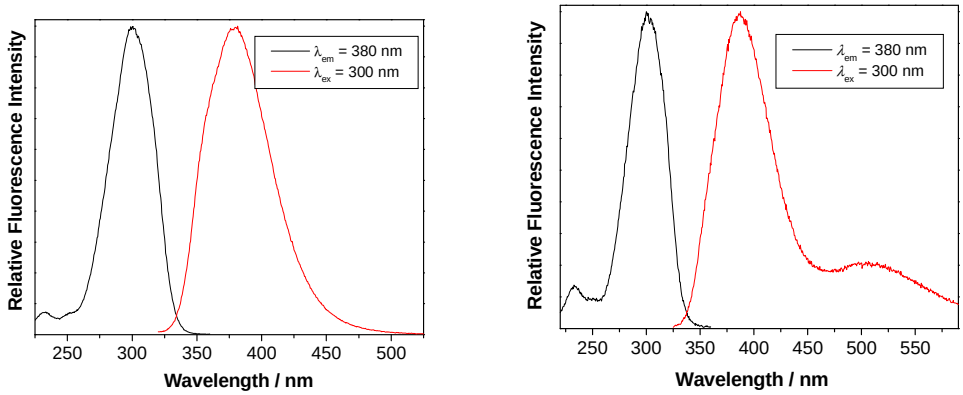

Fig S6. Excitation and emission spectra of **7** in CH_3CN (left) and CH_3CN-H_2O (1:1) (right).

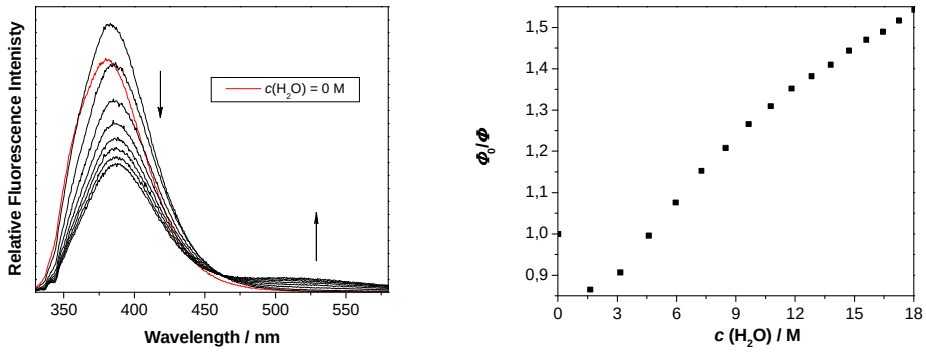

Fig S7. Fluorescence spectra of **7** in CH_3CN at different H_2O concentration (left) and the corresponding Stern-Volmer quenching plot (right).

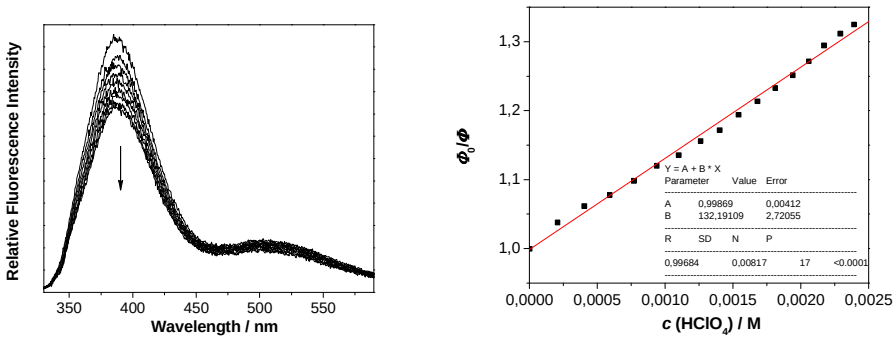

Fig S8. Fluorescence spectra of **7** in CH_3CN-H_2O (1:1) at different $HClO_4$ concentration (left) and the corresponding Stern-Volmer quenching plot (right).

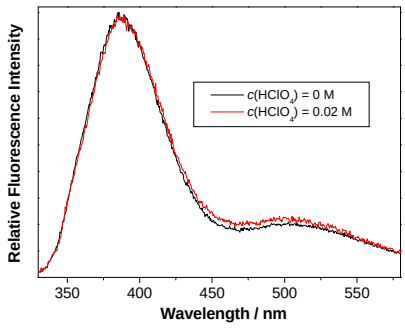

Fig S9. Normalized fluorescence spectra of **7** in CH_3CN-H_2O (1:1) at different $HClO_4$ concentration.

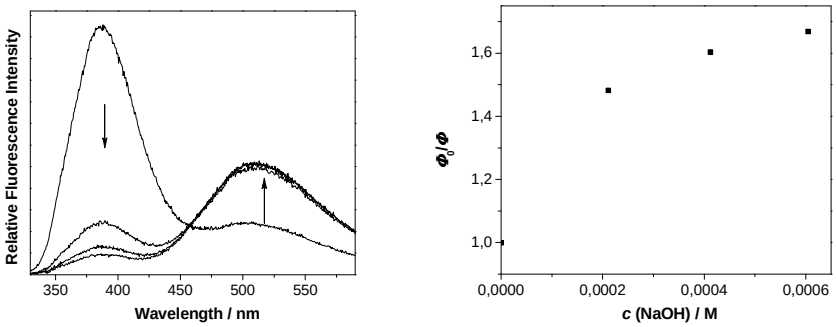

Fig S10. Fluorescence spectra of **7** in CH_3CN-H_2O (1:1) at different NaOH concentration (left) and the corresponding Stern-Volmer quenching plot (right).

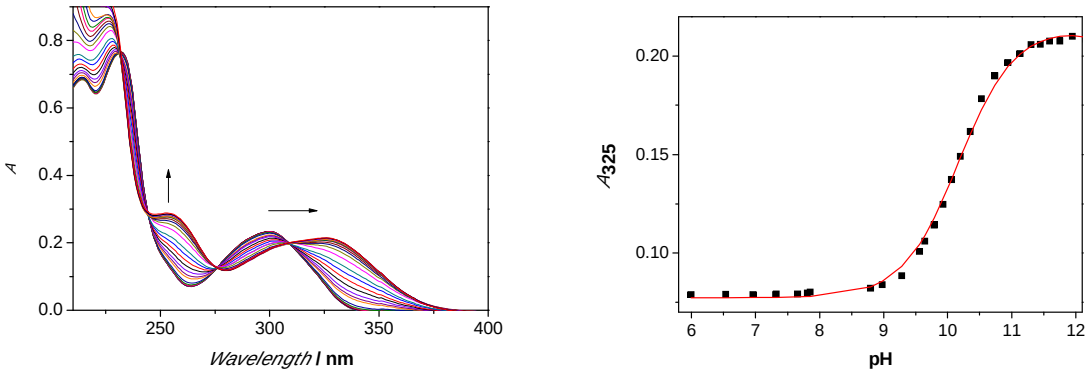

Fig S11. Absorption spectra of **7** in CH_3CN-H_2O (3:7) at different pH. Dependence of the absorbance at 326 nm on pH (right). Black dots are the experimental values, red line is the calculated fit.

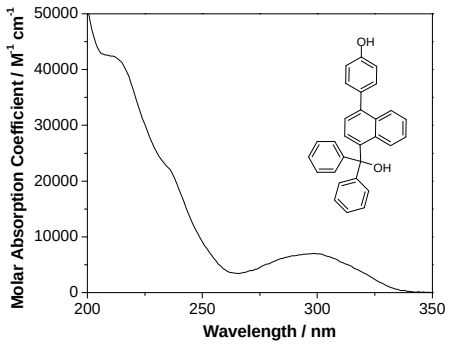

Fig S12. Absorption spectrum of **8** in CH_3CN.

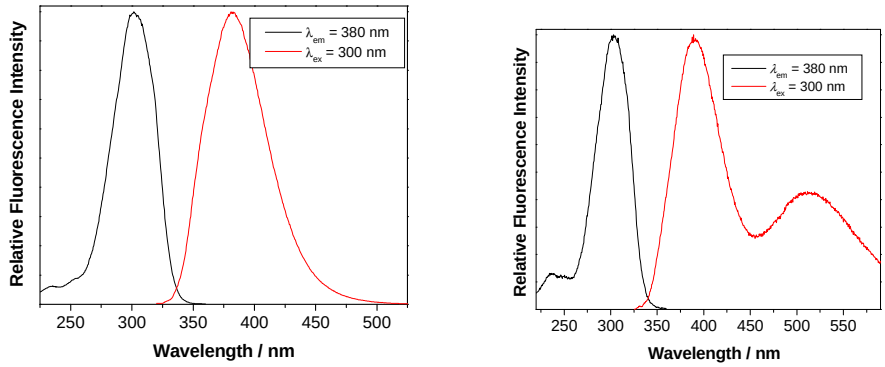

Fig S13. Excitation and emission spectra of **8** in CH_3CN (left) and CH_3CN-H_2O (1:1) (right).

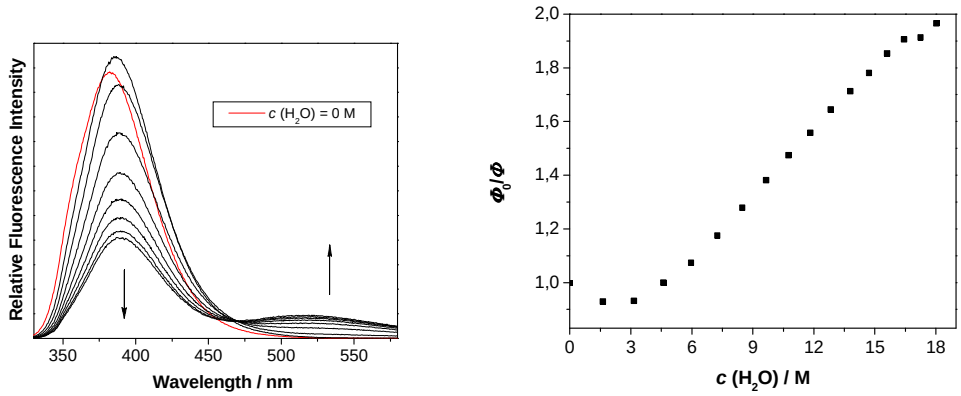

Fig S14. Fluorescence spectra of **8** in CH_3CN at different H_2O concentration (left) and the corresponding Stern-Volmer quenching plot (right).

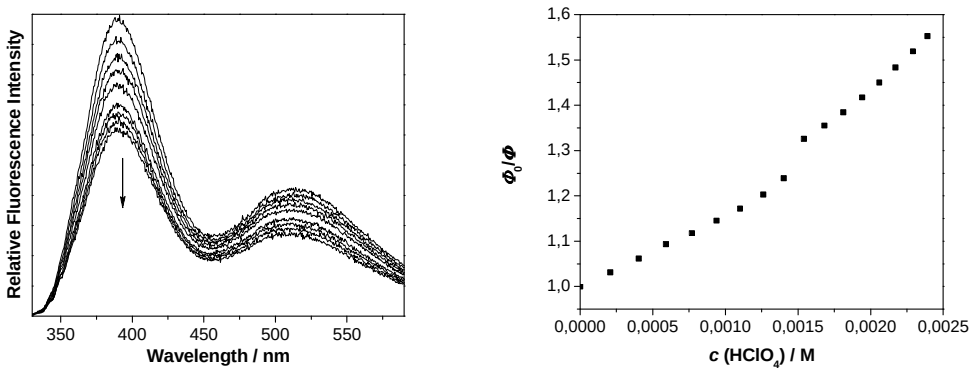

Fig S15. Fluorescence spectra of **8** in CH_3CN-H_2O (1:1) at different $HClO_4$ concentration (left) and the corresponding Stern-Volmer quenching plot (right).

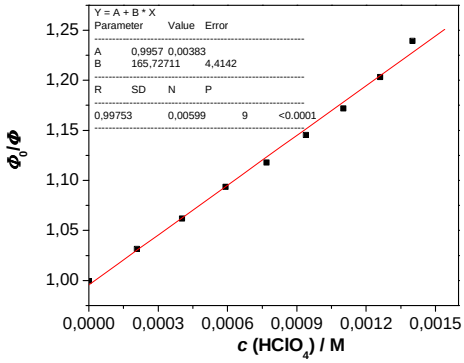

Fig S16. Stern-Volmer plot for the quenching of **8** in CH_3CN-H_2O (1:1) by $HClO_4$.

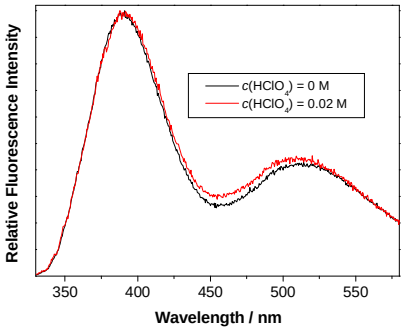

Fig S17. Normalized fluorescence spectra of **8** in CH_3CN-H_2O (1:1) at different $HClO_4$ concentration.

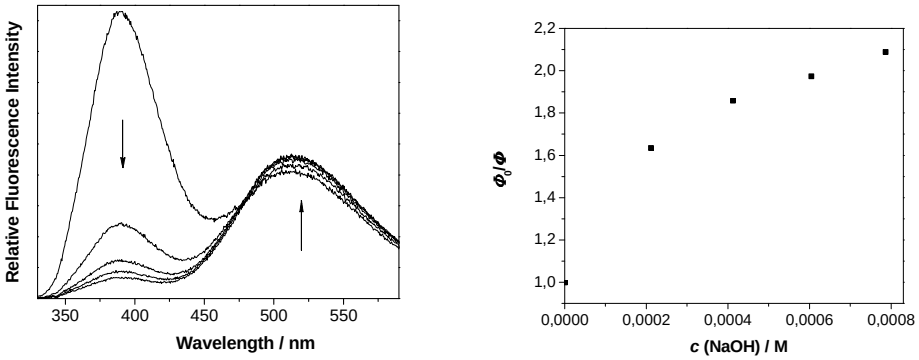

Fig S18. Fluorescence spectra of **8** in CH_3CN-H_2O (1:1) at different NaOH concentration (left) and the corresponding Stern-Volmer quenching plot (right).

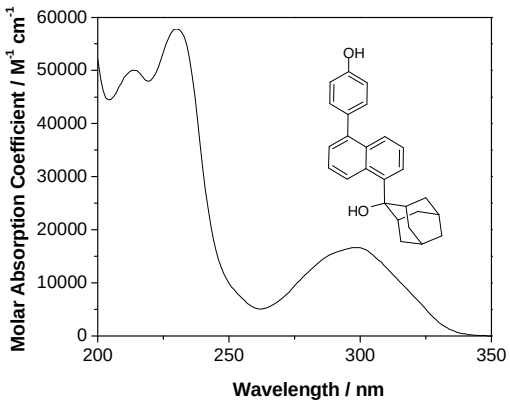

Fig S19. Absorption spectrum of **9** in CH_3CN.

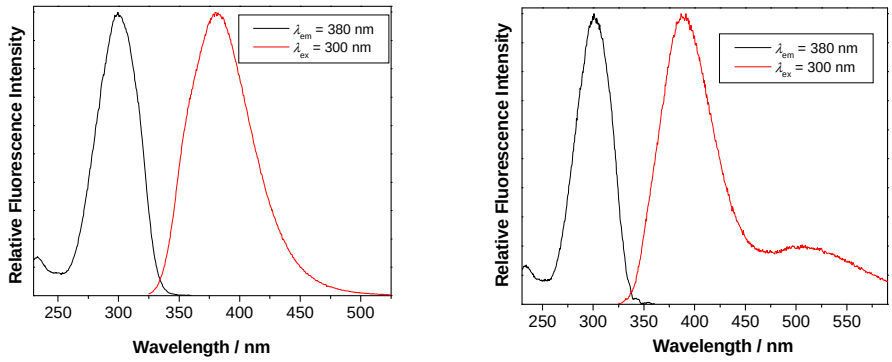

Fig S20. Excitation and emission spectra of **9** in CH_3CN (left) and CH_3CN-H_2O (1:1) (right).

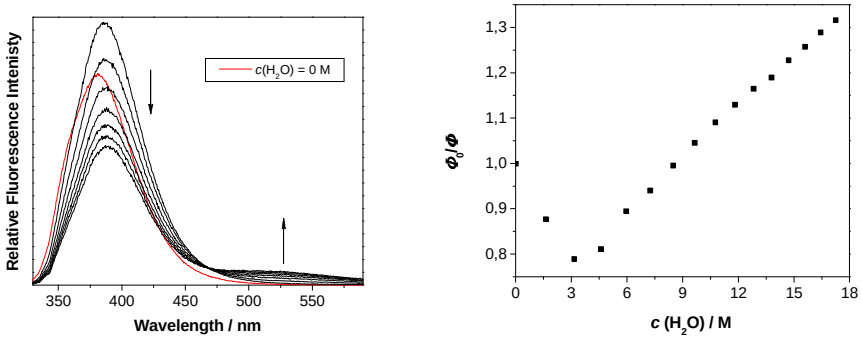

Fig S21. Fluorescence spectra of **9** in CH_3CN at different H_2O concentration (left) and the corresponding Stern-Volmer quenching plot (right).

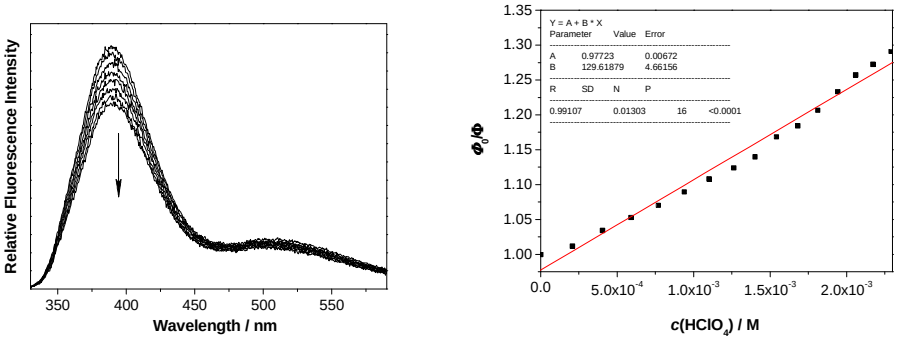

Fig S22. Fluorescence spectra of **9** in CH_3CN-H_2O (1:1) at different $HClO_4$ concentration (left) and the corresponding Stern-Volmer quenching plot (right).

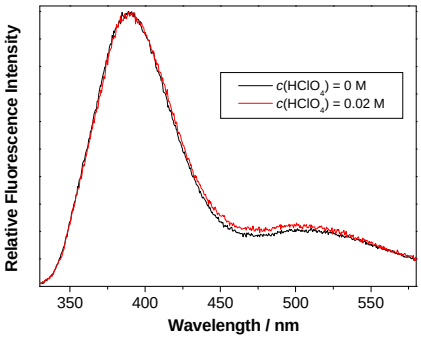

Fig S23. Normalized fluorescence spectra of **9** in CH_3CN-H_2O (1:1) at different $HClO_4$ concentration.

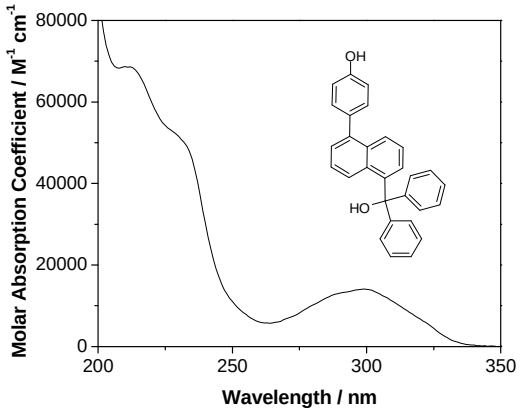

Fig S24. Absorption spectrum of **10** in CH_3CN.

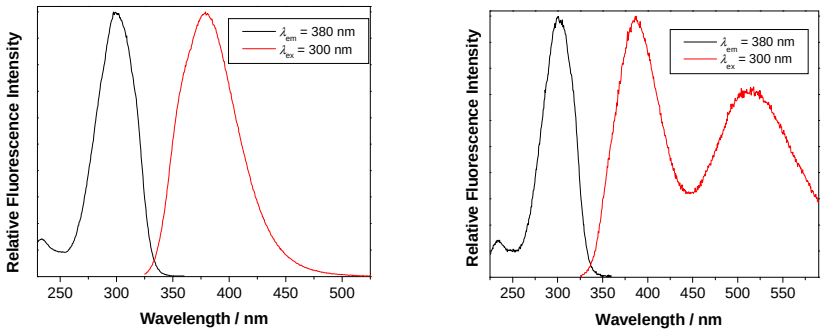

Fig S25. Excitation and emission spectra of **10** in CH_3CN (left) and CH_3CN-H_2O (1:1) (right).

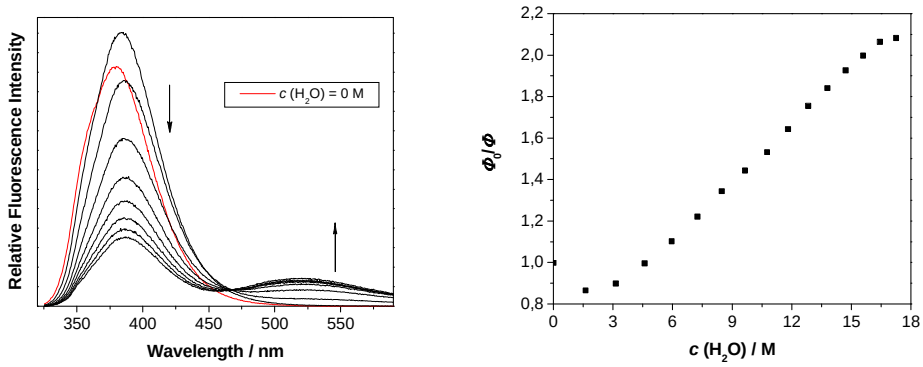

Fig S26. Fluorescence spectra of **10** in CH_3CN at different H_2O concentration (left) and the corresponding Stern-Volmer quenching plot (right).

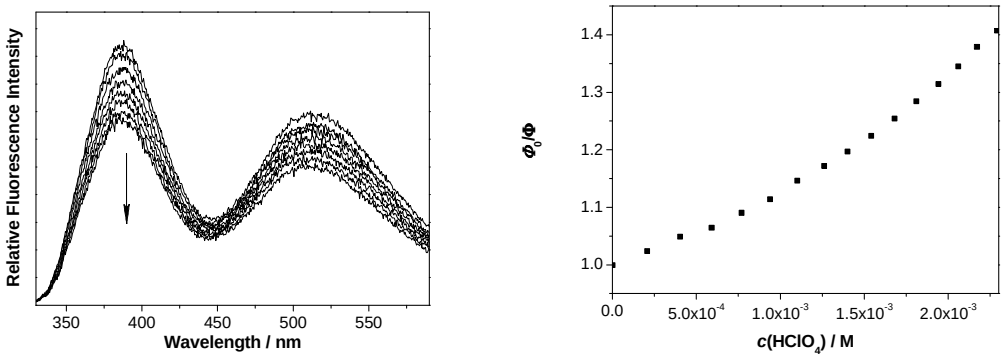

Fig S27. Fluorescence spectra of **10** in CH_3CN-H_2O (1:1) at different $HClO_4$ concentration (left) and the corresponding Stern-Volmer quenching plot (right).

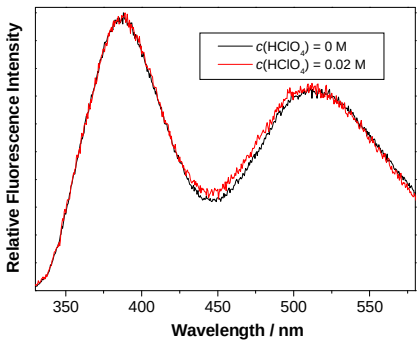

Fig S28. Normalized fluorescence spectra of **10** in CH_3CN-H_2O (1:1) at different $HClO_4$ concentration.

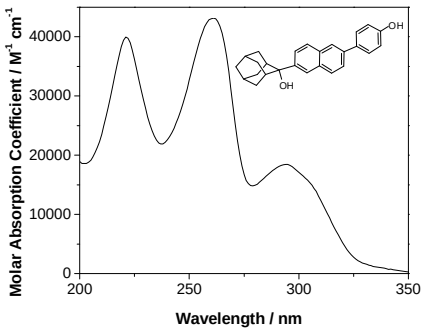

Fig S29. Absorption spectrum of **11** in CH_3CN.

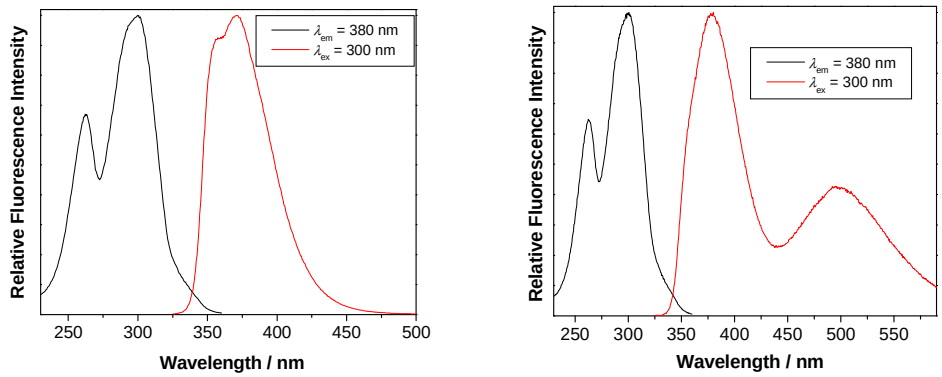

Fig S30. Excitation and emission spectra of **11** in CH_3CN (left) and CH_3CN-H_2O (1:1) (right).

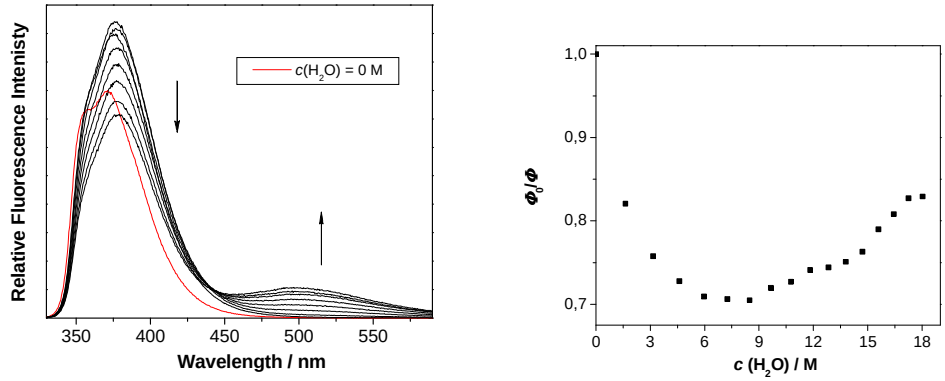

Fig S31. Fluorescence spectra of **11** in CH_3CN at different H_2O concentration (left) and the corresponding Stern-Volmer quenching plot (right).

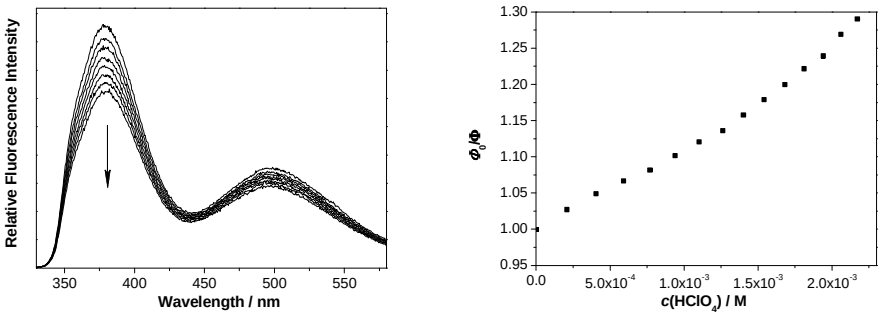

Fig S32. Fluorescence spectra of **11** in CH_3CN-H_2O (1:1) at different $HClO_4$ concentration (left) and the corresponding Stern-Volmer quenching plot (right).

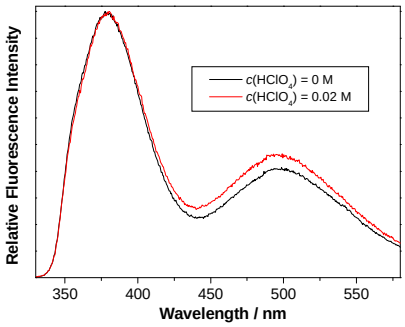

Fig S33. Normalized fluorescence spectra of **11** in CH_3CN-H_2O (1:1) at different $HClO_4$ concentration.

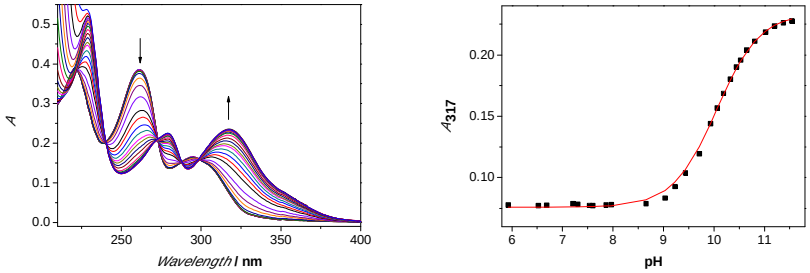

Fig S34. Absorption spectra of **11** in CH_3CN-H_2O (3:7) at different pH. Dependence of the absorbance at 317 nm on pH (right). Black dots are the experimental values, red line is the calculated fit.

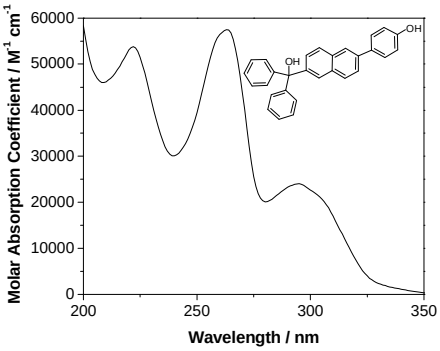

Fig S35. Absorption spectrum of **12** in CH_3CN.

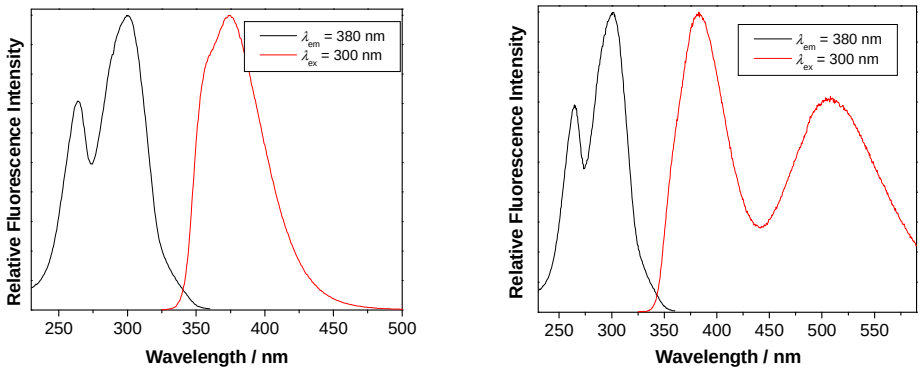

Fig S36. Excitation and emission spectra of **12** in CH_3CN (left) and CH_3CN-H_2O (1:1) (right).

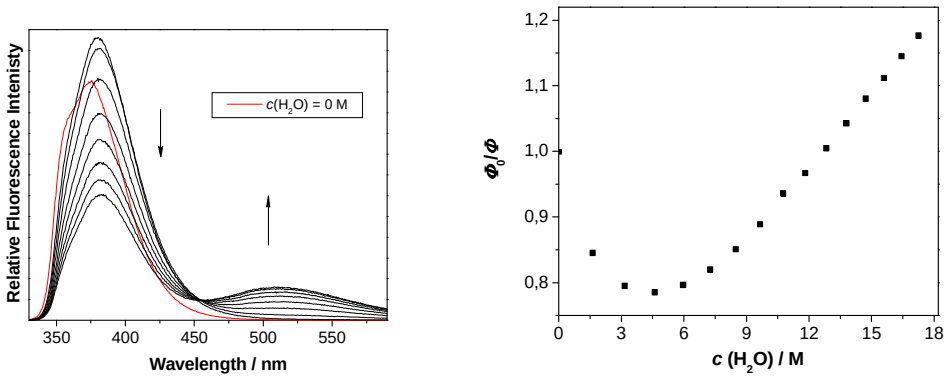

Fig S37. Fluorescence spectra of **12** in CH_3CN at different H_2O concentration (left) and the corresponding Stern-Volmer quenching plot (right).

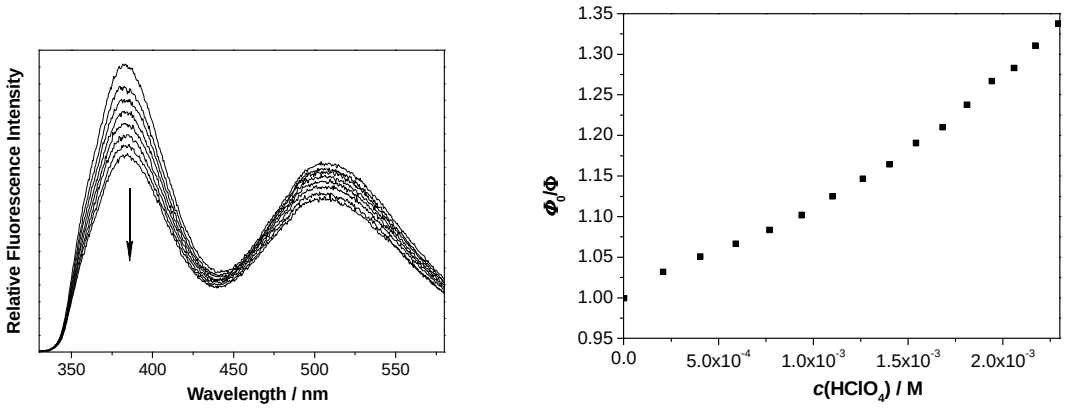

Fig S38. Fluorescence spectra of **12** in CH_3CN-H_2O (1:1) at different $HClO_4$ concentration (left) and the corresponding Stern-Volmer quenching plot (right).

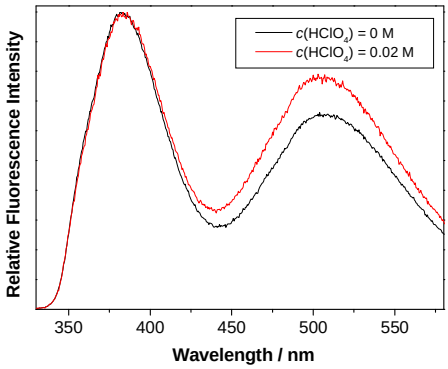

Fig S39. Normalized fluorescence spectra of **12** in CH_3CN-H_2O (1:1) at different $HClO_4$ concentration.

4. Laser Flash Photolysis (LFP)

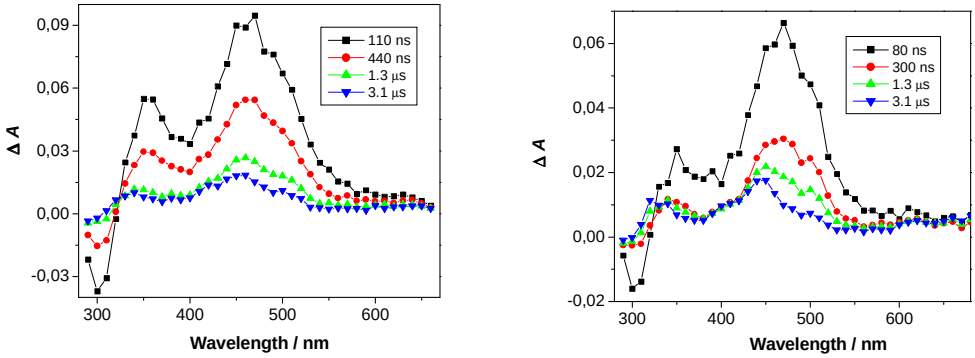

Fig S40. Transient absorption spectra of **7** in N_2-purged (left) and O_2-purged (right) CH_3CN solution.

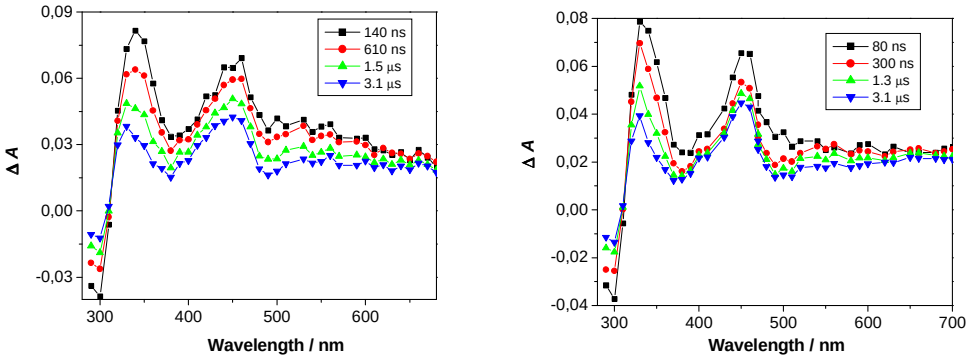

Fig S41. Transient absorption spectra of **7** in N_2-purged (left) and O_2-purged (right) CH_3CN-H_2O (1:1) solution.

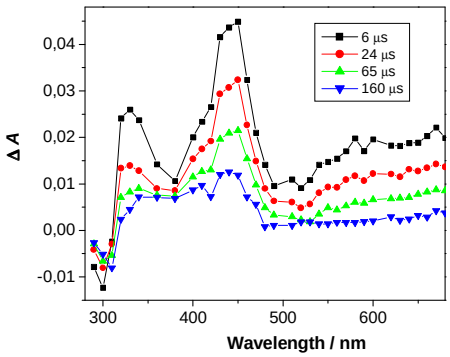

Fig S42. Transient absorption spectra of **7** in O_2-purged CH_3CN-H_2O (1:1) solution.

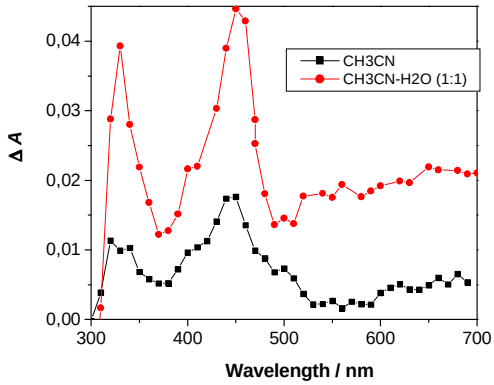

Fig S43. Transient absorption spectra of **7** in O_2-purged CH_3CN and CH_3CN-H_2O (1:1) solution 3 µs after the laser pulse.

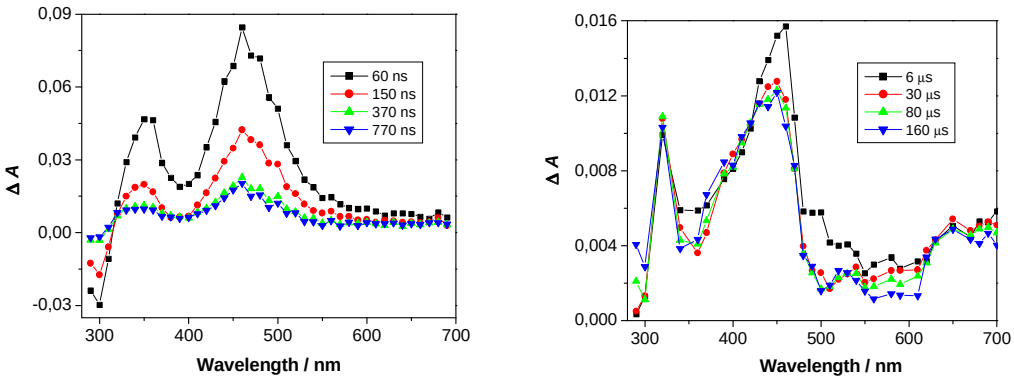

Fig S44. Transient absorption spectra of **7** in O_2-purged TFE solution.

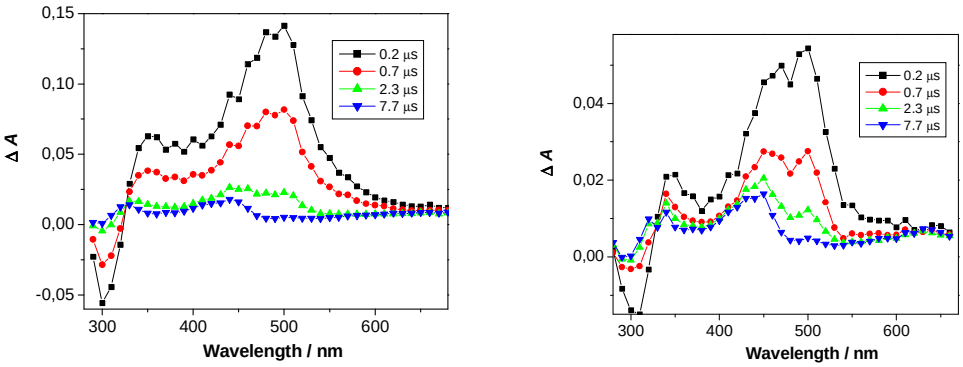

Fig S45. Transient absorption spectra of **8** in N_2-purged (left) and O_2-purged (right) CH_3CN solution.

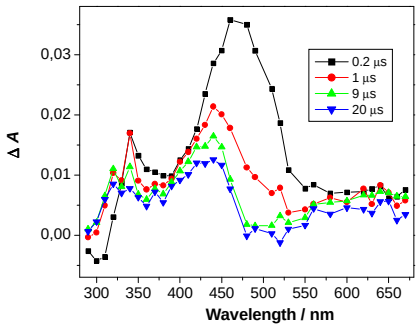

Fig S46. Transient absorption spectra of **8** in O_2-purged CH_3CN solution.

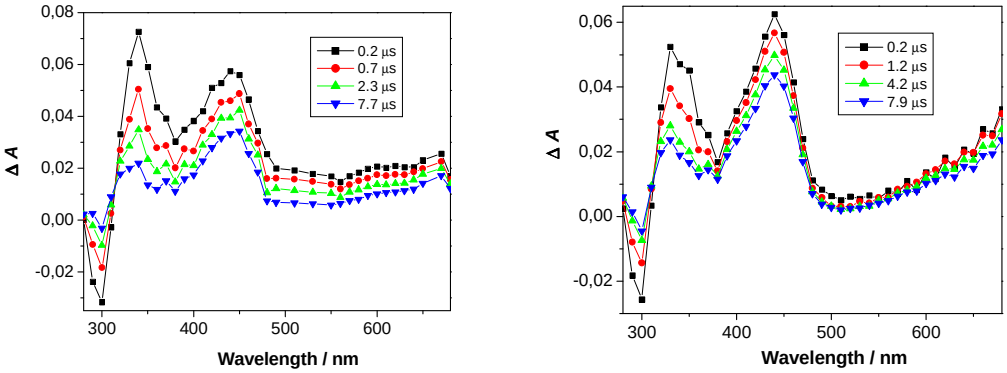

Fig S47. Transient absorption spectra of **8** in N_2-purged (left) and O_2-purged (right) CH_3CN-H_2O (1:1) solution.

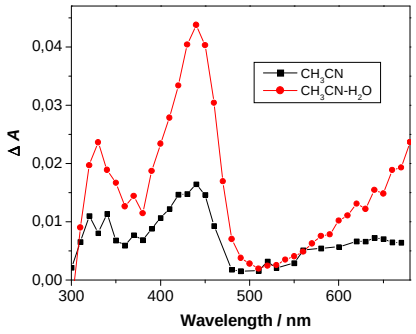

Fig S48. Transient absorption spectra of **8** in O_2-purged CH_3CN and CH_3CN-H_2O (1:1) solution 8 µs after the laser pulse.

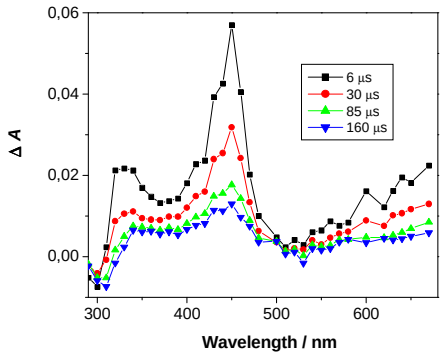

Fig S49. Transient absorption spectra of **8** in O_2-purged CH_3CN-H_2O (1:1) solution.

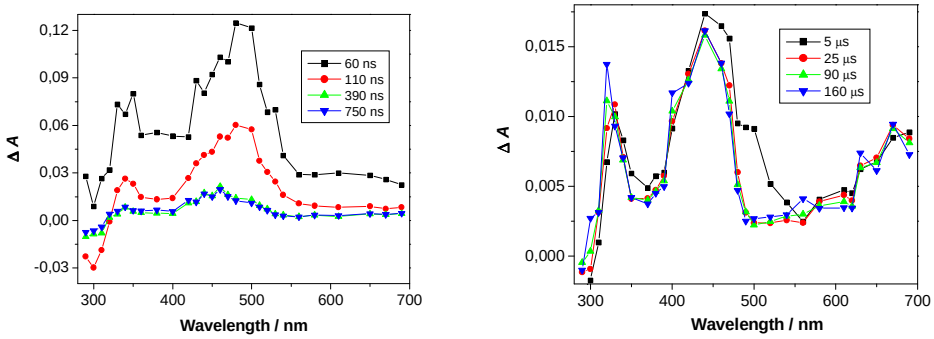

Fig S50. Transient absorption spectra of **8** in O_2-purged TFE solution.

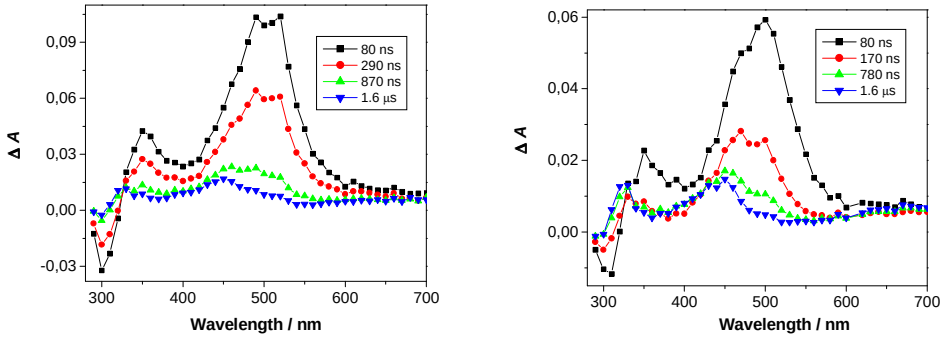

Fig S51. Transient absorption spectra of **9** in N_2-purged (left) and O_2-purged (right) CH_3CN solution.

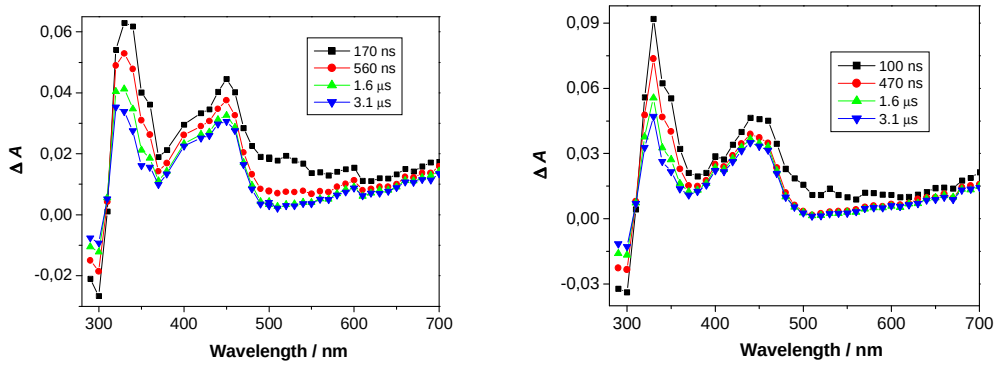

Fig S52. Transient absorption spectra of **9** in N_2-purged (left) and O_2-purged (right) CH_3CN-H_2O (1:1) solution.

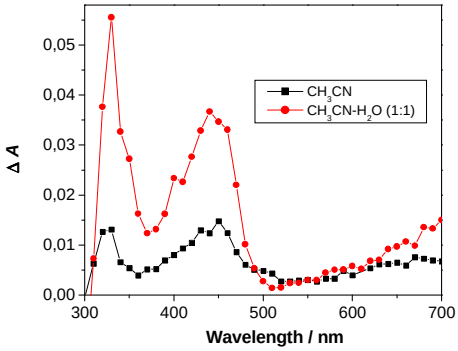

Fig S53. Transient absorption spectra of **9** in O_2-purged CH_3CN and CH_3CN-H_2O (1:1) solution 1.6 μs after the laser pulse.

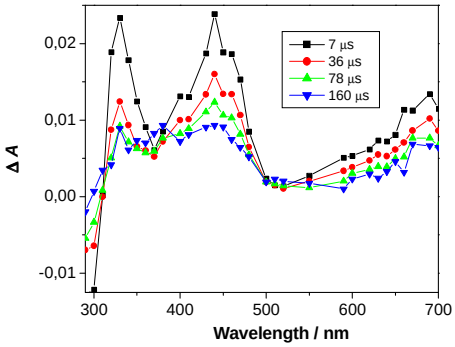

Fig S54. Transient absorption spectra of **9** in O_2-purged CH_3CN-H_2O (1:1) solution.

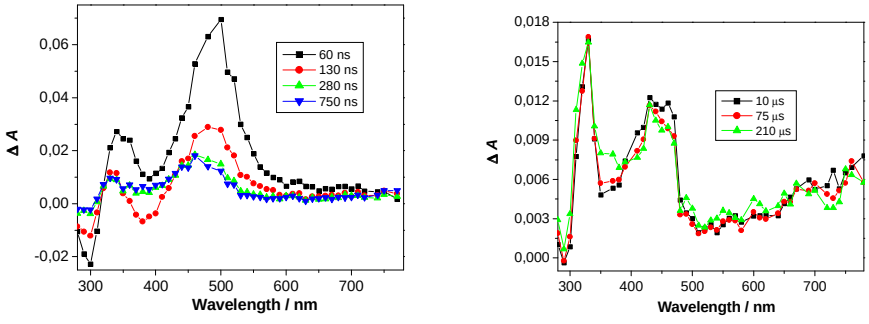

Fig S55. Transient absorption spectra of **9** in O_2-purged TFE solution.

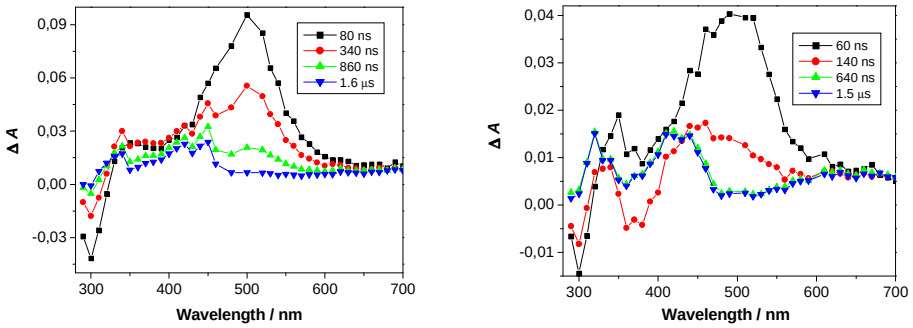

Fig S56. Transient absorption spectra of **10** in N_2-purged (left) and O_2-purged (right) CH_3CN solution.

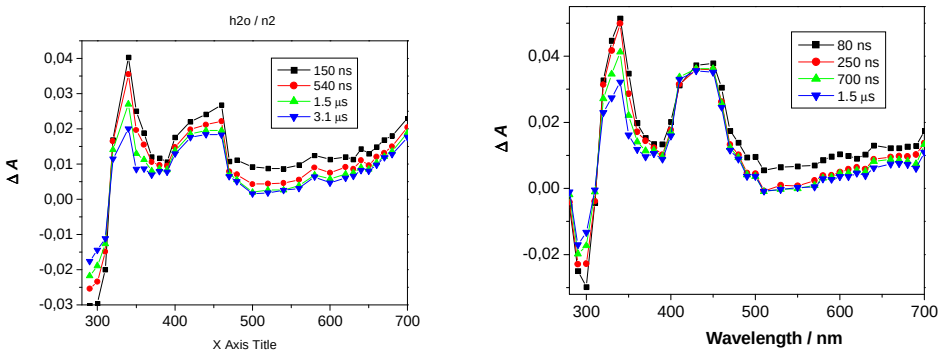

Fig S57. Transient absorption spectra of **10** in N_2-purged (left) and O_2-purged (right) CH_3CN-H_2O (1:1) solution.

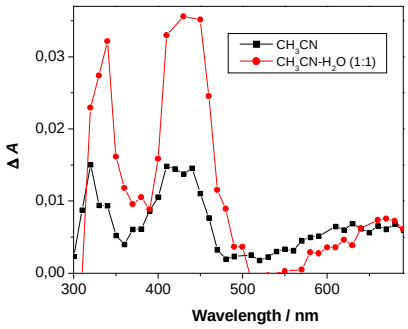

Fig S58. Transient absorption spectra of **10** in O_2-purged CH_3CN and CH_3CN-H_2O (1:1) solution 1.5 µs after the laser pulse.

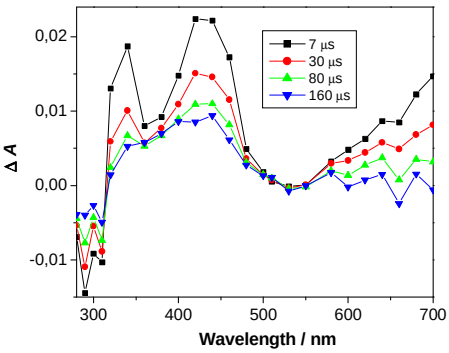

Fig S59. Transient absorption spectra of **10** in O_2-purged CH_3CN-H_2O (1:1) solution.

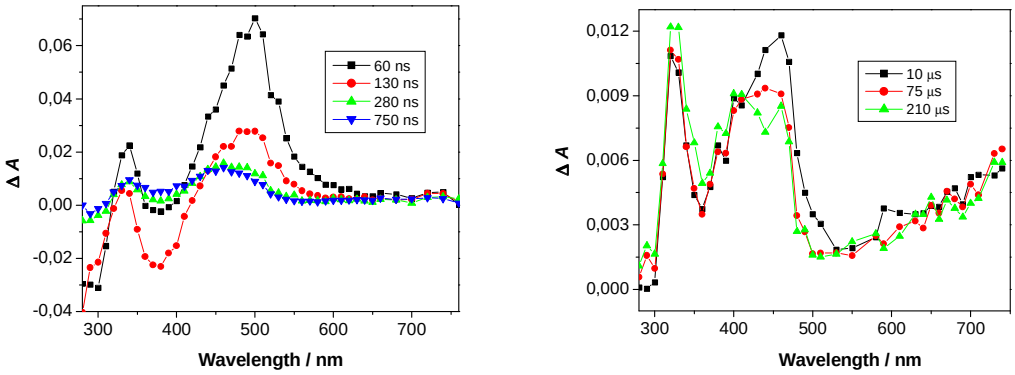

Fig S60. Transient absorption spectra of **10** in O_2-purged TFE solution.

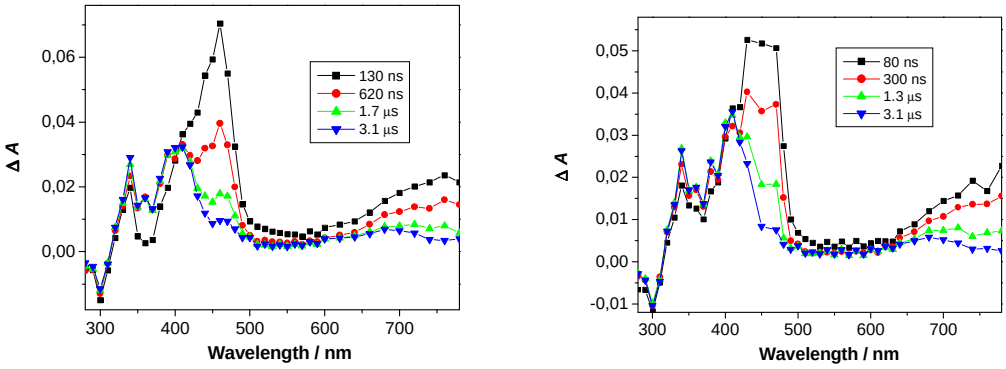

Fig S61. Transient absorption spectra of **11** in N_2-purged (left) and O_2-purged (right) CH_3CN solution.

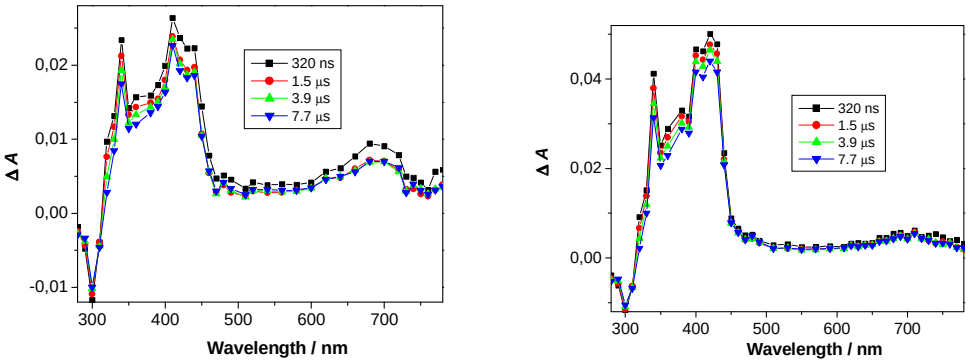

Fig S62. Transient absorption spectra of **11** in N_2-purged (left) and O_2-purged (right) CH_3CN-H_2O (1:1) solution.

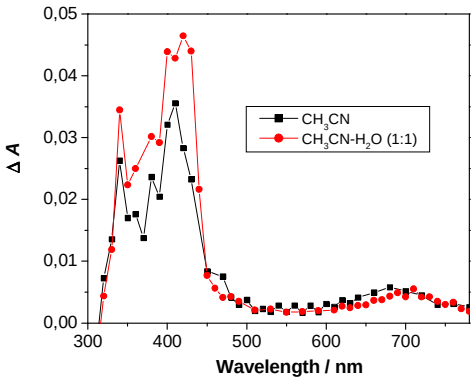

Fig S63. Transient absorption spectra of **11** in O_2-purged CH_3CN and CH_3CN-H_2O (1:1) solution, 4 µs after the laser pulse.

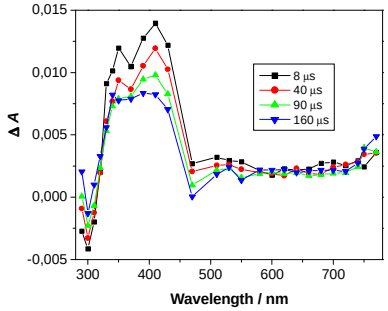

Fig S64. Transient absorption spectra of **11** in O_2-purged CH_3CN-H_2O (1:1) solution.

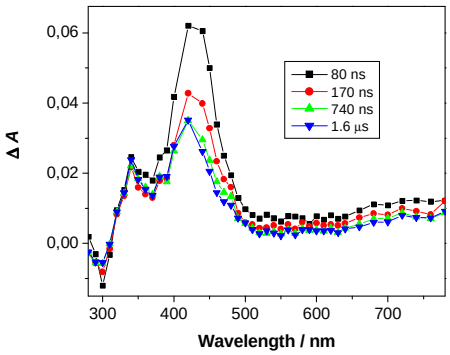

Fig S65. Transient absorption spectra of **11** in O_2-purged TFE solution.

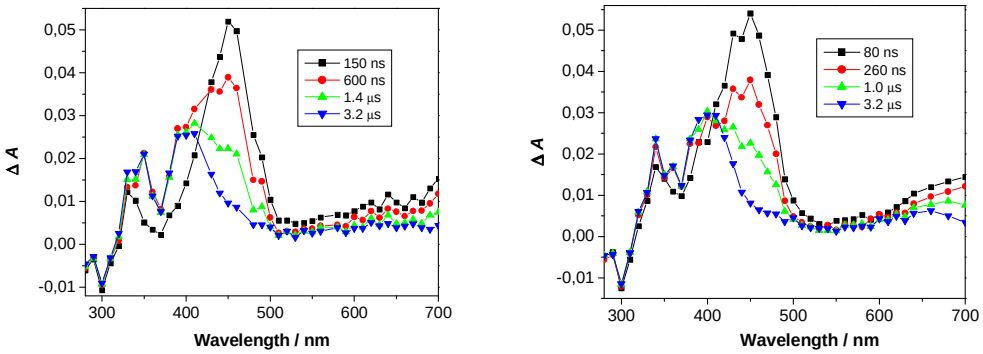

Fig S66. Transient absorption spectra of **12** in N_2-purged (left) and O_2-purged (right) CH_3CN solution.

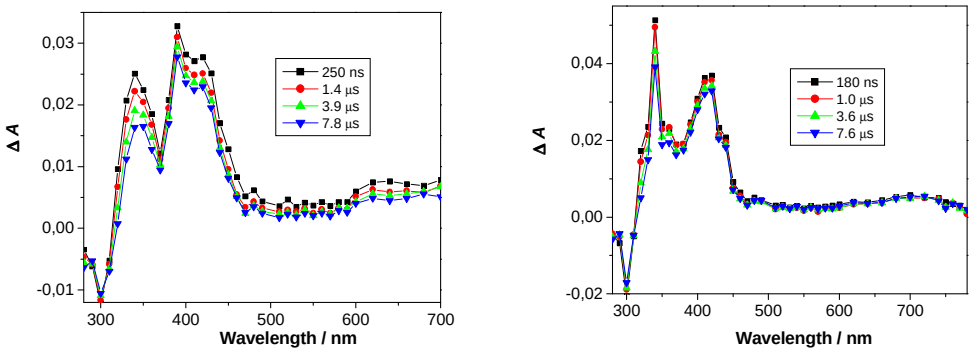

Fig S67. Transient absorption spectra of **12** in N_2-purged (left) and O_2-purged (right) CH_3CN-H_2O (1:1) solution.

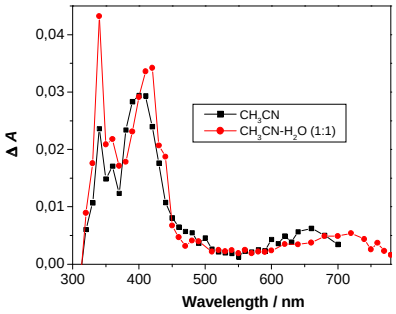

Fig S68. Transient absorption spectra of **12** in O_2-purged CH_3CN and CH_3CN-H_2O (1:1) solution 3 μs after the laser pulse.

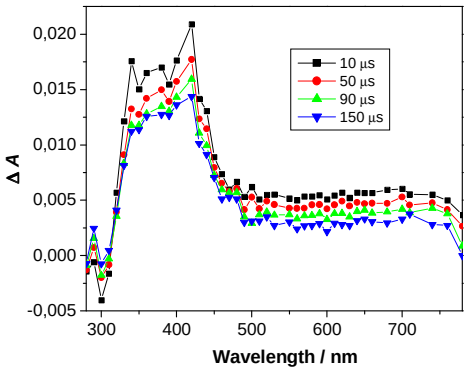

Fig S69. Transient absorption spectra of **12** in O_2-purged CH_3CN-H_2O (1:1) solution.

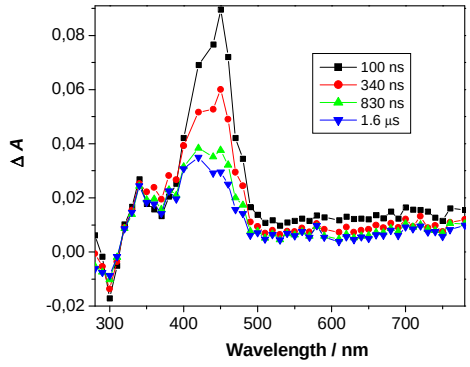

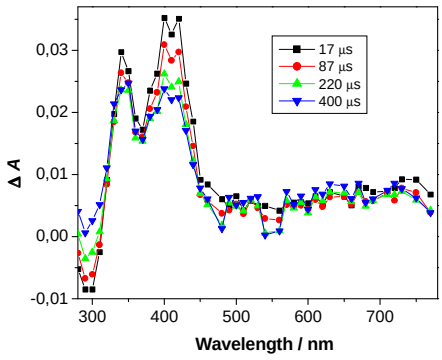

Fig S70. Transient absorption spectra of **12** in O_2-purged TFE solution.

5. Theoretical calculations

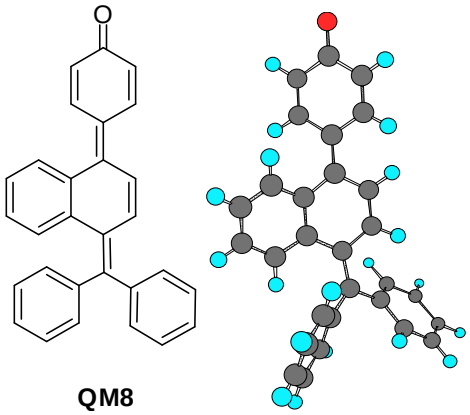

QM8

SCF Energy: -1192.03626 hartrees

Center Number	Atomic Number	Atomic Type	Coordinates (Angstroms) X	Y	Z
1	6	0	-0.067509	-1.014910	-0.322491
2	6	0	-1.490956	-1.039940	-0.119776
3	6	0	-2.163598	-2.283050	-0.250876
4	6	0	-1.522599	-3.414906	-0.733574
5	6	0	-0.174421	-3.333730	-1.114750
6	6	0	0.534661	-2.159286	-0.898366
7	6	0	0.709047	0.199316	0.006494
8	6	0	-0.059673	1.338161	0.446314
9	6	0	-1.415342	1.310842	0.611809
10	6	0	-2.217697	0.177442	0.257625
11	6	0	-3.632847	0.315542	0.219295

12	6	0	2.110684	0.303696	0.001231
13	6	0	3.029542	-0.841371	0.222404
14	6	0	2.767623	1.626134	-0.147062
15	6	0	3.893120	1.974852	0.634598
16	6	0	4.520759	3.211434	0.475617
17	6	0	4.053399	4.123689	-0.479626
18	6	0	2.950167	3.788910	-1.274720
19	6	0	2.313812	2.556814	-1.111026
20	6	0	2.799829	-1.752987	1.277506
21	6	0	3.693486	-2.795000	1.528256
22	6	0	4.834038	-2.955312	0.729346
23	6	0	5.080362	-2.055363	-0.314662
24	6	0	4.194892	-1.002011	-0.558597
25	6	0	-4.303945	1.278951	1.068137
26	6	0	-5.657520	1.442897	1.056102
27	6	0	-6.517279	0.696558	0.140241
28	6	0	-5.827565	-0.226223	-0.756970
29	6	0	-4.476811	-0.414180	-0.703529
30	8	0	-7.774591	0.852855	0.115371
31	1	0	-3.198665	-2.354560	0.053526
32	1	0	-2.065094	-4.350303	-0.821660
33	1	0	0.325555	-4.191772	-1.551954
34	1	0	1.579468	-2.128209	-1.170083
35	1	0	0.476112	2.239476	0.714273

36	1	0	-1.908687	2.215482	0.944931
37	1	0	4.259908	1.275489	1.377681
38	1	0	5.373356	3.465115	1.097441
39	1	0	4.547362	5.081494	-0.607006
40	1	0	2.591705	4.482859	-2.028254
41	1	0	1.472709	2.294014	-1.743558
42	1	0	1.920392	-1.629026	1.900001
43	1	0	3.504738	-3.478910	2.349555
44	1	0	5.526067	-3.768283	0.923809
45	1	0	5.962407	-2.171398	-0.936341
46	1	0	4.393318	-0.303985	-1.364930
47	1	0	-3.716070	1.830219	1.794322
48	1	0	-6.149725	2.126005	1.740021
49	1	0	-6.437401	-0.735621	-1.495428
50	1	0	-4.006689	-1.062728	-1.433016

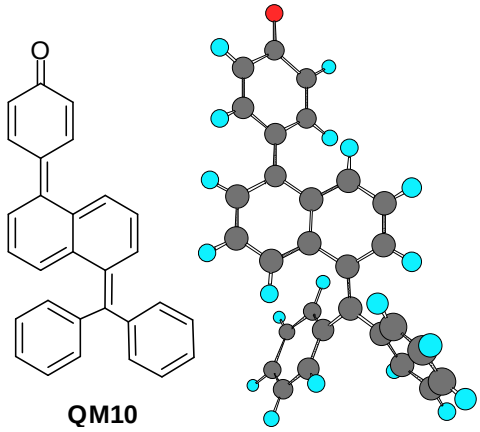

QM10

SCF Energy: -1192.01954 hartrees

Center Number	Atomic Number	Atomic Type	Coordinates (Angstroms) X	Y	Z
1	6	0	0.463871	-2.564080	-0.469800
2	6	0	-0.810610	-2.038395	-0.402494
3	6	0	-1.050888	-0.700863	0.053907
4	6	0	0.108419	0.037334	0.589757
5	6	0	1.450388	-0.476802	0.354248
6	6	0	1.586093	-1.790447	-0.110004
7	6	0	-0.034265	1.131558	1.444225
8	6	0	1.089565	1.786088	1.979803
9	6	0	2.376253	1.405757	1.631693
10	6	0	2.612358	0.316225	0.753994
11	6	0	3.940894	0.043943	0.276013
12	6	0	-3.541730	-1.026445	-0.010694
13	6	0	-2.353954	-0.152304	-0.063990

14	6	0	-2.586994	1.287183	-0.313811
15	6	0	-4.657505	-0.801928	-0.853911
16	6	0	-5.780440	-1.627174	-0.792365
17	6	0	-5.829967	-2.688136	0.122190
18	6	0	-4.742348	-2.918395	0.974591
19	6	0	-3.612753	-2.101616	0.909413
20	6	0	-1.766517	2.007090	-1.214894
21	6	0	-2.006587	3.353787	-1.481150
22	6	0	-3.068755	4.021470	-0.853350
23	6	0	-3.896240	3.323212	0.033692
24	6	0	-3.666052	1.969797	0.293883
25	6	0	5.096159	0.356422	1.075389
26	6	0	6.368133	0.105698	0.638329
27	6	0	6.632639	-0.457696	-0.681883
28	6	0	5.456318	-0.722739	-1.499645
29	6	0	4.188167	-0.493215	-1.036952
30	8	0	7.813934	-0.683047	-1.094942
31	1	0	0.611742	-3.573898	-0.837510
32	1	0	-1.647264	-2.616786	-0.773871
33	1	0	2.571561	-2.236604	-0.158983
34	1	0	-1.023268	1.482597	1.709154
35	1	0	0.941486	2.633543	2.641364
36	1	0	3.216283	1.997719	1.975491
37	1	0	-4.625220	0.011329	-1.570067

38	1	0	-6.616760	-1.446593	-1.460043
39	1	0	-6.707609	-3.324251	0.173116
40	1	0	-4.779269	-3.727588	1.696854
41	1	0	-2.783770	-2.270087	1.588038
42	1	0	-0.948591	1.494524	-1.708830
43	1	0	-1.371454	3.883958	-2.183481
44	1	0	-3.251340	5.070993	-1.059828
45	1	0	-4.720277	3.831797	0.523931
46	1	0	-4.309626	1.436490	0.985149
47	1	0	4.946211	0.742566	2.078868
48	1	0	7.230314	0.303152	1.266414
49	1	0	5.632000	-1.081407	-2.508191
50	1	0	3.341467	-0.659063	-1.695155

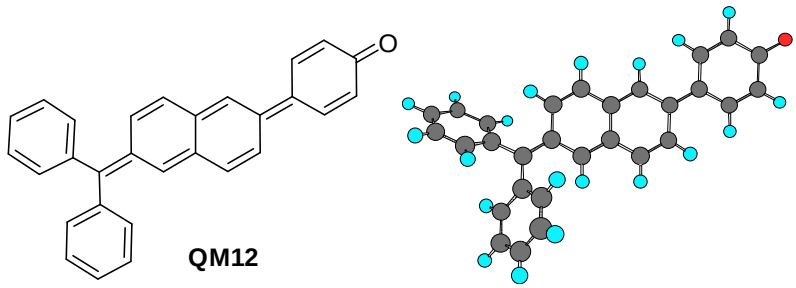

QM12

SCF Energy: -1192.04308 hartrees

Center Number	Atomic Number	Atomic Type	Coordinates (Angstroms) X	Y	Z
1	6	0	-1.015466	-1.536382	-0.477442
2	6	0	-1.612590	-0.264323	-0.096513
3	6	0	-0.696718	0.796212	0.222572
4	6	0	0.677304	0.628970	0.189592
5	6	0	1.251847	-0.645764	-0.202522
6	6	0	0.334916	-1.706816	-0.539683
7	6	0	1.594874	1.679172	0.546236
8	6	0	2.945783	1.495979	0.500298
9	6	0	3.543498	0.236543	0.098197
10	6	0	2.627685	-0.808262	-0.240785
11	6	0	4.959324	0.057261	0.051032
12	6	0	-3.009286	-0.082072	-0.045615
13	6	0	5.878913	1.111556	0.410609
14	6	0	7.233418	0.946892	0.368168
15	6	0	7.844637	-0.311749	-0.046054
16	6	0	6.910415	-1.373040	-0.408936
17	6	0	5.558863	-1.191520	-0.360316
18	8	0	9.101955	-0.473067	-0.088278

19	6	0	-3.939159	-1.229204	0.029785
20	6	0	-3.613303	1.268238	-0.065514
21	6	0	-3.676843	-2.338966	0.867678
22	6	0	-4.571992	-3.407945	0.944193
23	6	0	-5.748950	-3.398966	0.185203
24	6	0	-6.029591	-2.304993	-0.644049
25	6	0	-5.142702	-1.229976	-0.714695
26	6	0	-4.706242	1.580964	0.776959
27	6	0	-5.285160	2.850559	0.759588
28	6	0	-4.802093	3.835476	-0.112287
29	6	0	-3.733575	3.538848	-0.967452
30	6	0	-3.144331	2.272898	-0.944682
31	1	0	-1.671244	-2.346981	-0.769076
32	1	0	-1.095674	1.748332	0.553358
33	1	0	0.747877	-2.657226	-0.865610
34	1	0	1.186450	2.638297	0.851974
35	1	0	3.585786	2.324031	0.773273
36	1	0	3.006446	-1.778773	-0.536429
37	1	0	5.490779	2.071674	0.728852
38	1	0	7.908032	1.750650	0.642859
39	1	0	7.341982	-2.317830	-0.721647
40	1	0	4.920160	-2.019244	-0.644968
41	1	0	-2.780390	-2.341746	1.477999
42	1	0	-4.356260	-4.242840	1.603201
43	1	0	-6.442656	-4.231358	0.243984
44	1	0	-6.938833	-2.291425	-1.236487
45	1	0	-5.364963	-0.388473	-1.361572
46	1	0	-5.083112	0.824462	1.456418
47	1	0	-6.111933	3.073398	1.426414
48	1	0	-5.257993	4.820062	-0.129692

49	1	0	-3.366124	4.289871	-1.659455
50	1	0	-2.334834	2.042128	-1.628566

---

6. Antiproliferative investigation

The experiments were carried out on three human carcinoma cell lines HCT 116, MCF-7 and H 460. Cells were cultured as monolayers and maintained in Dulbecco's modified Eagle medium (DMEM) supplemented with 10% fetal bovine serum (FBS), 2mM L-glutamine, 100 U/ml penicillin, and 100 µg/ml streptomycin in a humidified atmosphere with 5% CO_2 at 37 °C.

The cells were inoculated in parallel on two 96-well microtiter plates on day 0, at 1.5×10^4 cells/mL. Test agents were added in ten-fold dilutions (10^{-8} to 10^{-4} M) on the next day and incubated for further 72 h. Working dilutions were freshly prepared on the day of testing. One of the plates was left in the dark, while the other was irradiated in a Luzchem reactor (6 lamps 300 nm, 1 min) 4, 24, and 48 hours after the addition of the compounds. After 72 h of incubation the cell growth rate was evaluated by performing the MTT assay which detects dehydrogenase activity in viable cells. The absorbance (A) was measured on a microplate reader at 570 nm. The absorbance is directly proportional to the number of living, metabolically active cells. The percentage of growth (PG) of the cell lines was calculated according to one or the other of the following two expressions:

If (mean A_{test} – mean A_{tzero}) ≥ 0, then PG = 100 × (mean A_{test} – mean A_{tzero}) / (mean A_{ctrl} – mean A_{tzero}).

If (mean A_{test} – mean A_{tzero}) < 0, then: PG = 100 × (mean A_{test} – mean A_{tzero}) / A_{tzero}, where the mean A_{tzero} is the average of absorbance measurements before exposure of cells to the test compound, the mean A_{test} is the average of absorbance measurements after the desired period of time and the mean A_{ctrl} is the average of optical density measurements after the desired period of time with no exposure of cells to the test compound. In the experiments where the cells were irradiated, A_{ctrl} represents irradiated control cells, which typically showed the 25% growth inhibition compared to A_{ctrl} without irradiation.

The results are expressed as IC_{50}, which is the concentration necessary for 50% of inhibition. The IC_{50} values for each compound are calculated from concentration-response curves using linear regression analysis by fitting the test concentrations that give PG values above and below the reference value (*i.e.* 50%). Each test was performed in quadruplicate in at least two individual experiments.

Table S1. IC_{50} values (in μM)

Compound	Structure	Cell lines					
		HCT116		MCF-7		H 460	
		Not irradiated	300 nm 3×1 min	Not irradiated	300 nm 3×1 min	Not irradiated	300 nm 3×1 min
11	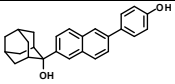	5±0.1	5±2	4±2	3±1	10±1	7±3
12	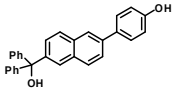	19±1	21±1	19±2	18±2	17±1	18±1
7	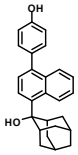	18±1	15±1	17±2	13±1	16±2	15±3
9	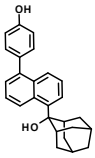	17±2	13±1	16±4	14±2	15±1	12±1

[a] GI_{50}; the concentration that causes 50% growth inhibition

[b] LET; Laboratory of Experimental Therapy

^{1}H NMR (300 MHz, $CDCl_3$) of 1-amino-5-bromonaphthalene.

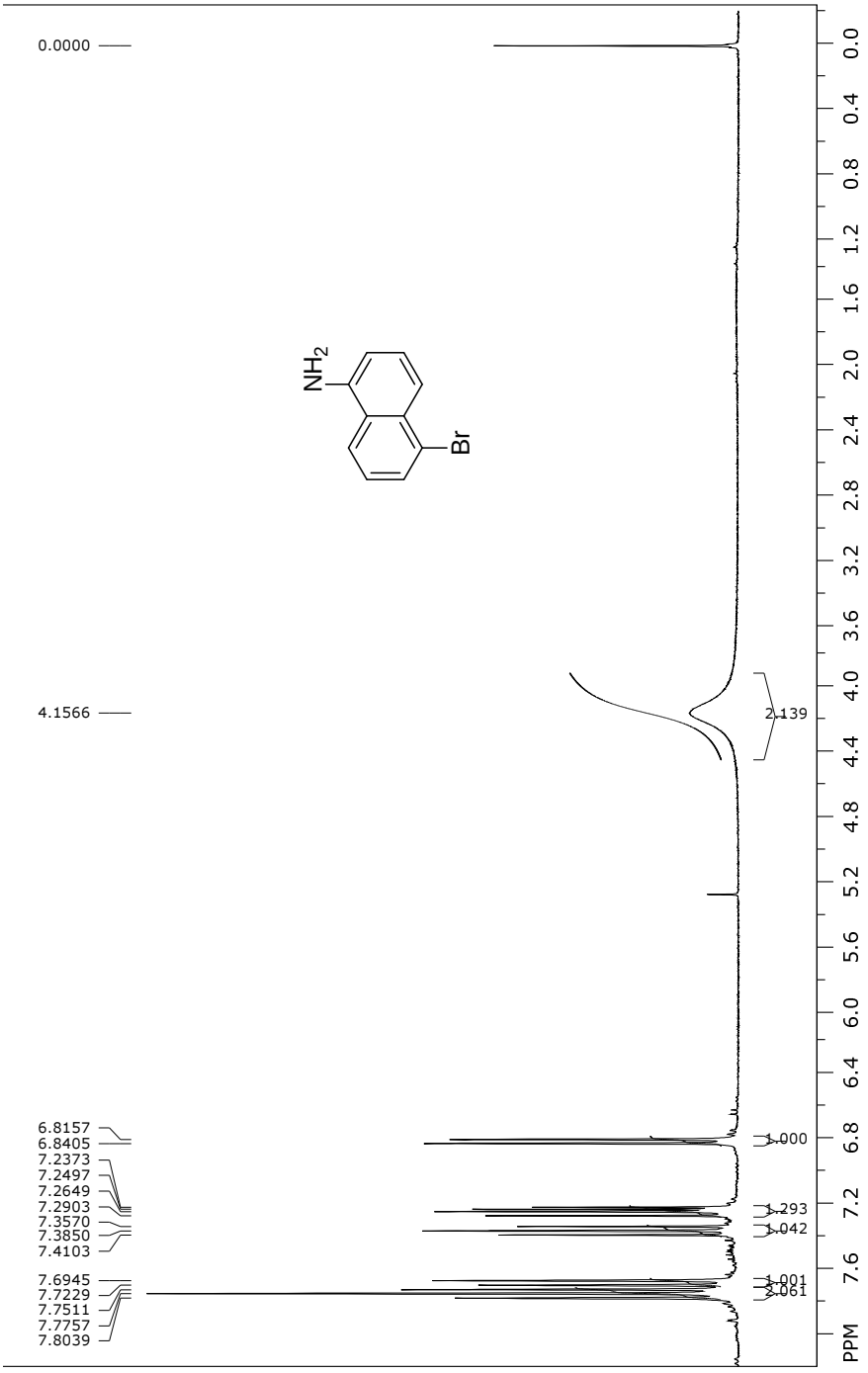

^{1}H NMR (300 MHz, $CDCl_3$) of 1-bromo-5-iodonaphthalene.

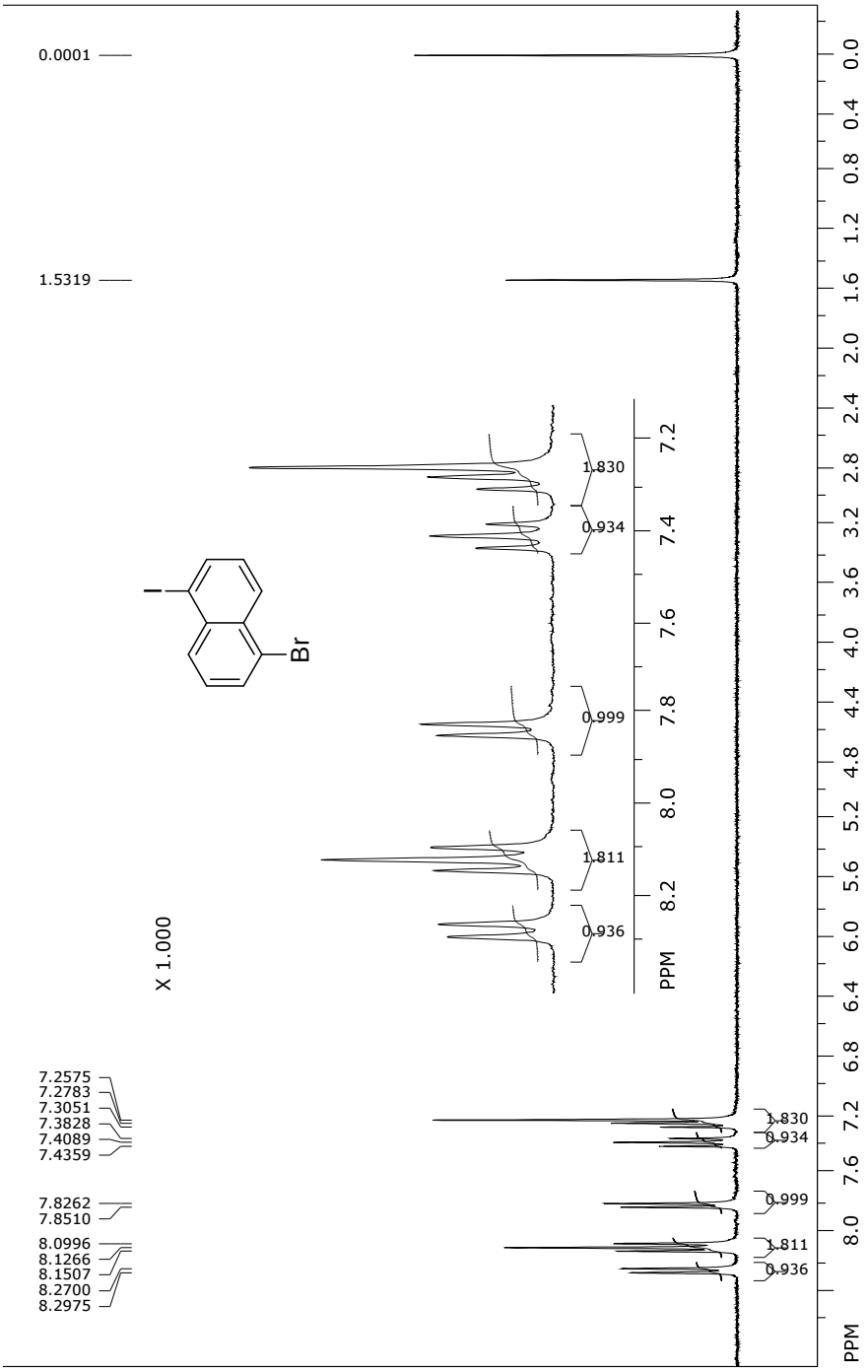

^{1}H NMR (600 MHz, $CDCl_3$) of compound **13**.

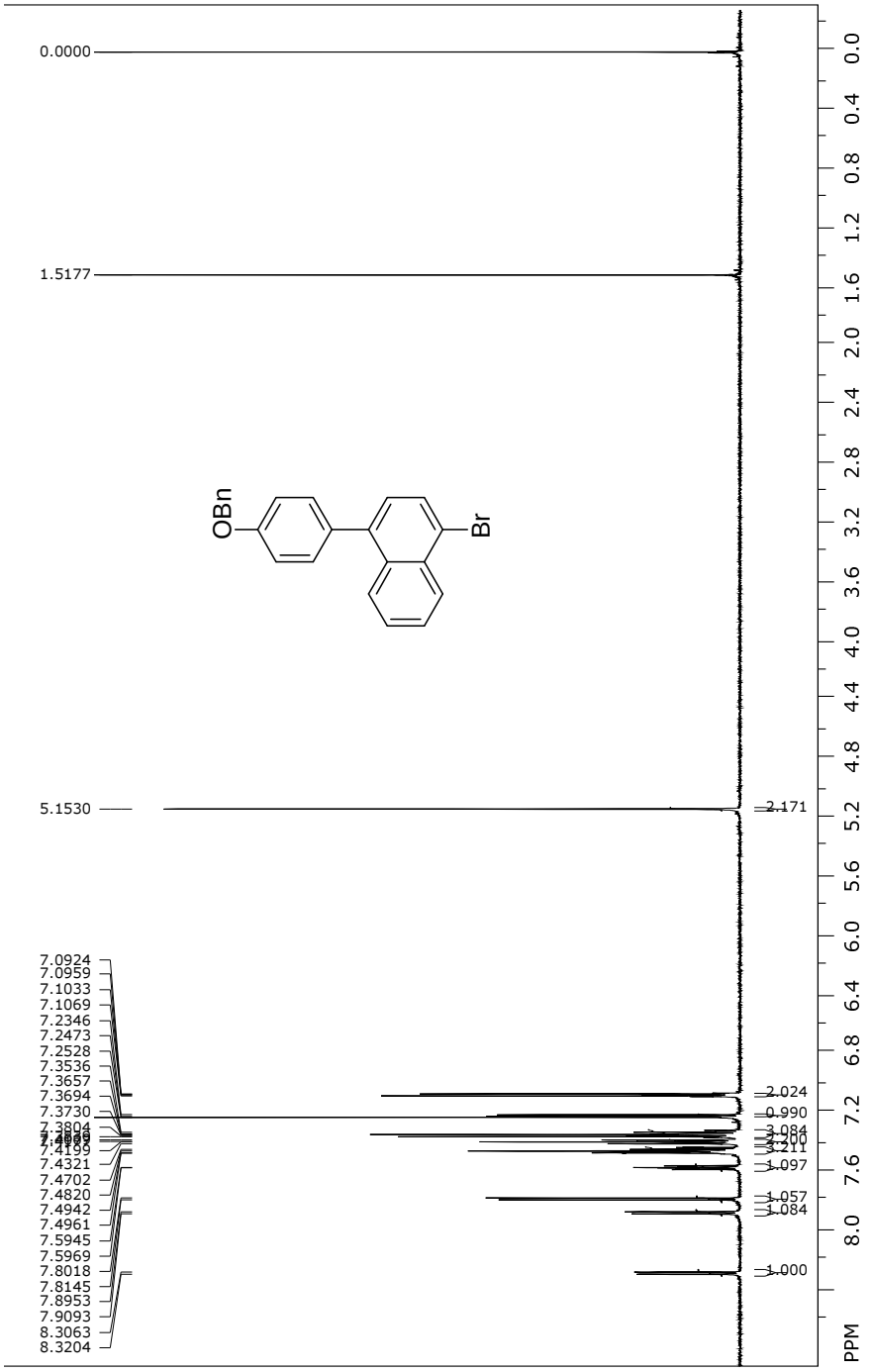

^{13}C NMR (150 MHz, $CDCl_3$) of compound **13**.

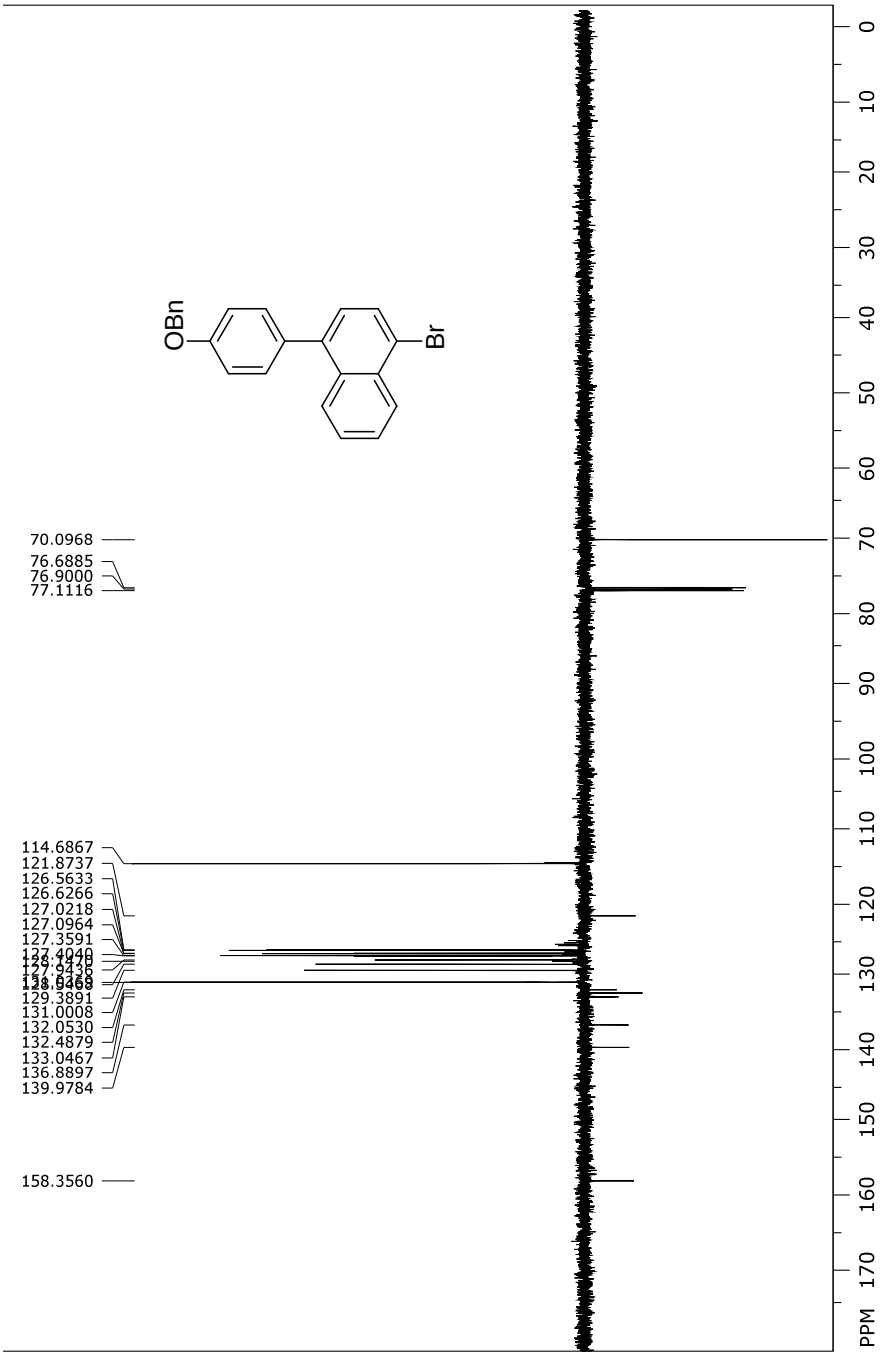

^{1}H NMR (600 MHz, $CDCl_3$) of compound **14**.

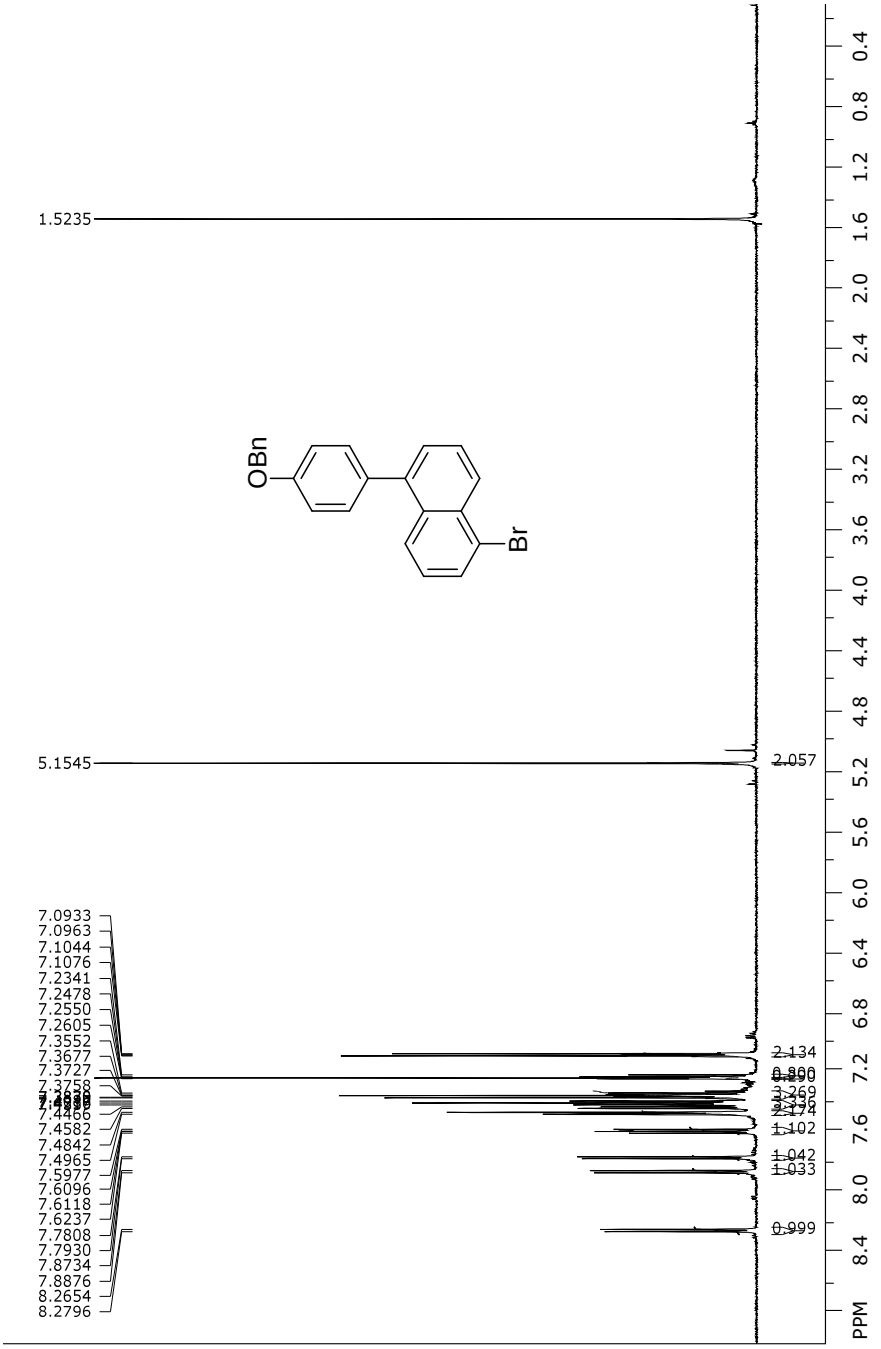

^{13}C NMR (150 MHz, $CDCl_3$) of compound **14**.

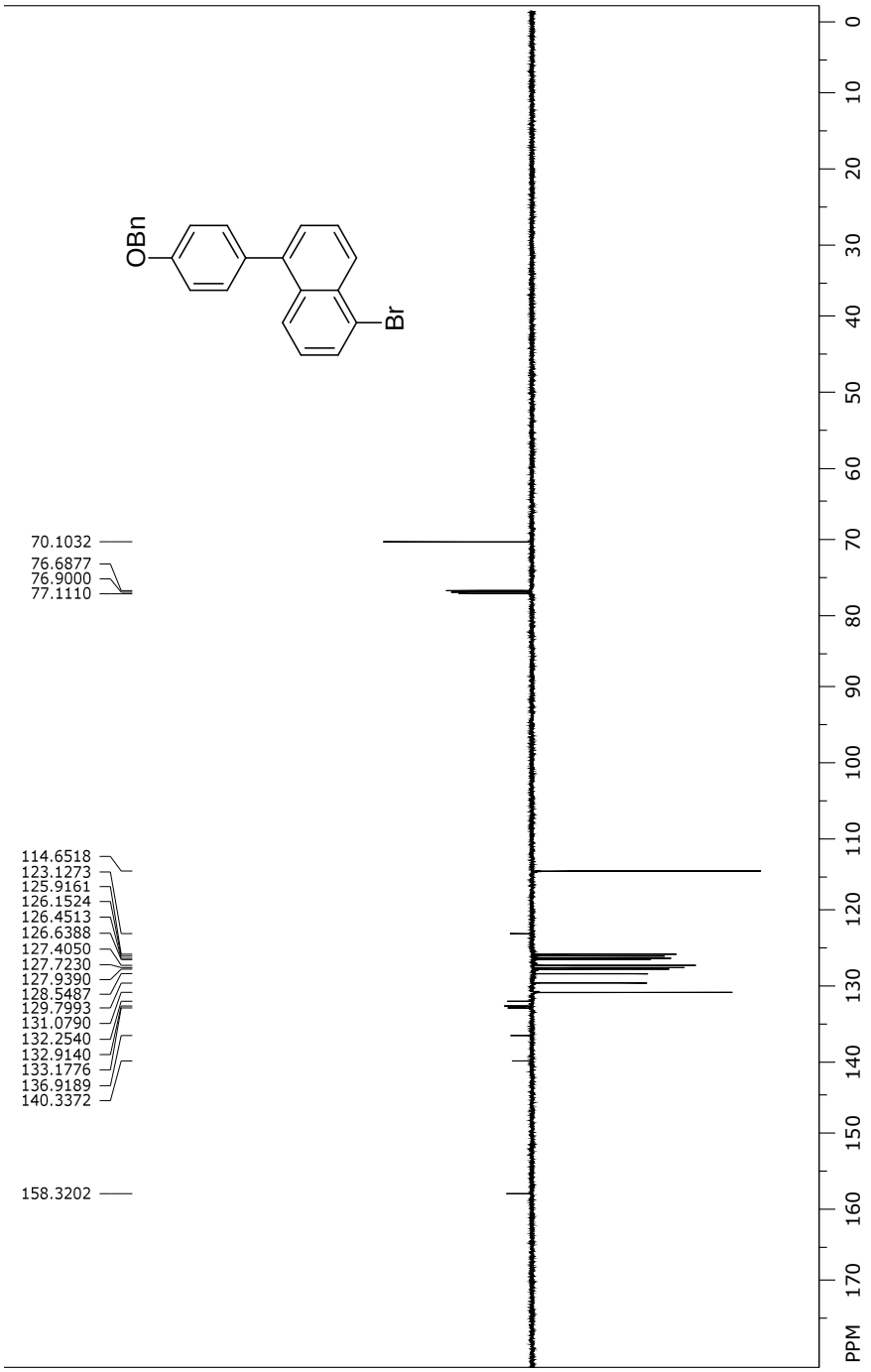

^{1}H NMR (300 MHz, $CDCl_3$) of compound **19**.

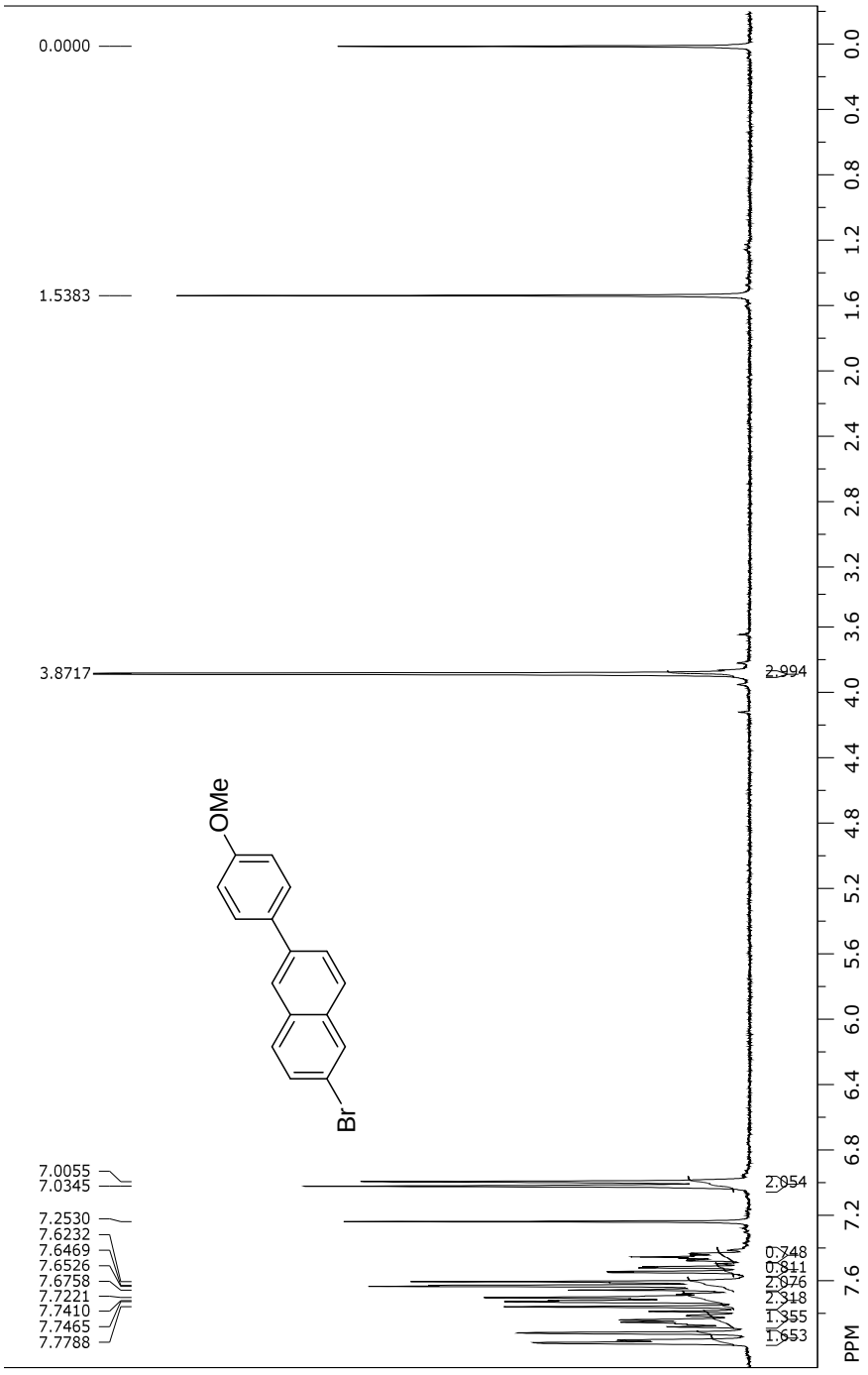

^{13}C NMR (150 MHz, $CDCl_3$) of compound **19**.

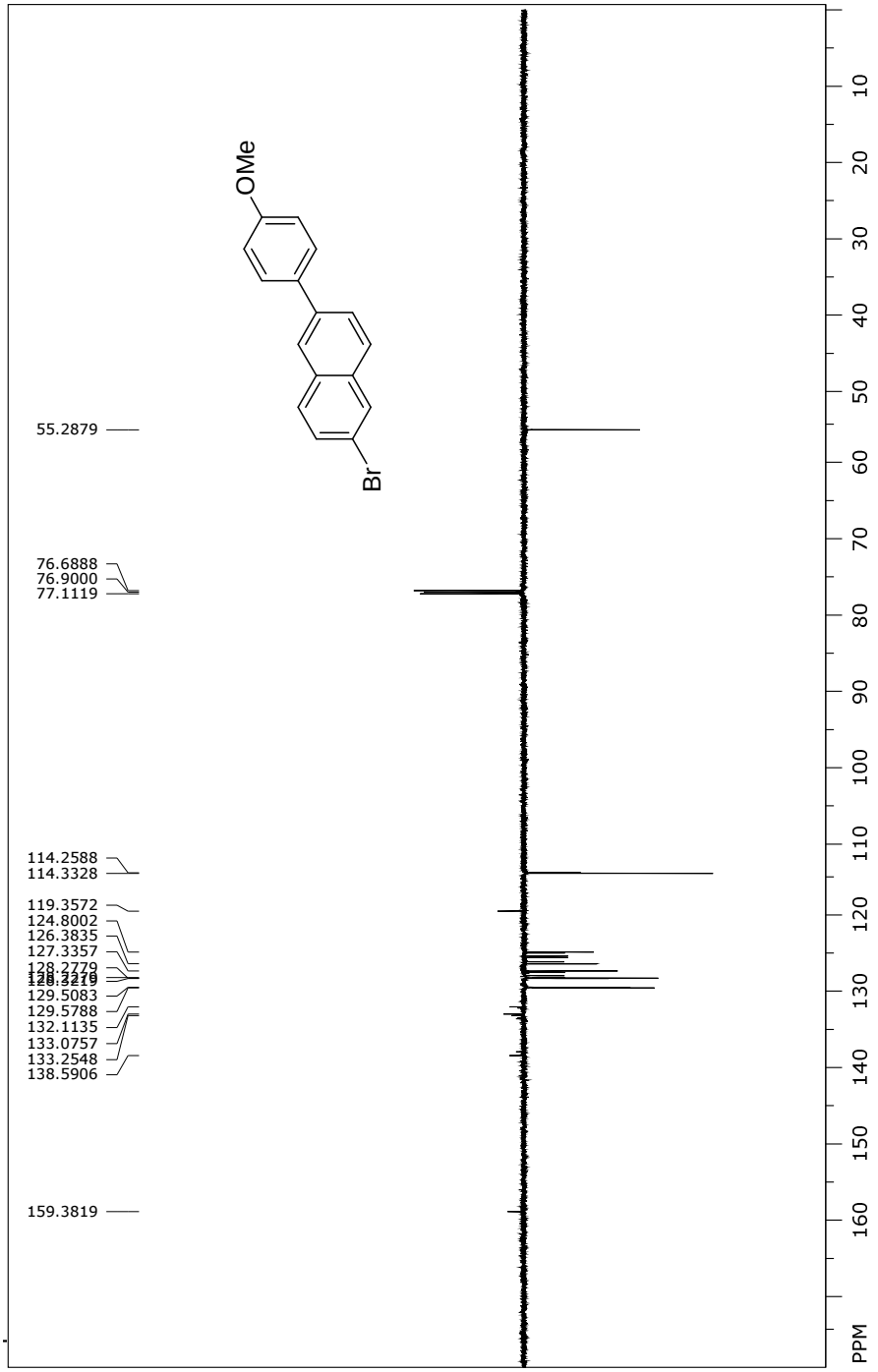

^{1}H NMR (300 MHz, $CDCl_3$) of compound **15**.

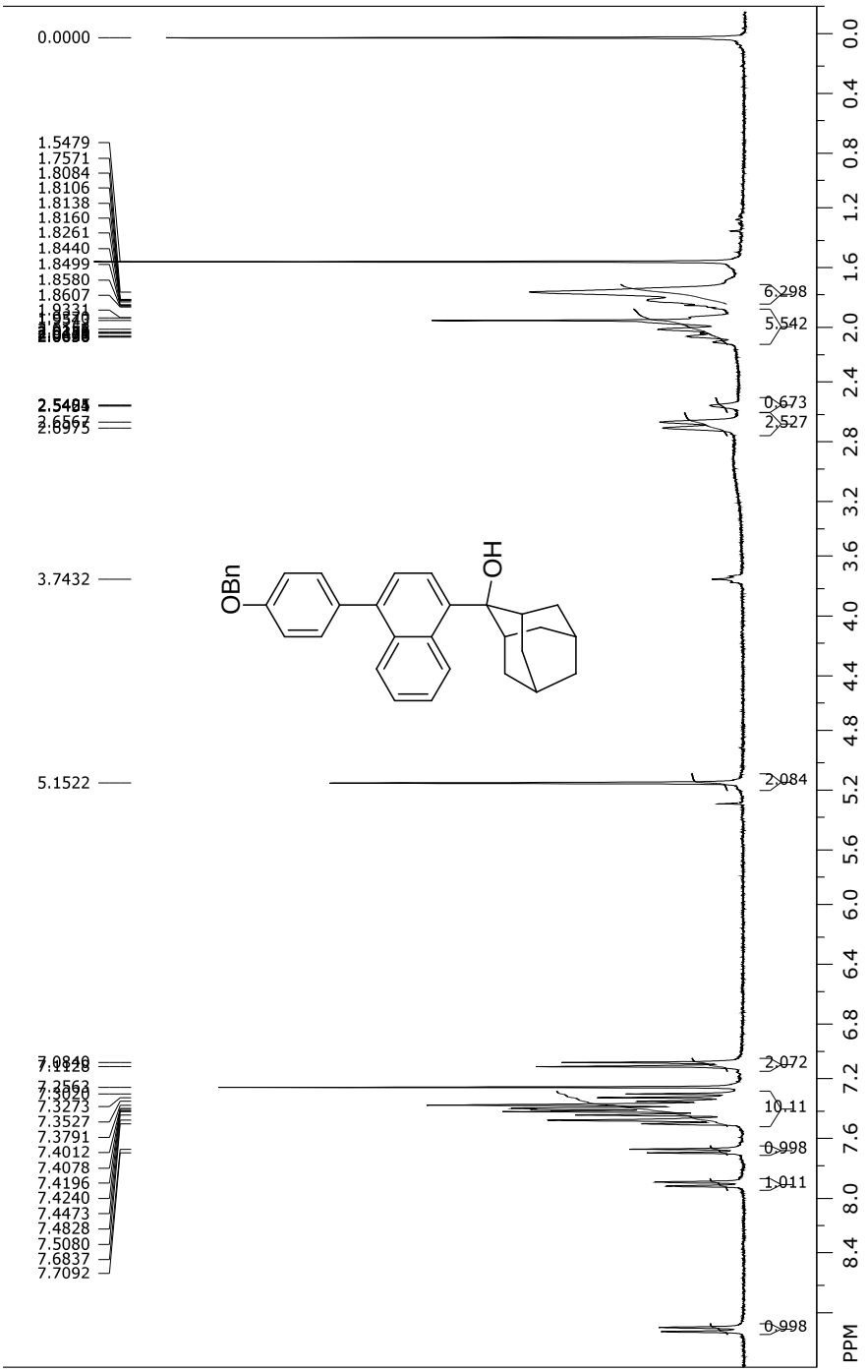

^{13}C NMR (150 MHz, $CDCl_3$) of compound **15**.

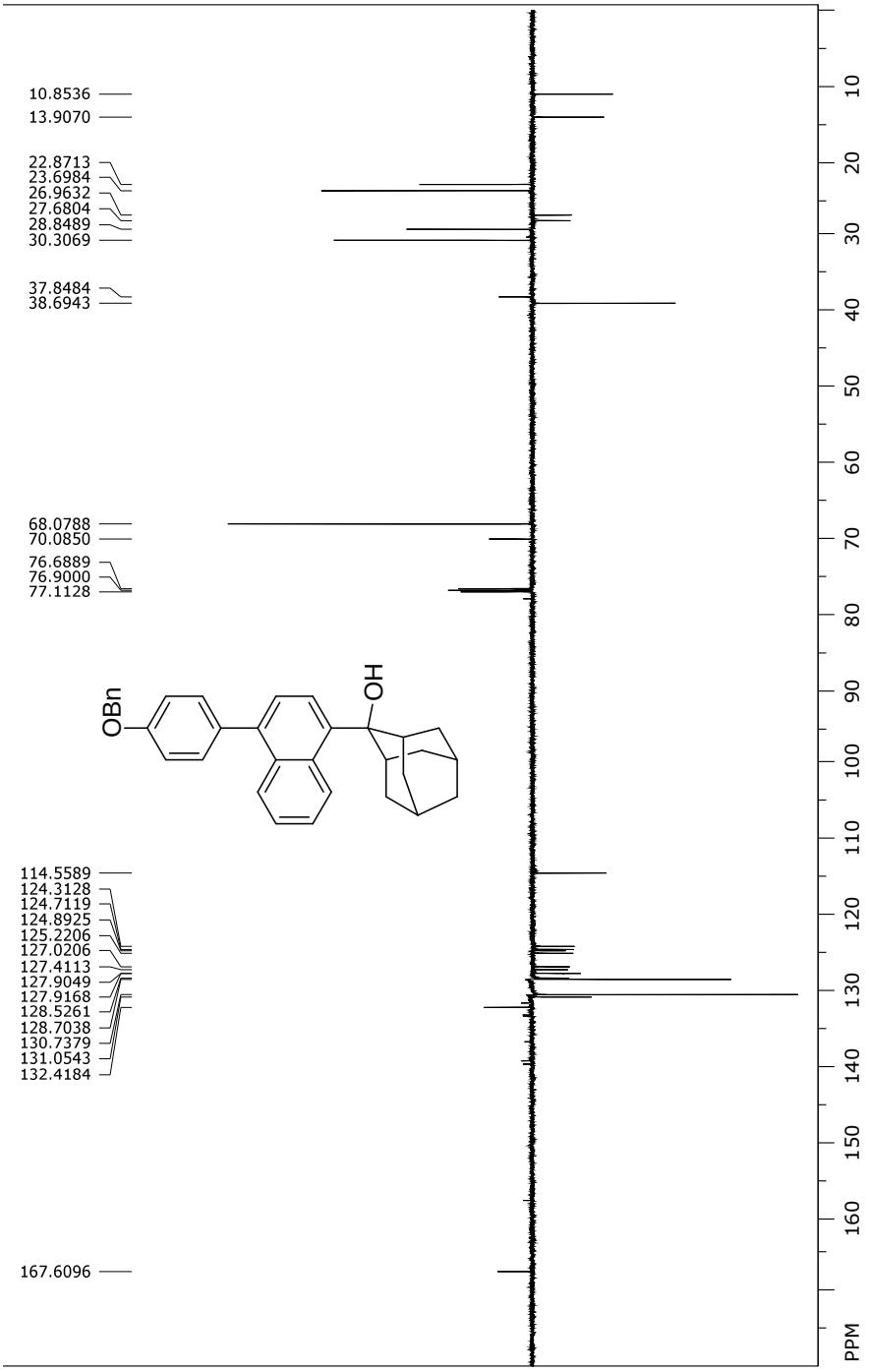

^{1}H NMR (300 MHz, $CDCl_3$) of compound **16**.

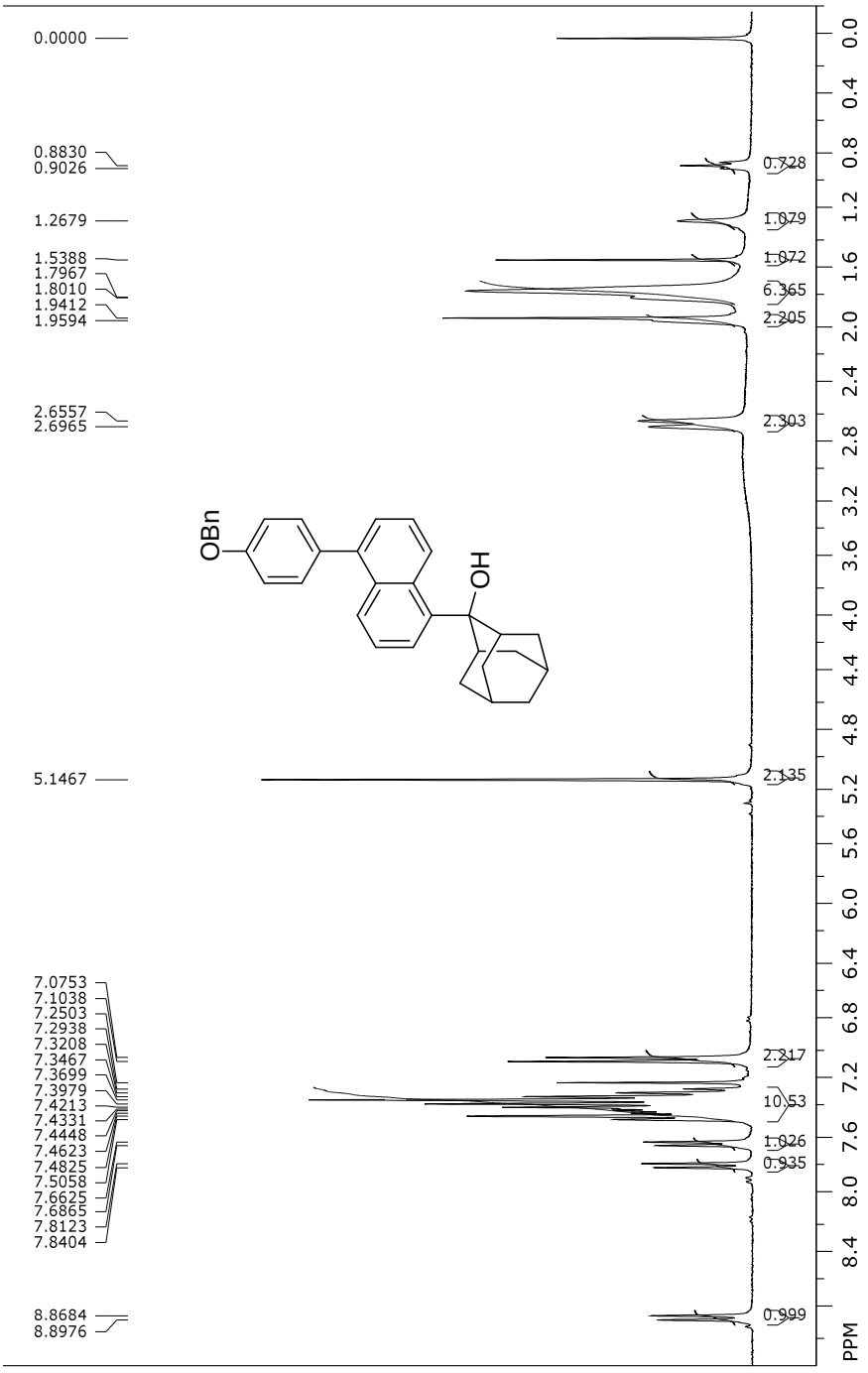

^{13}C NMR (75 MHz, $CDCl_3$) of compound **16**.

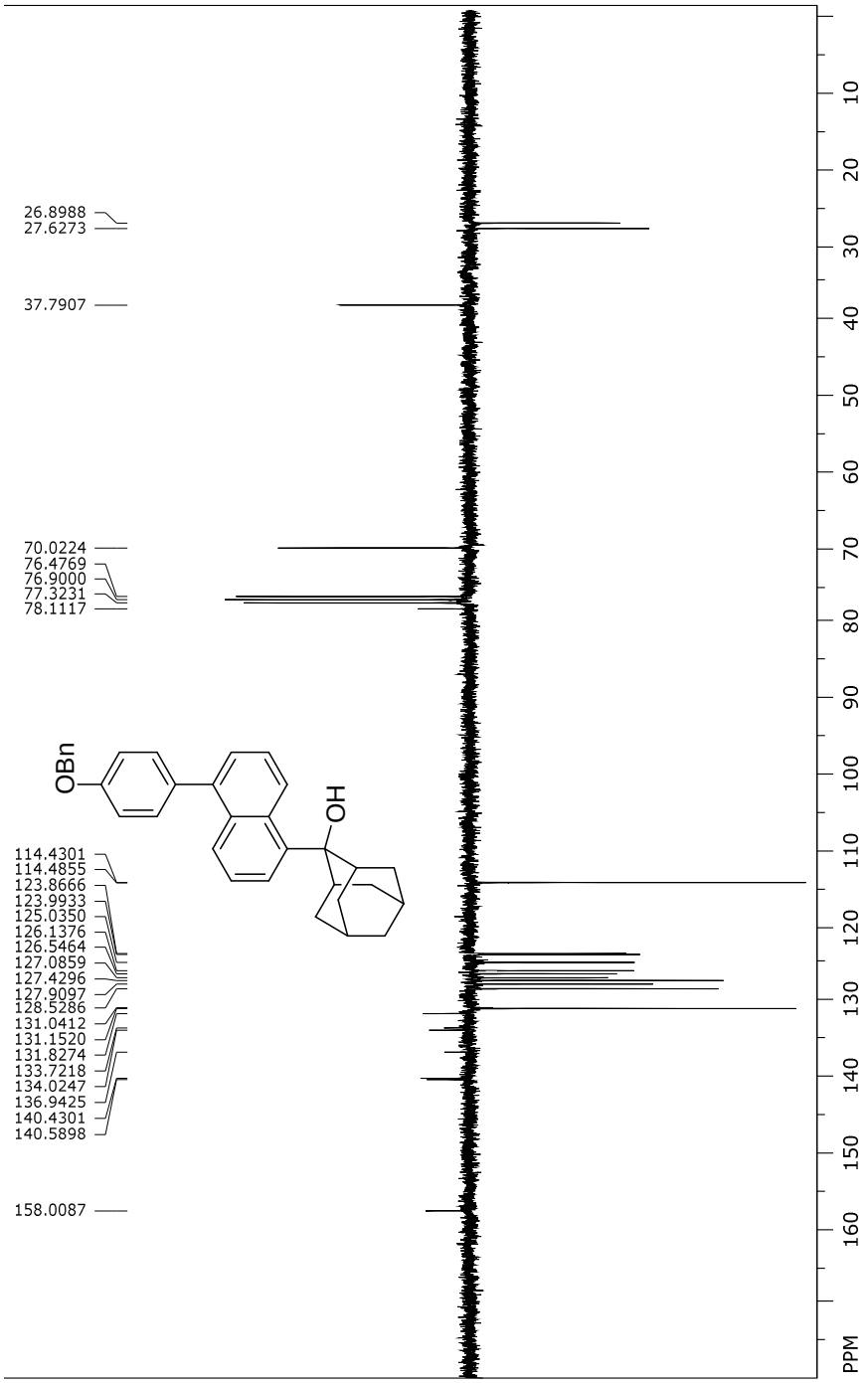

^{1}H NMR (600 MHz, $CDCl_3$) of compound **20**.

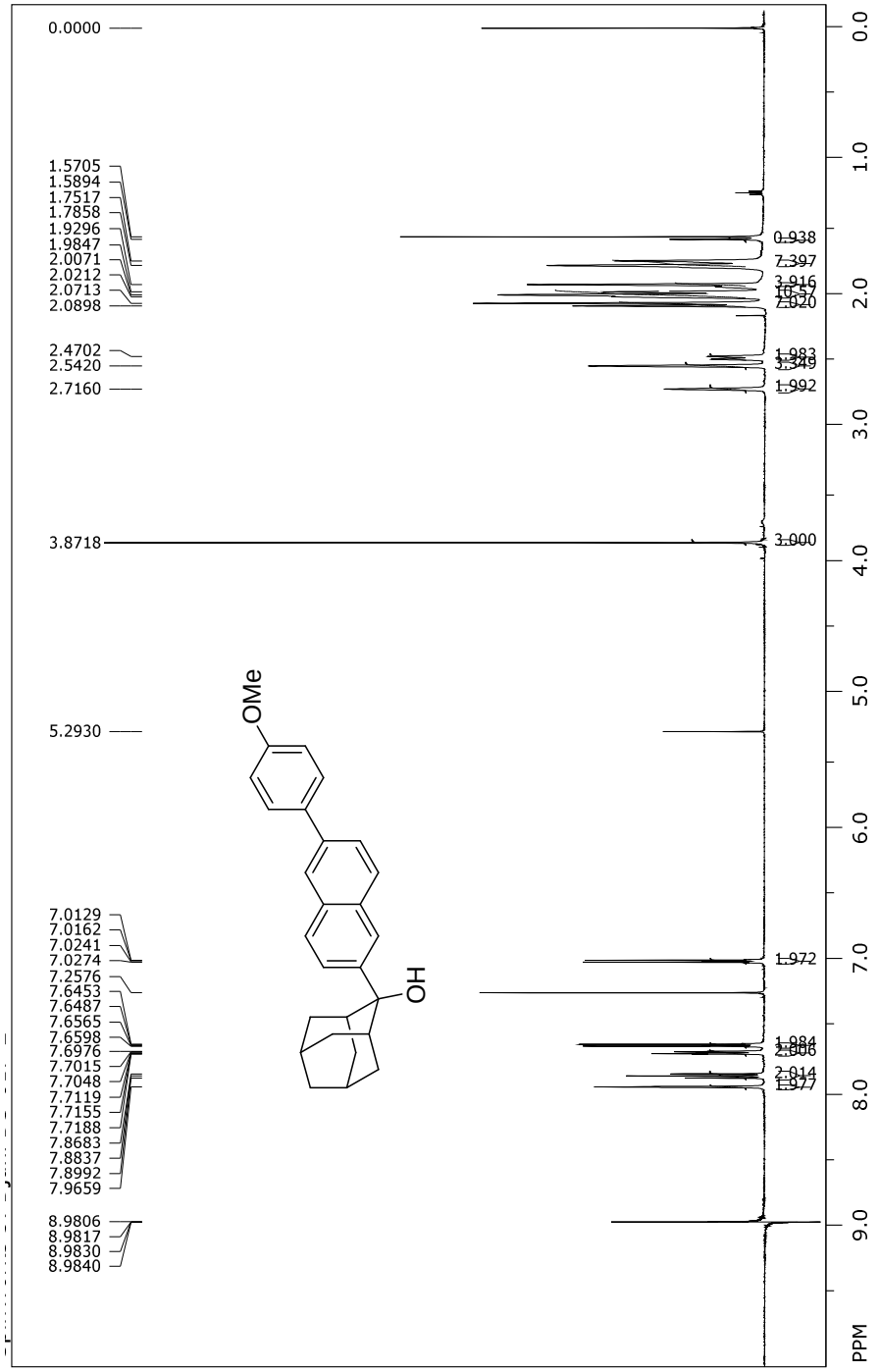

^{13}C NMR (150 MHz, $CDCl_3$) of compound **20**.

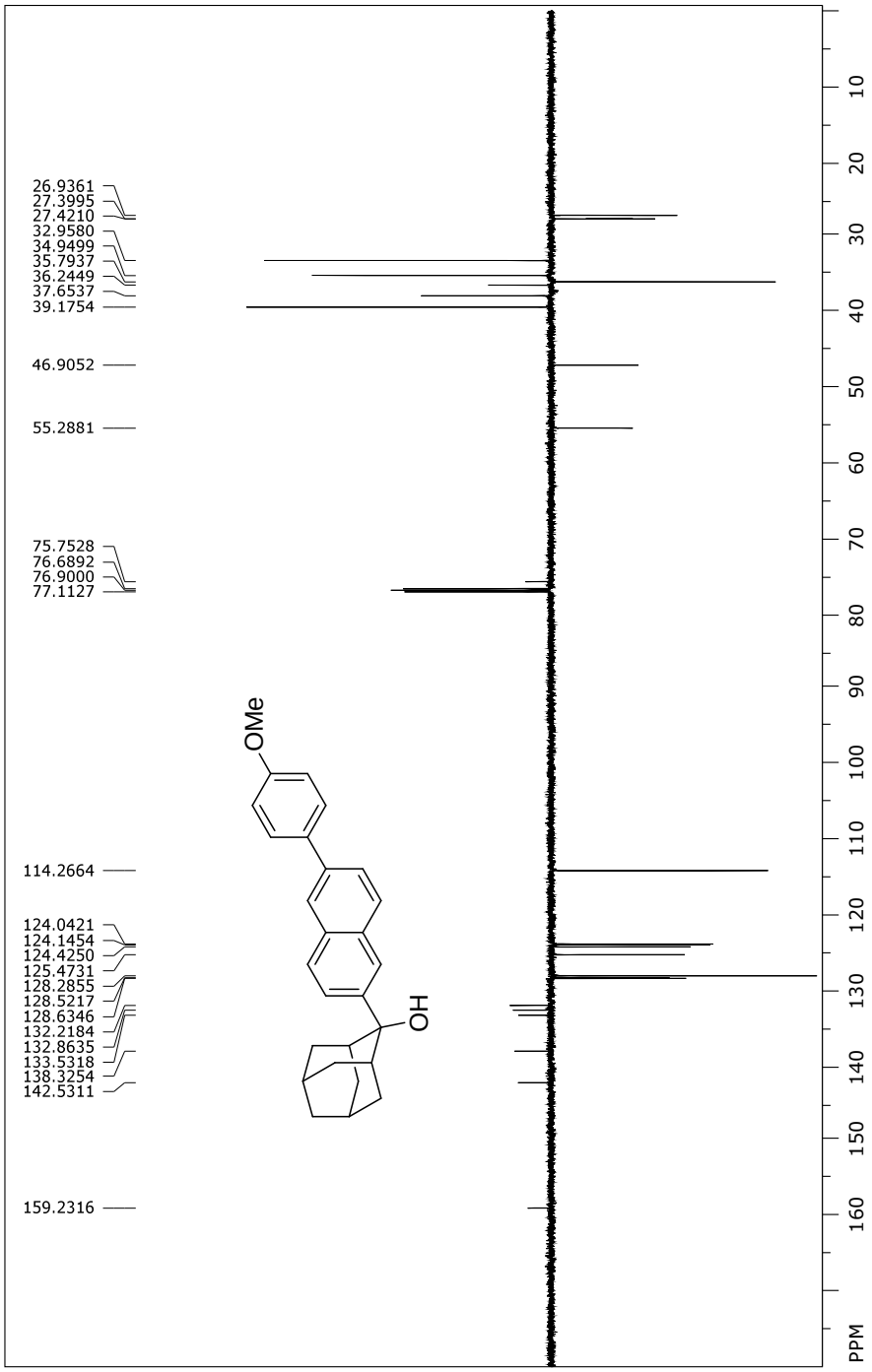

^{1}H NMR (300 MHz, $CDCl_3$) of compound **17**.

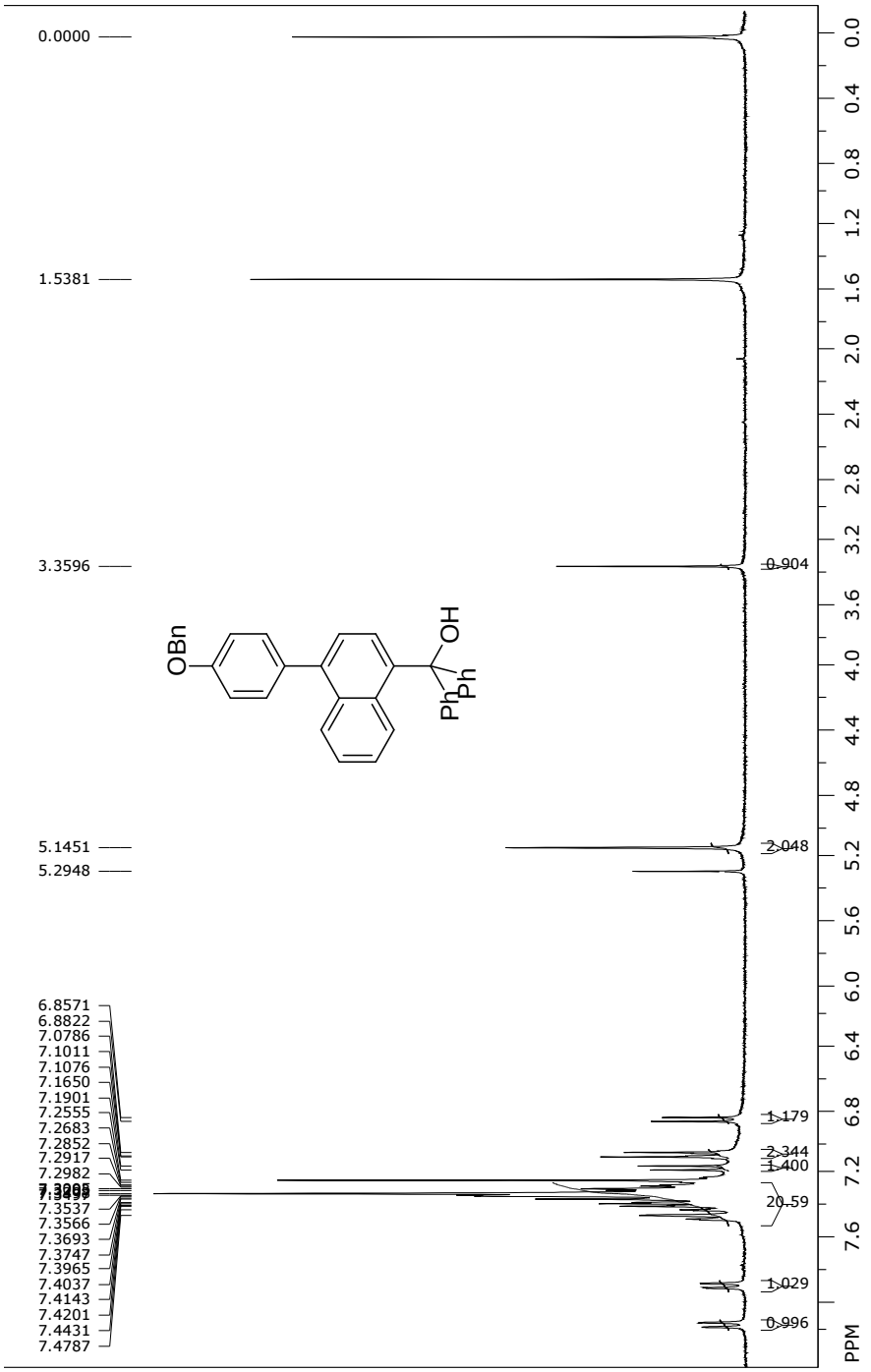

^{13}C NMR (75 MHz, $CDCl_3$) of compound **17**.

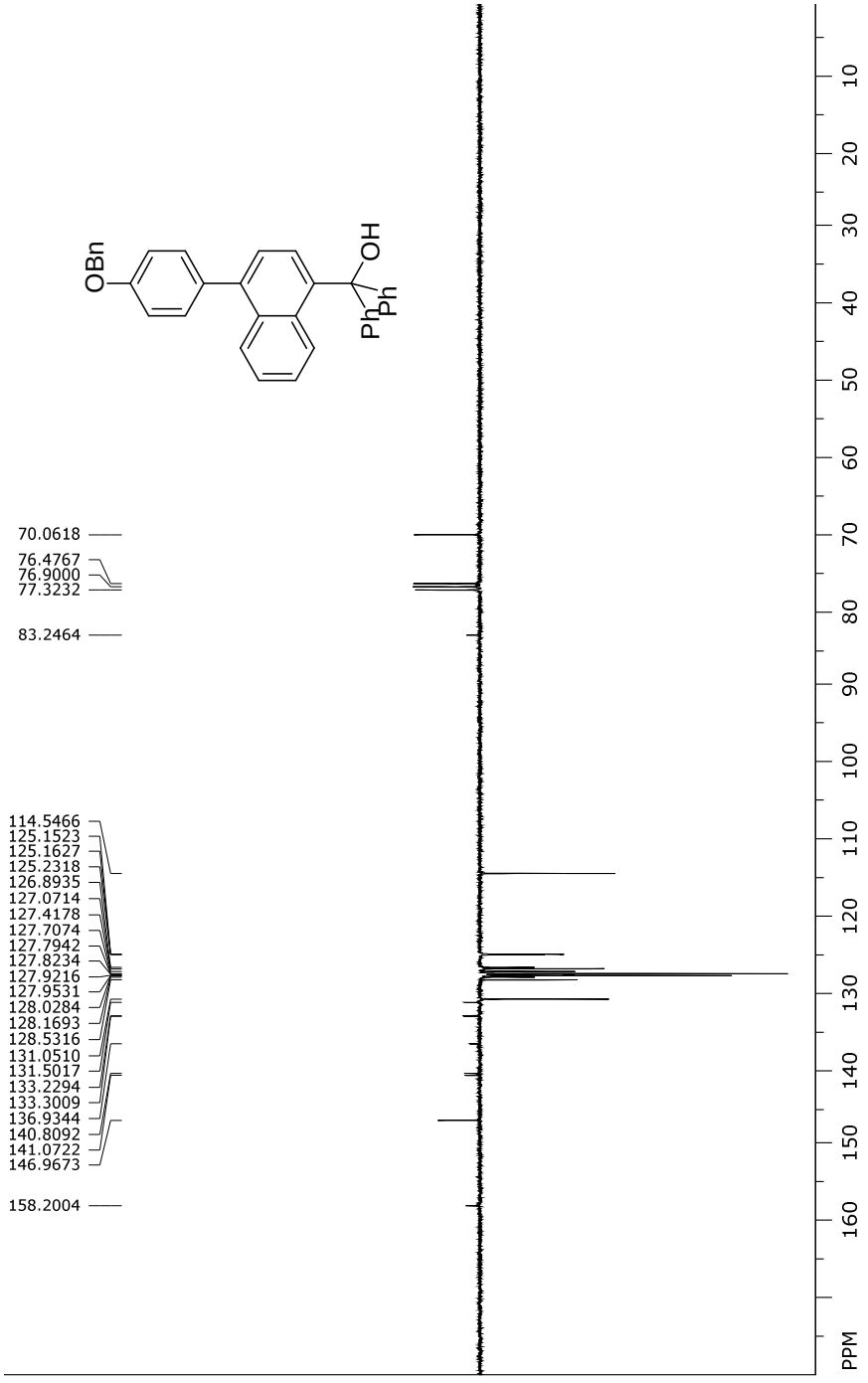

^{1}H NMR (300 MHz, $CDCl_3$) of compound **18**.

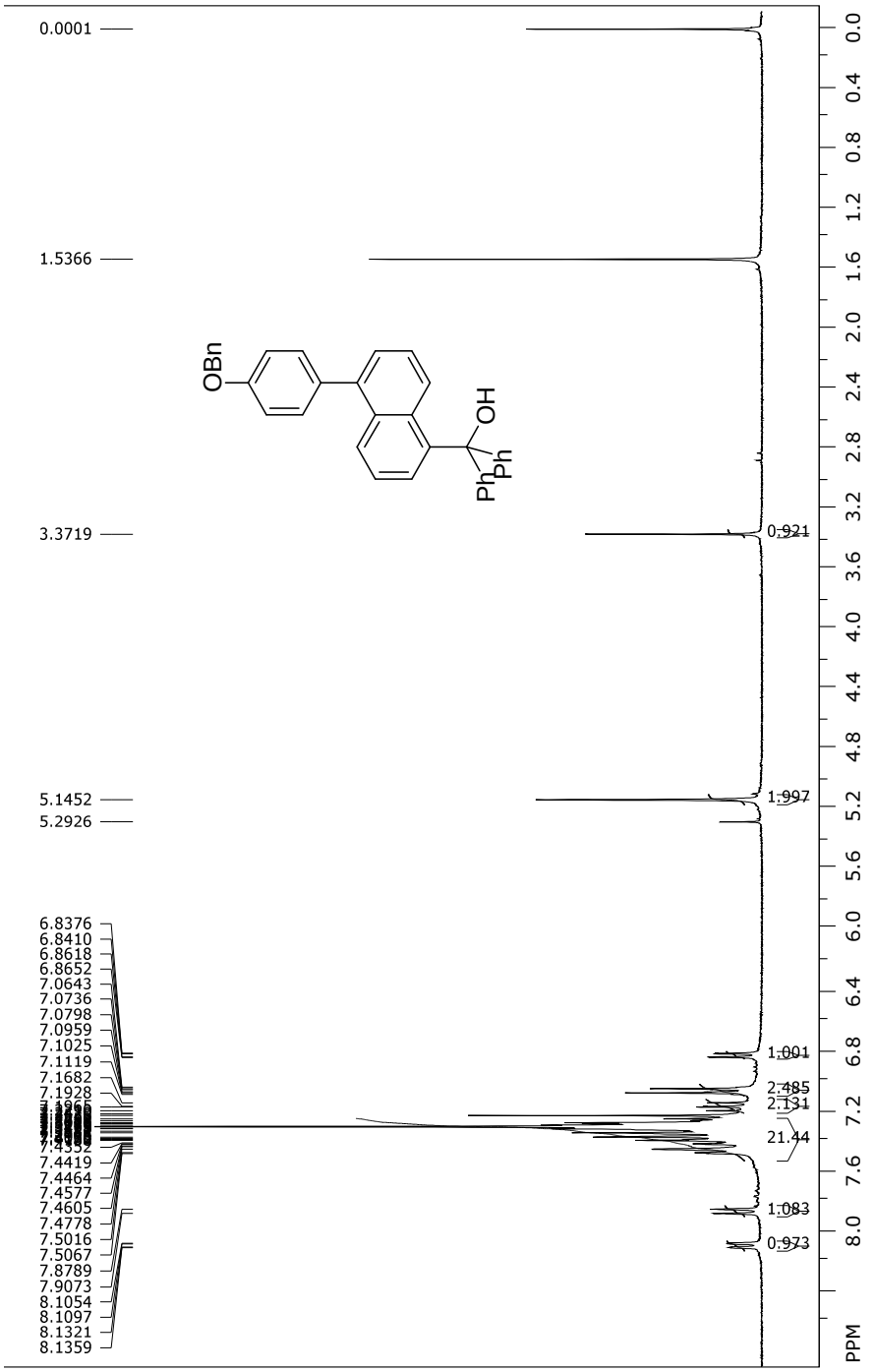

^{13}C NMR (75 MHz, $CDCl_3$) of compound **18**.

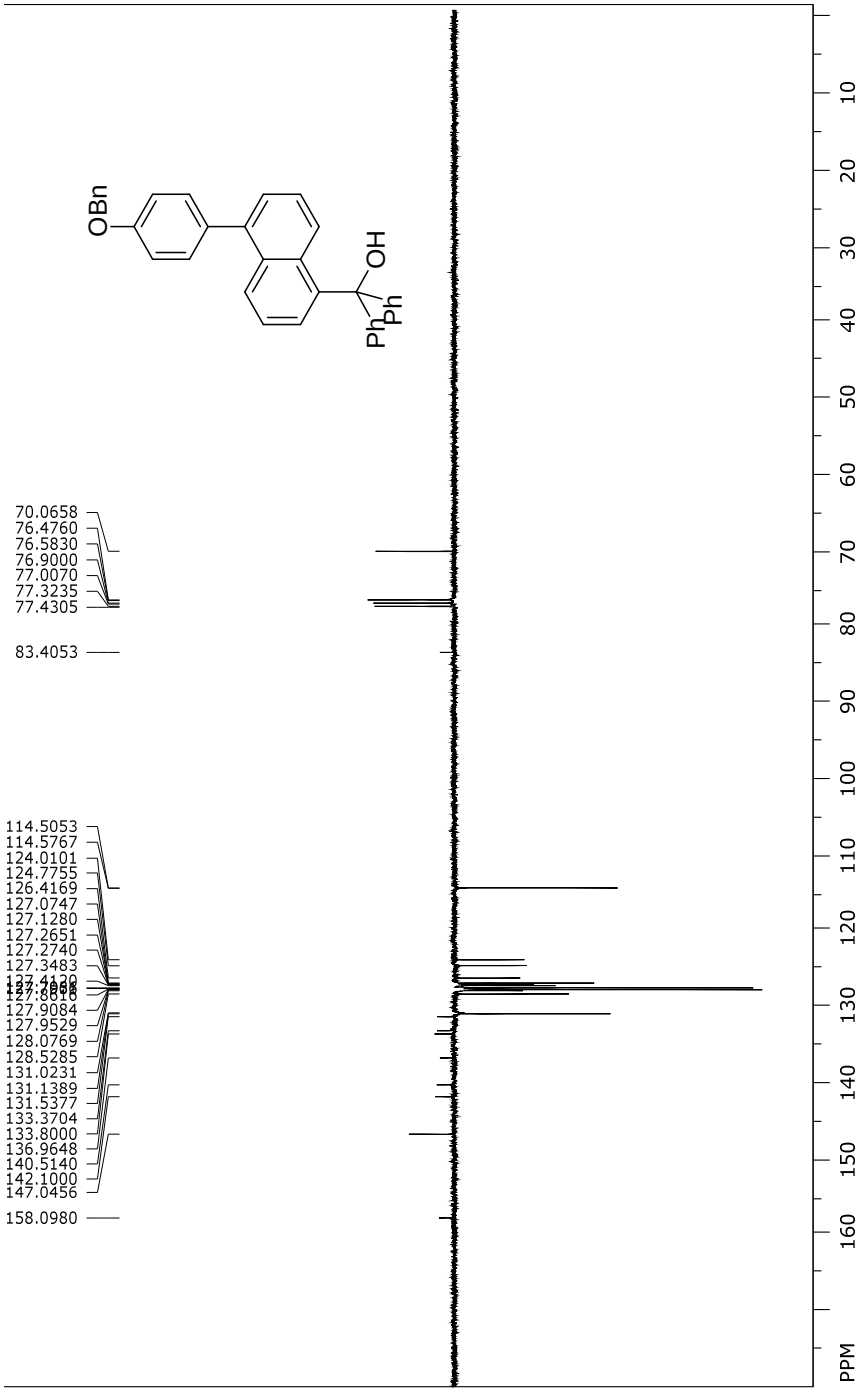

^{1}H NMR (300 MHz, $CDCl_3$) of compound **21**.

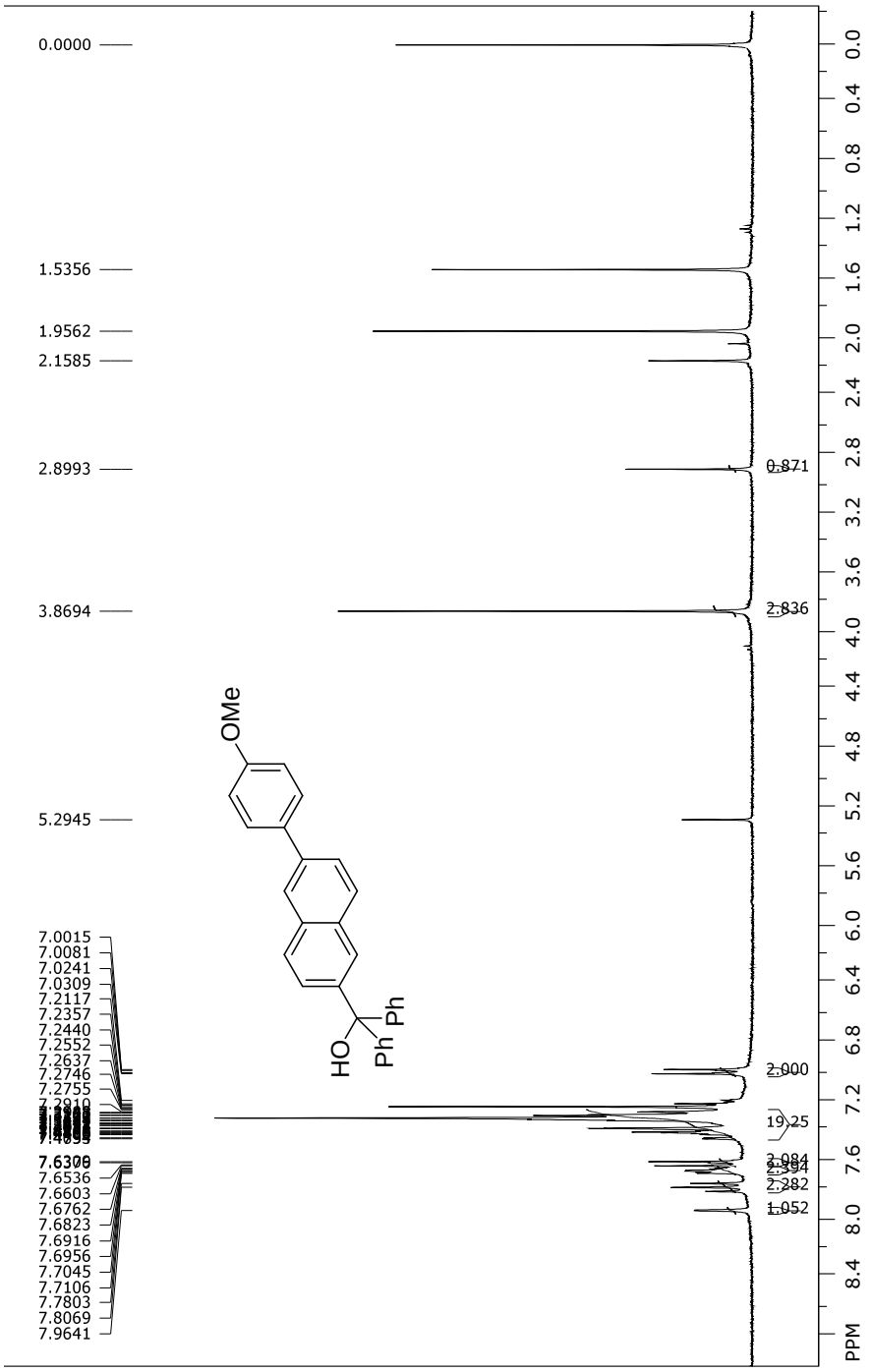

^{13}C NMR (75 MHz, $CDCl_3$) of compound **21**.

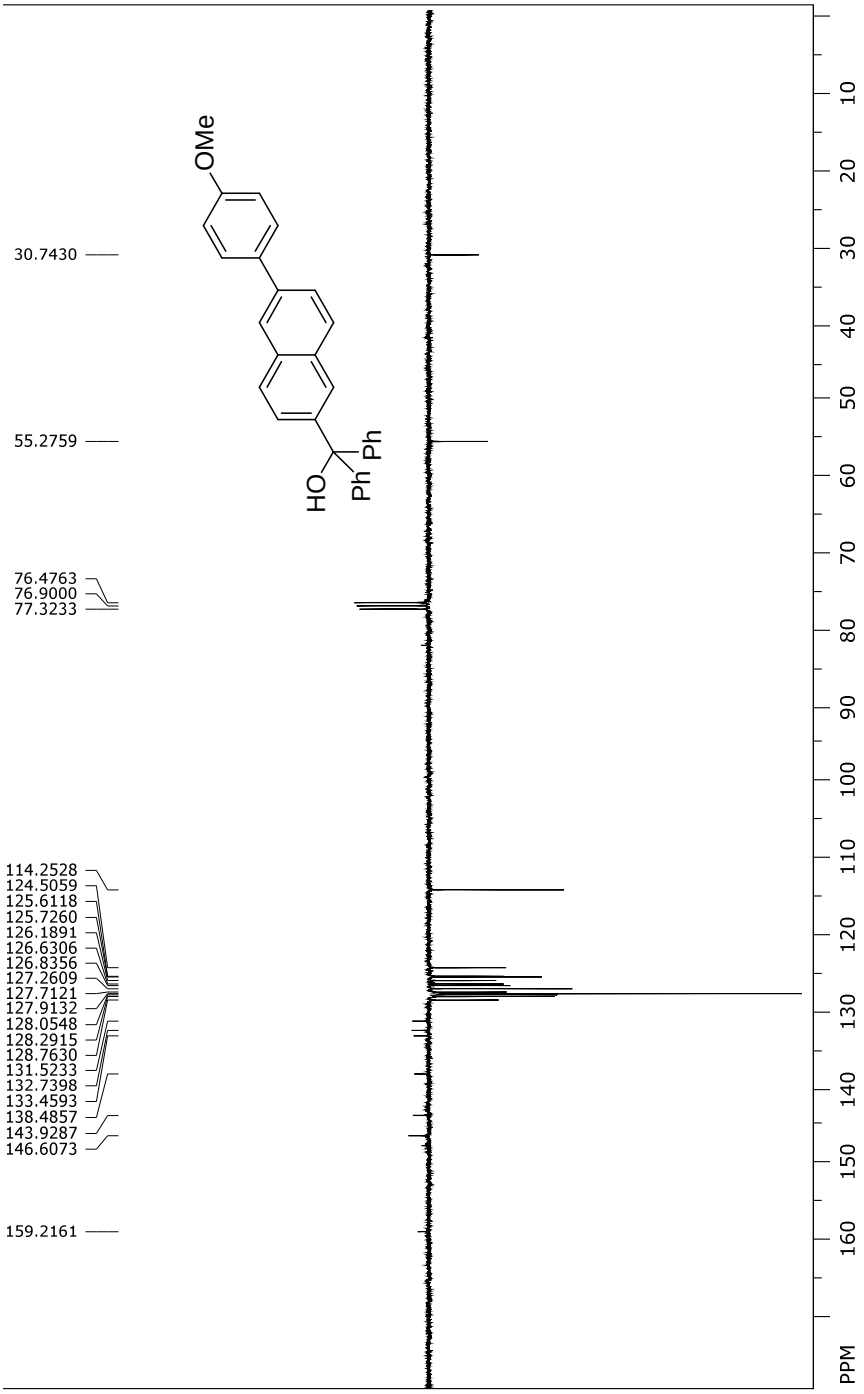

^{1}H NMR (300 MHz, $CDCl_3$) of compound **7**.

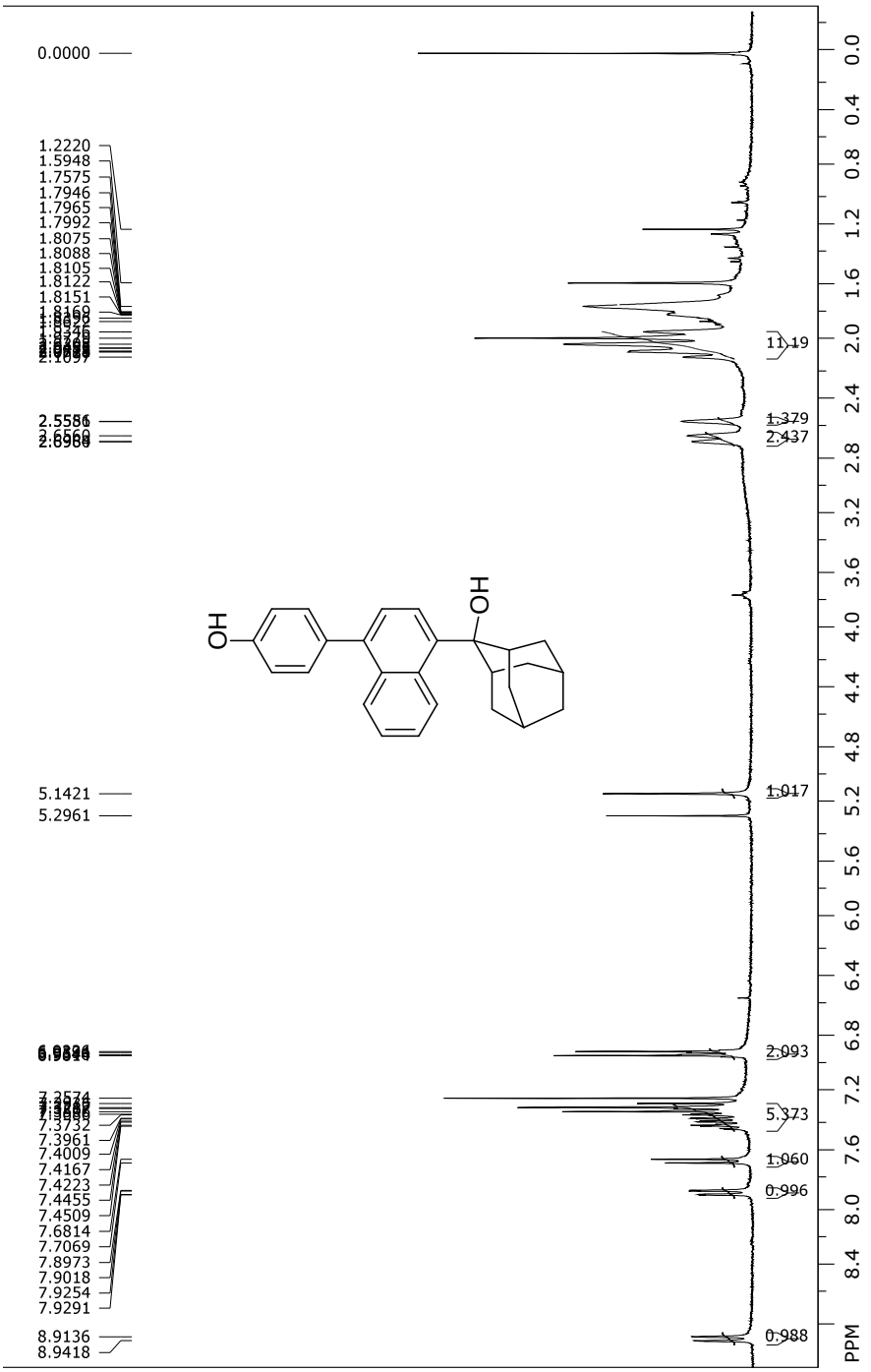

^{13}C NMR (75 MHz, DMSO-d_6) of compound **7**.

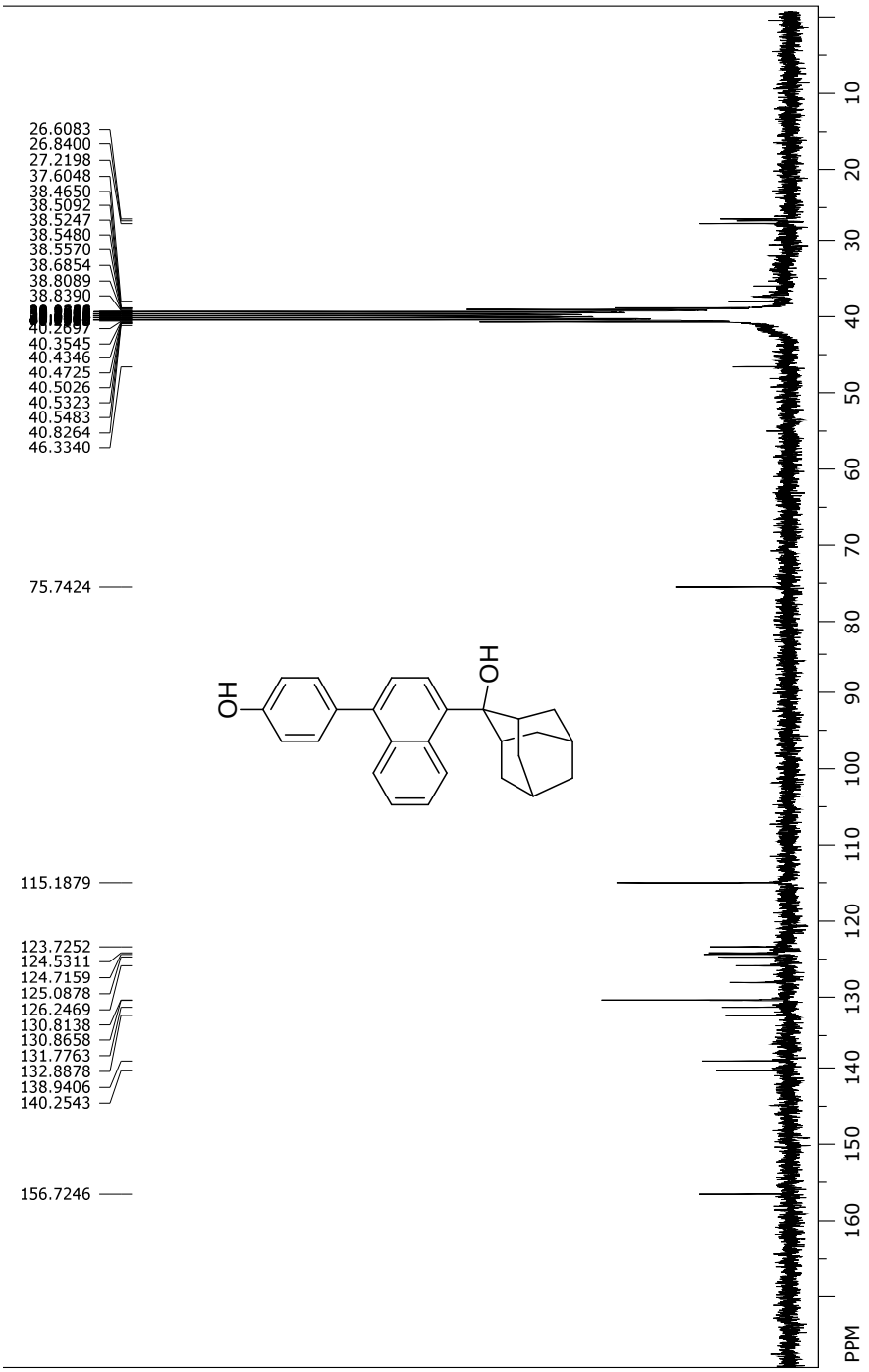

^{1}H NMR (600 MHz, $CDCl_3$) of compound **8**.

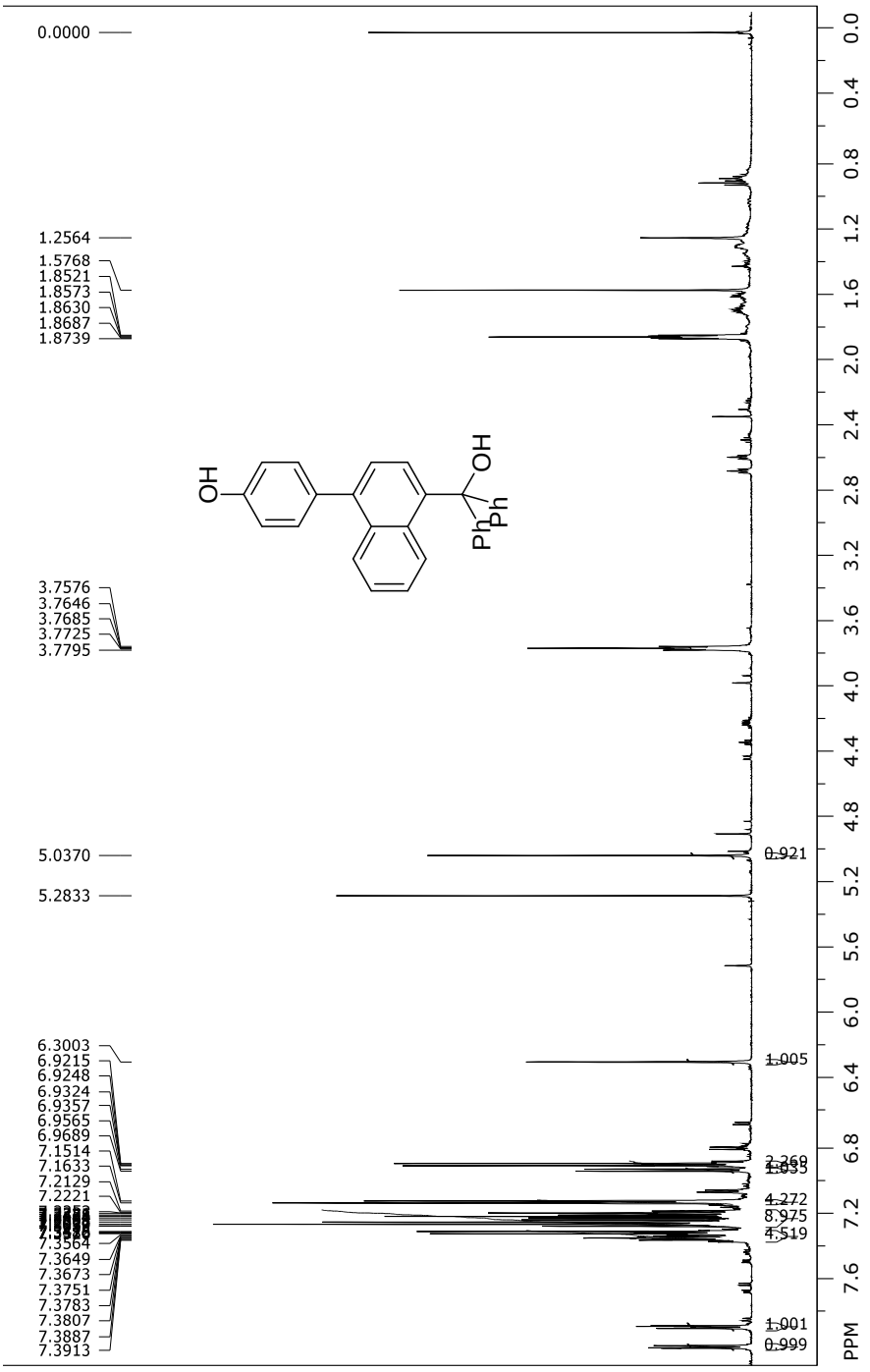

^{13}C NMR (150 MHz, $CDCl_3$) of compound **8**.

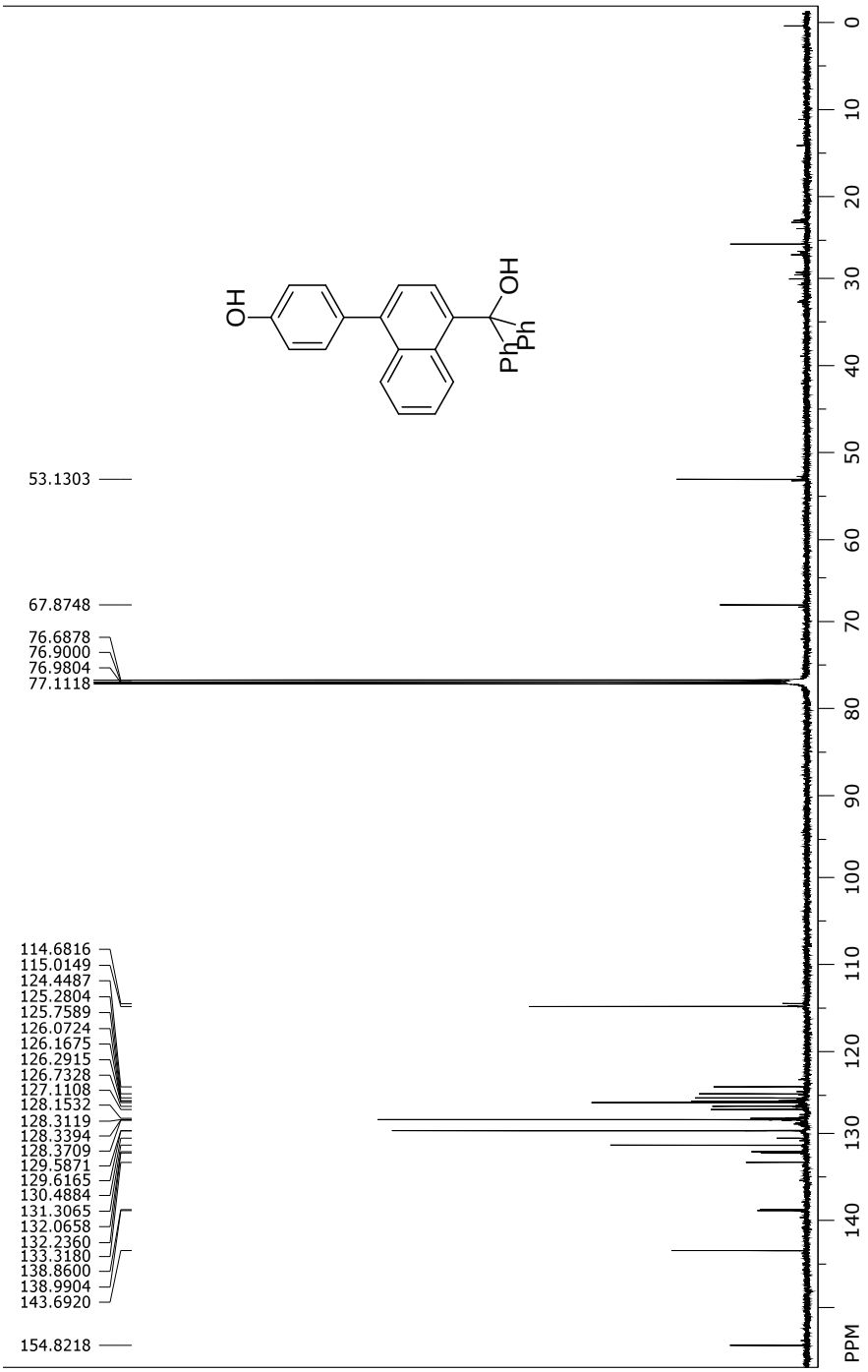

^{1}H NMR (300 MHz, $CDCl_3$) of compound **9**.

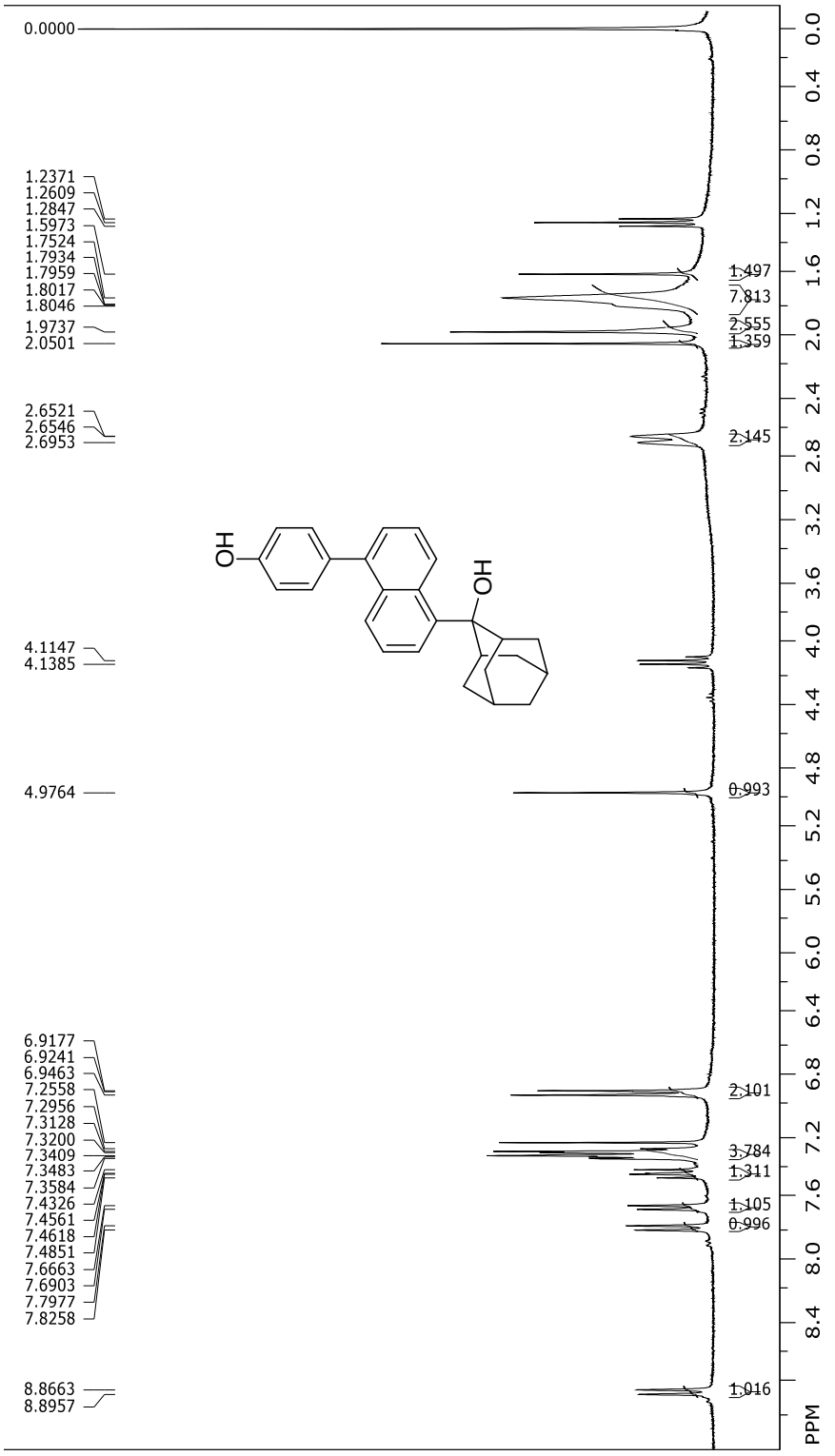

^{13}C NMR (75 MHz, $CDCl_3$) of compound **9**.

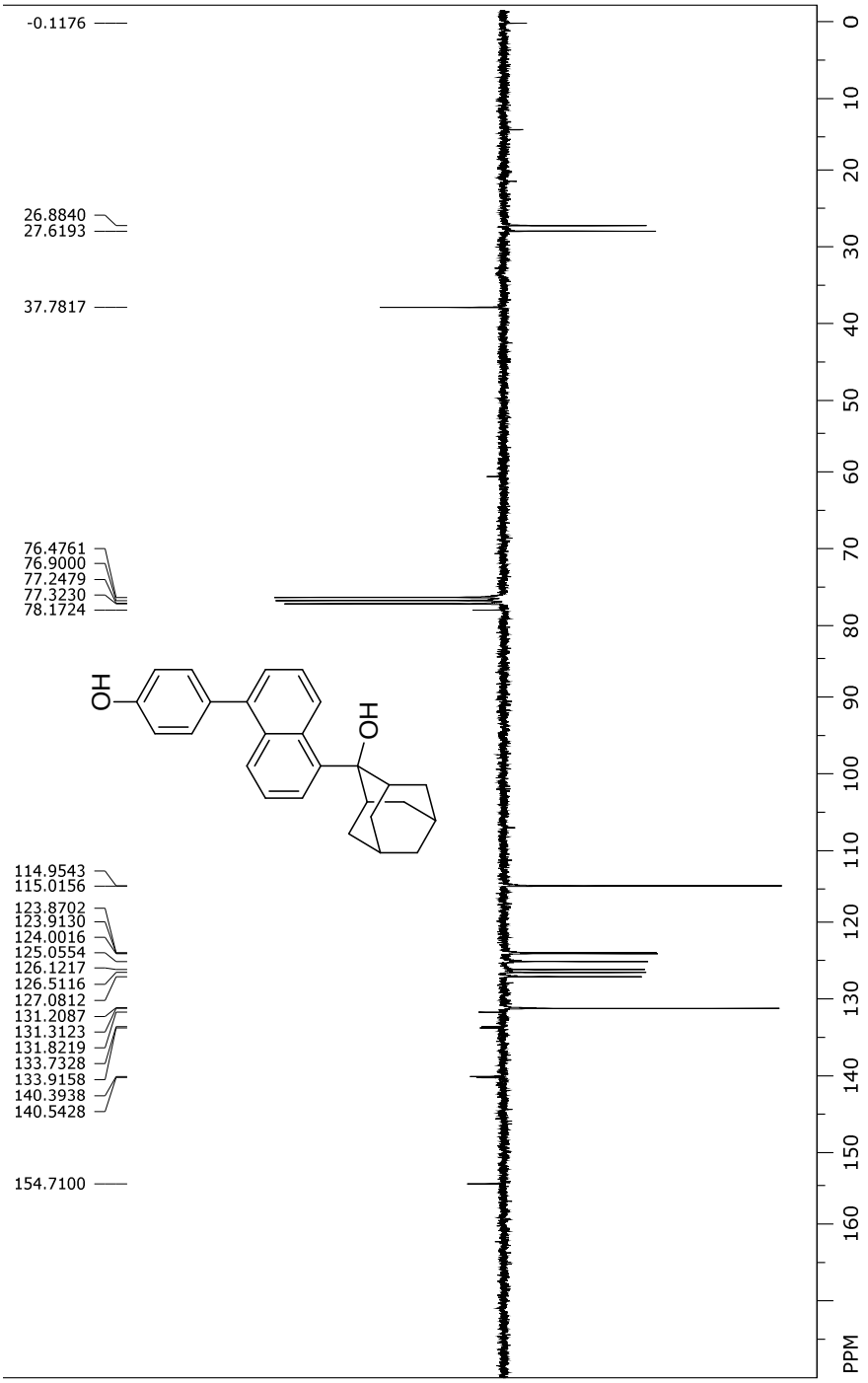

^{1}H NMR (300 MHz, $CDCl_3$) of compound **10**.

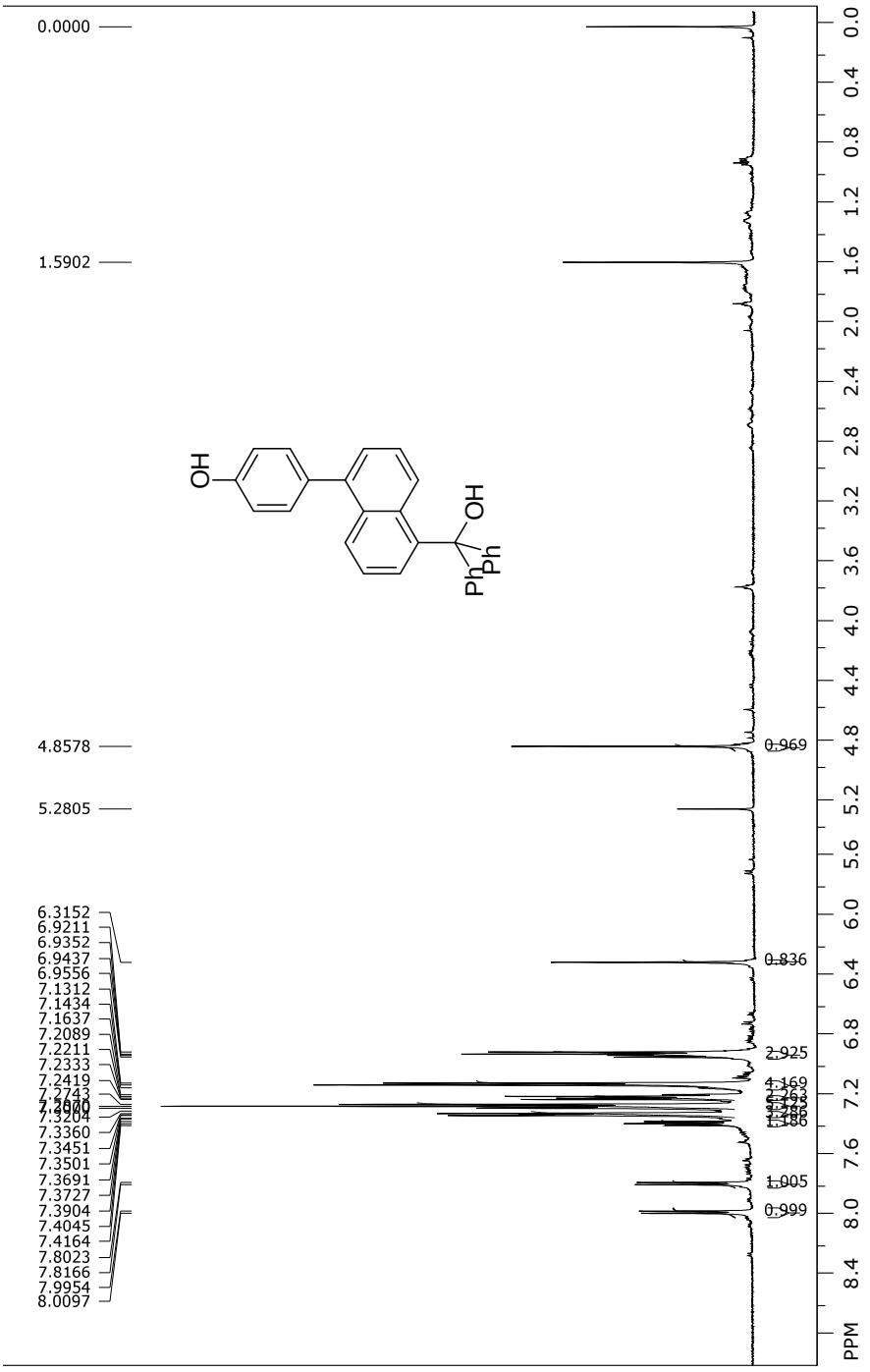

^{13}C NMR (150 MHz, $CDCl_3$) of compound **10**.

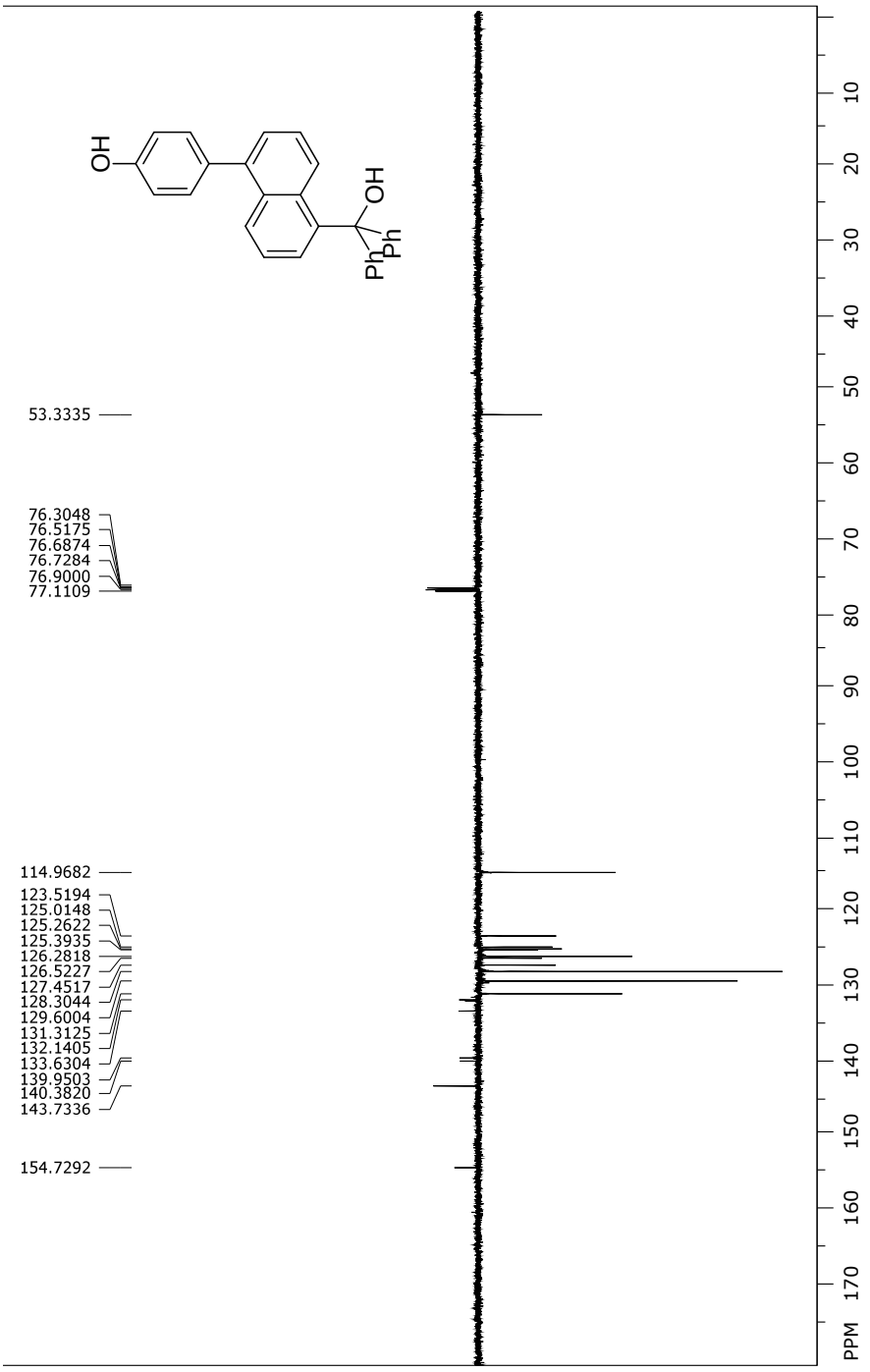

^{1}H NMR (600 MHz, $CDCl_3$) of compound **11**.

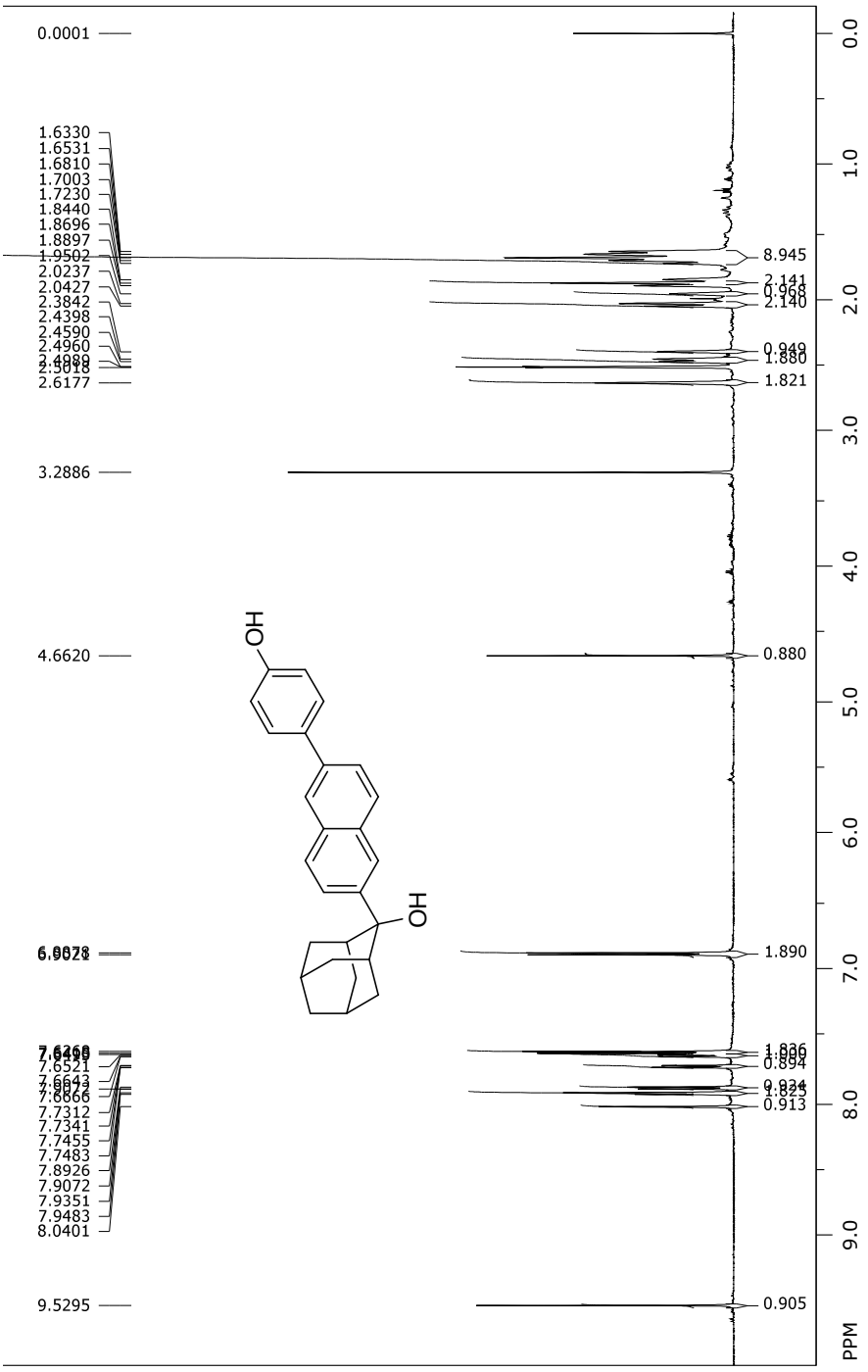

^{13}C NMR (150 MHz, $CDCl_3$) of compound **11**.

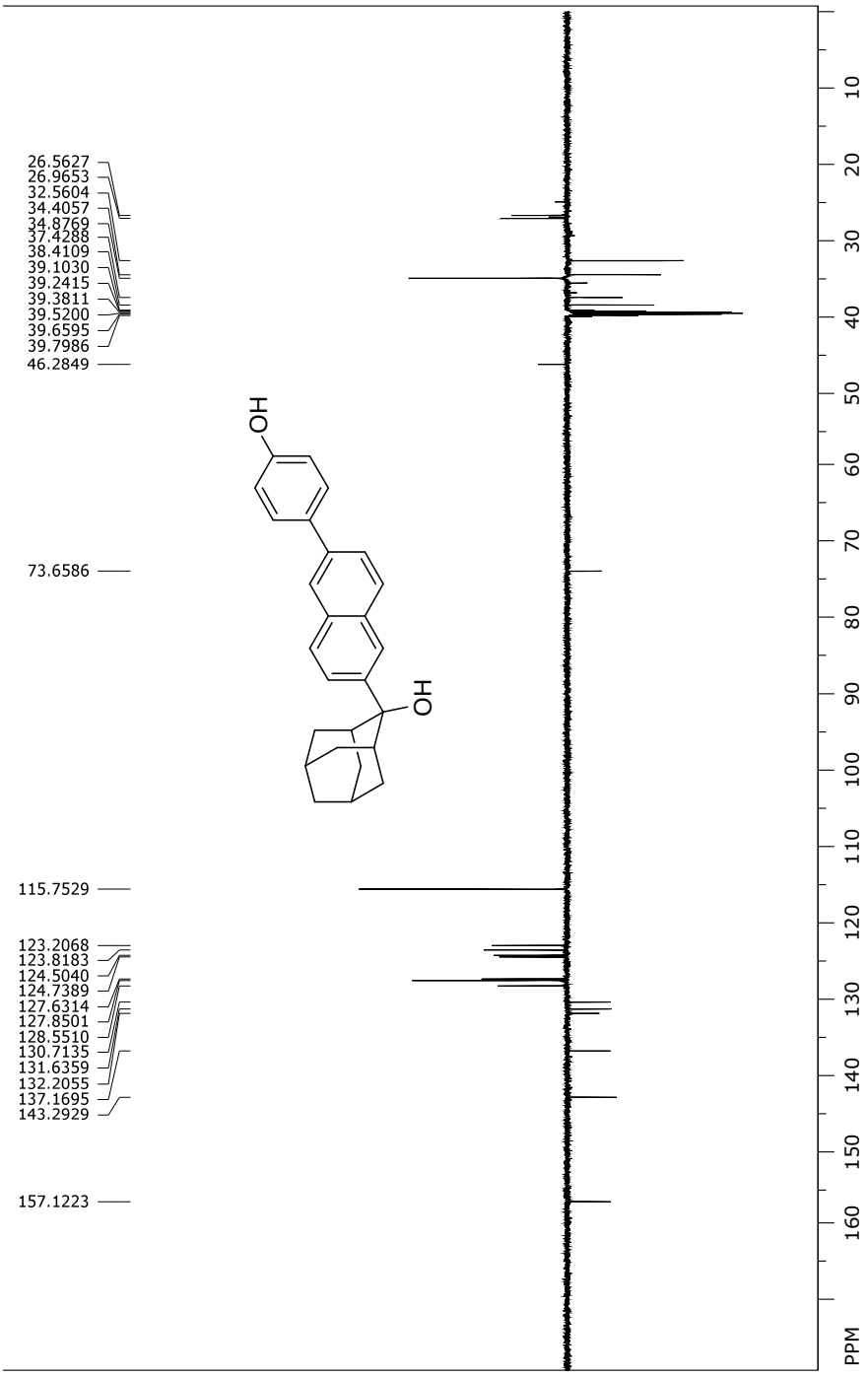

^{1}H NMR (600 MHz, $CDCl_3$) of compound **12**.

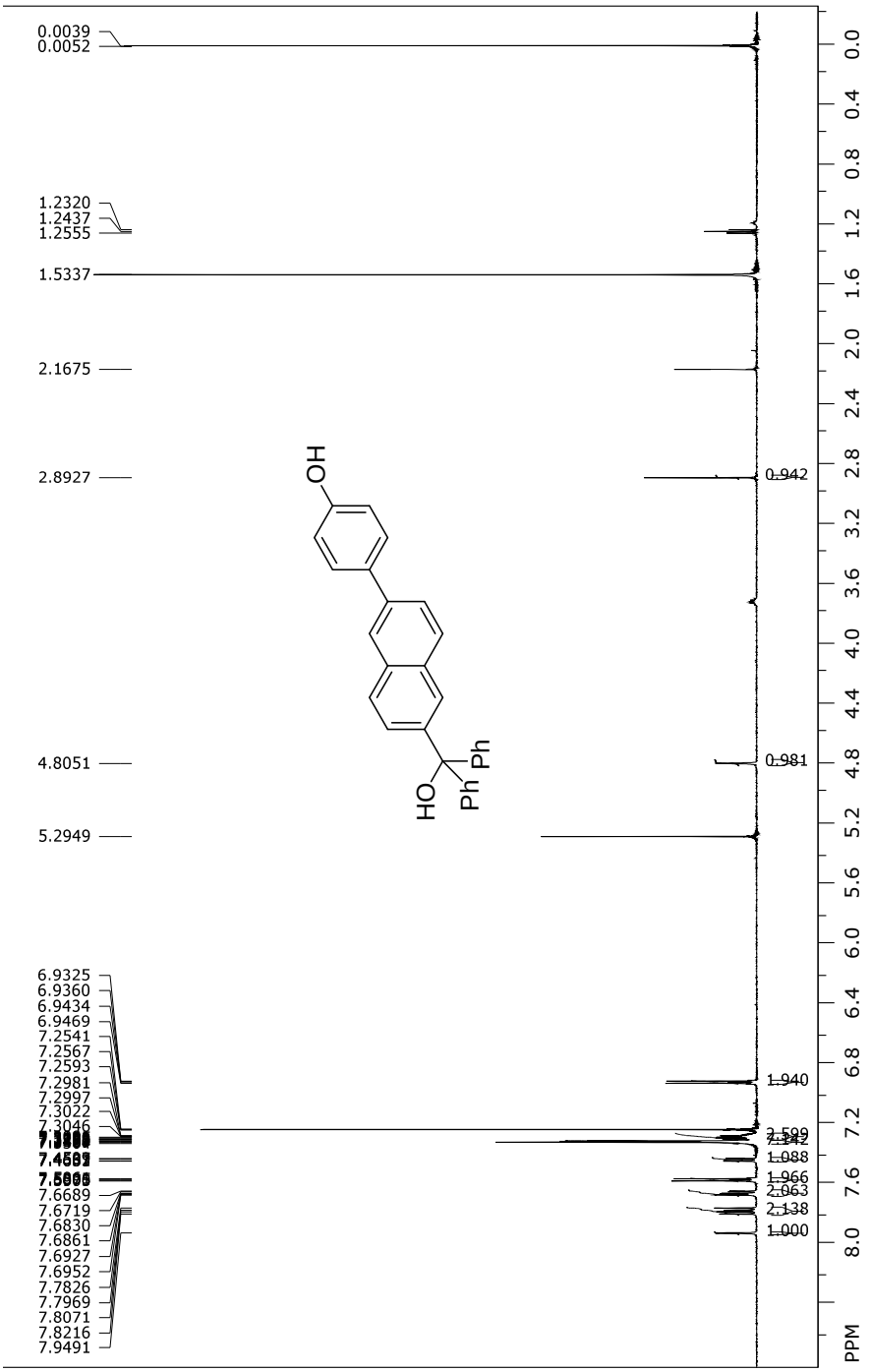

^{13}C NMR (150 MHz, $CDCl_3$) of compound **12**.

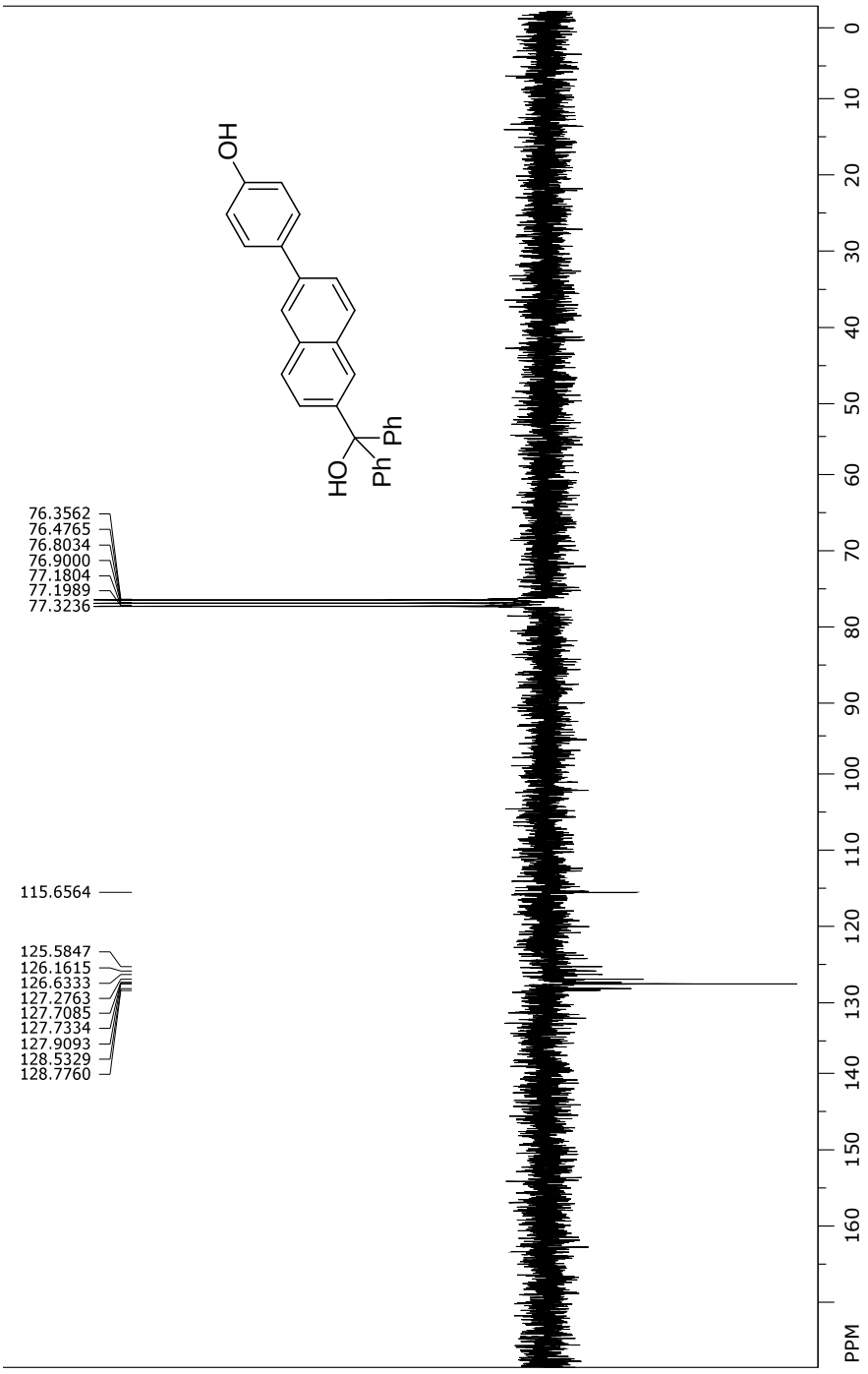

^{1}H NMR (300 MHz, $CDCl_3$) of compound **22**.

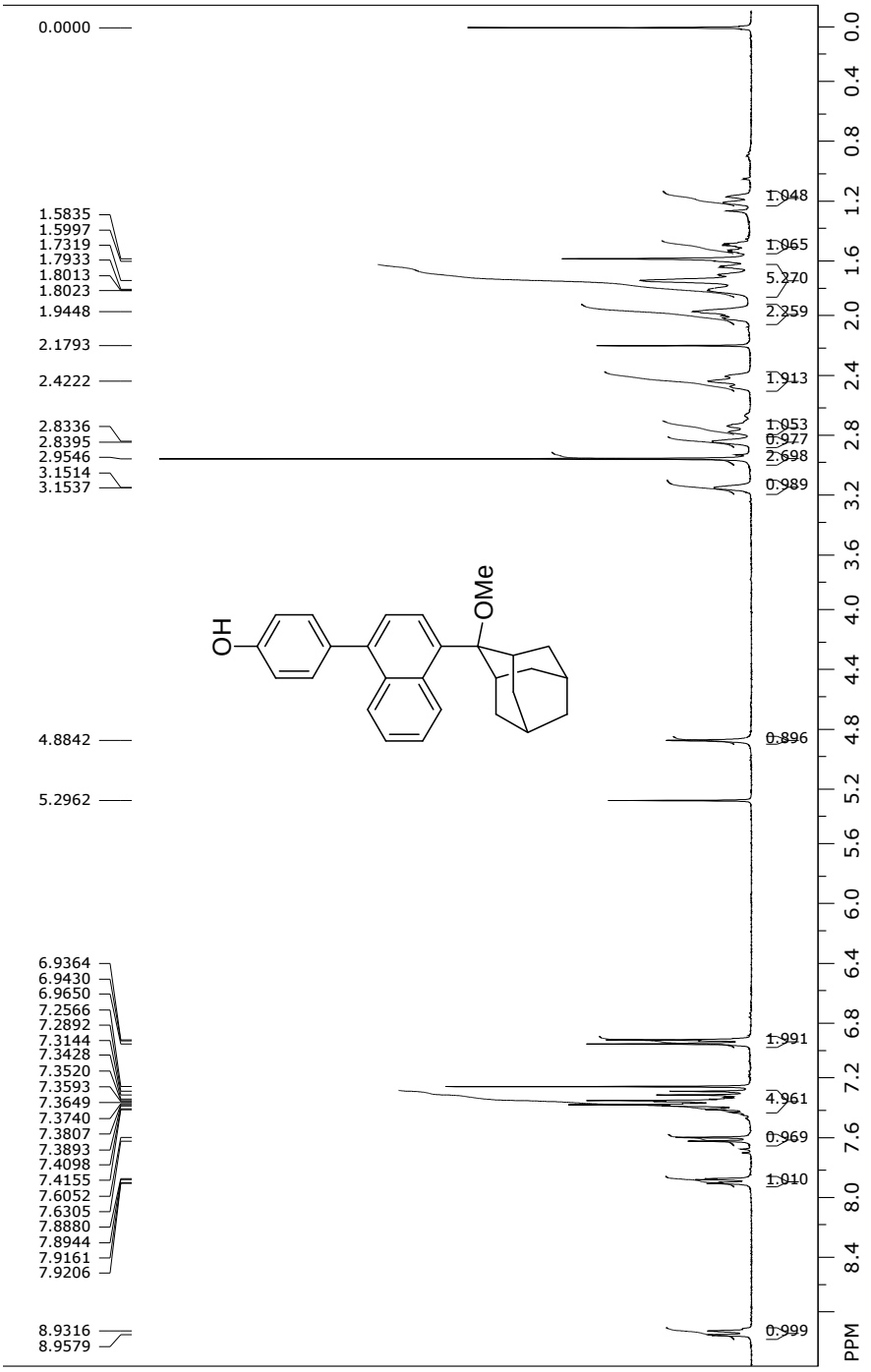

^{13}C NMR (150 MHz, $CDCl_3$) of compound **22**.

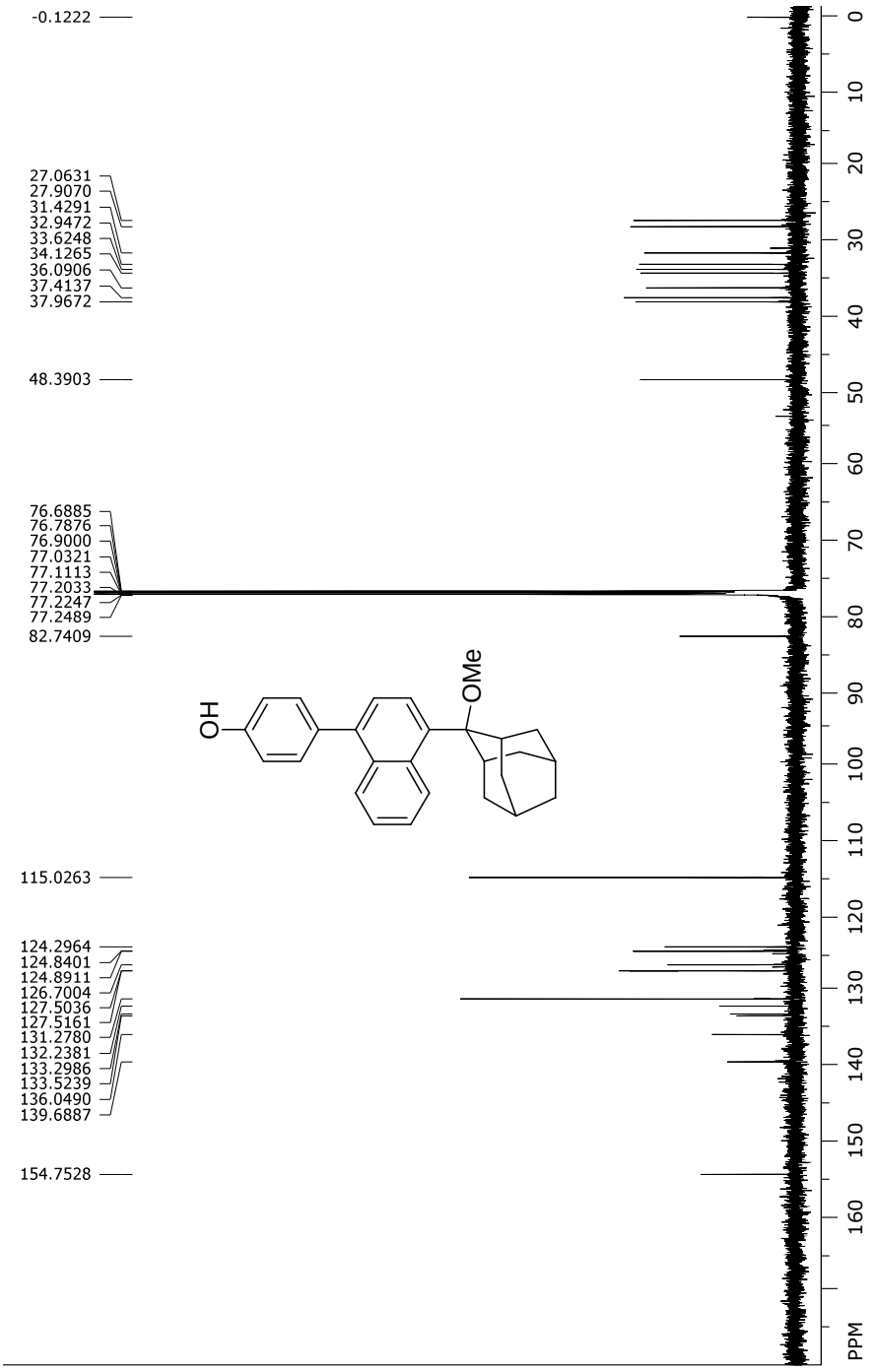

^{1}H NMR (600 MHz, $CDCl_3$) of compound **23**.

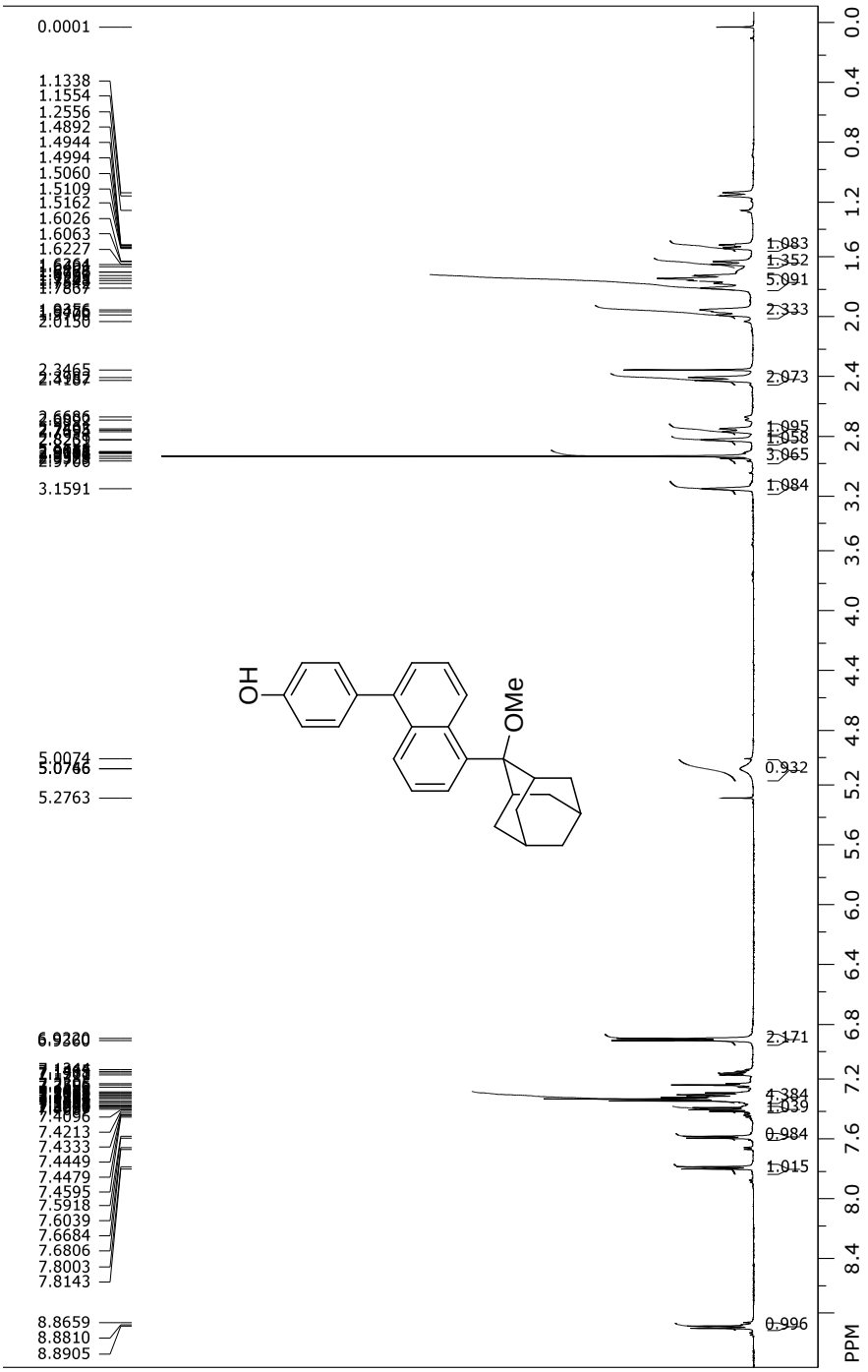

^{13}C NMR (150 MHz, $CDCl_3$) of compound **23**.

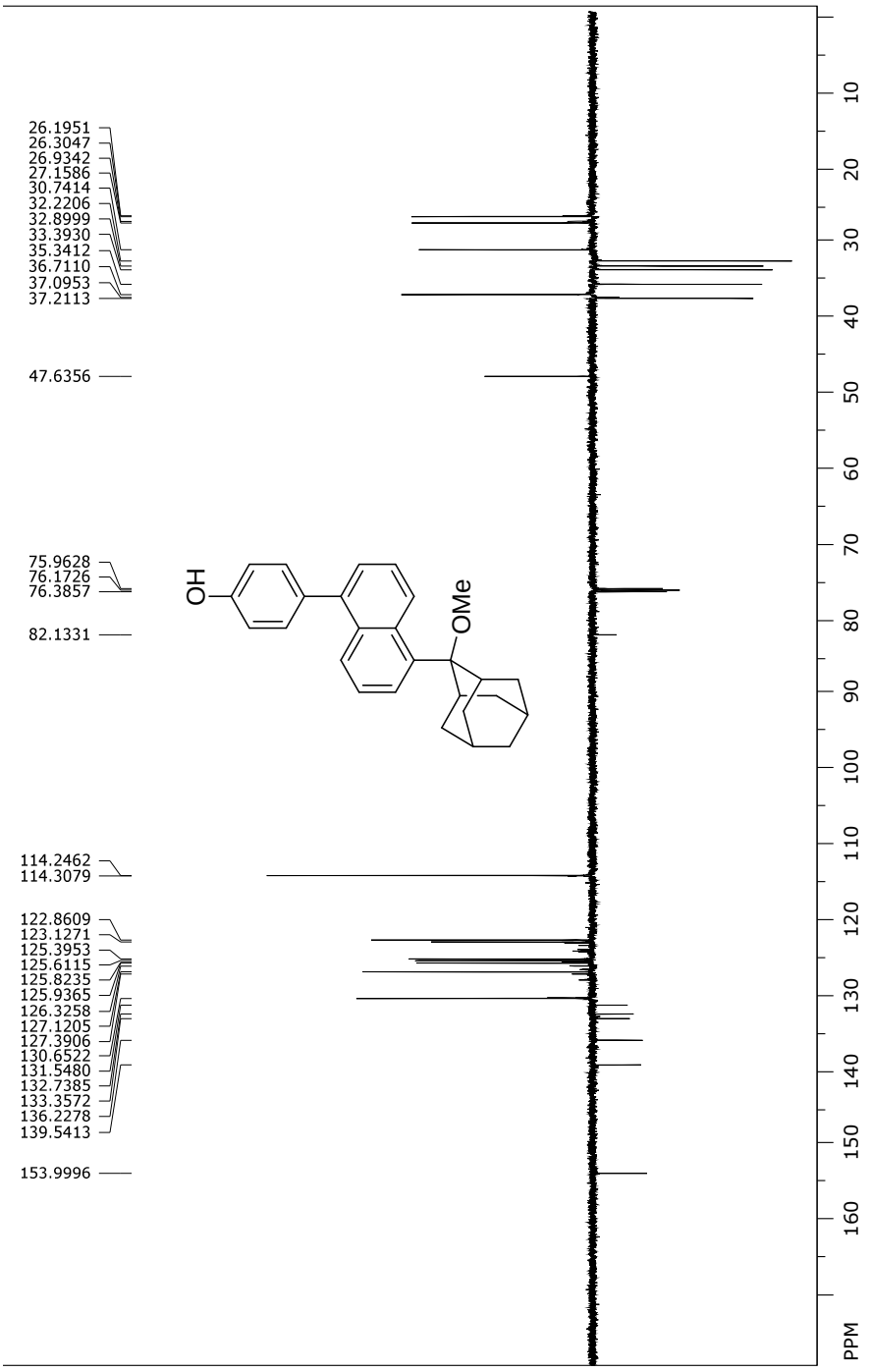

^{1}H NMR (300 MHz, $CDCl_3$) of compound **24**.

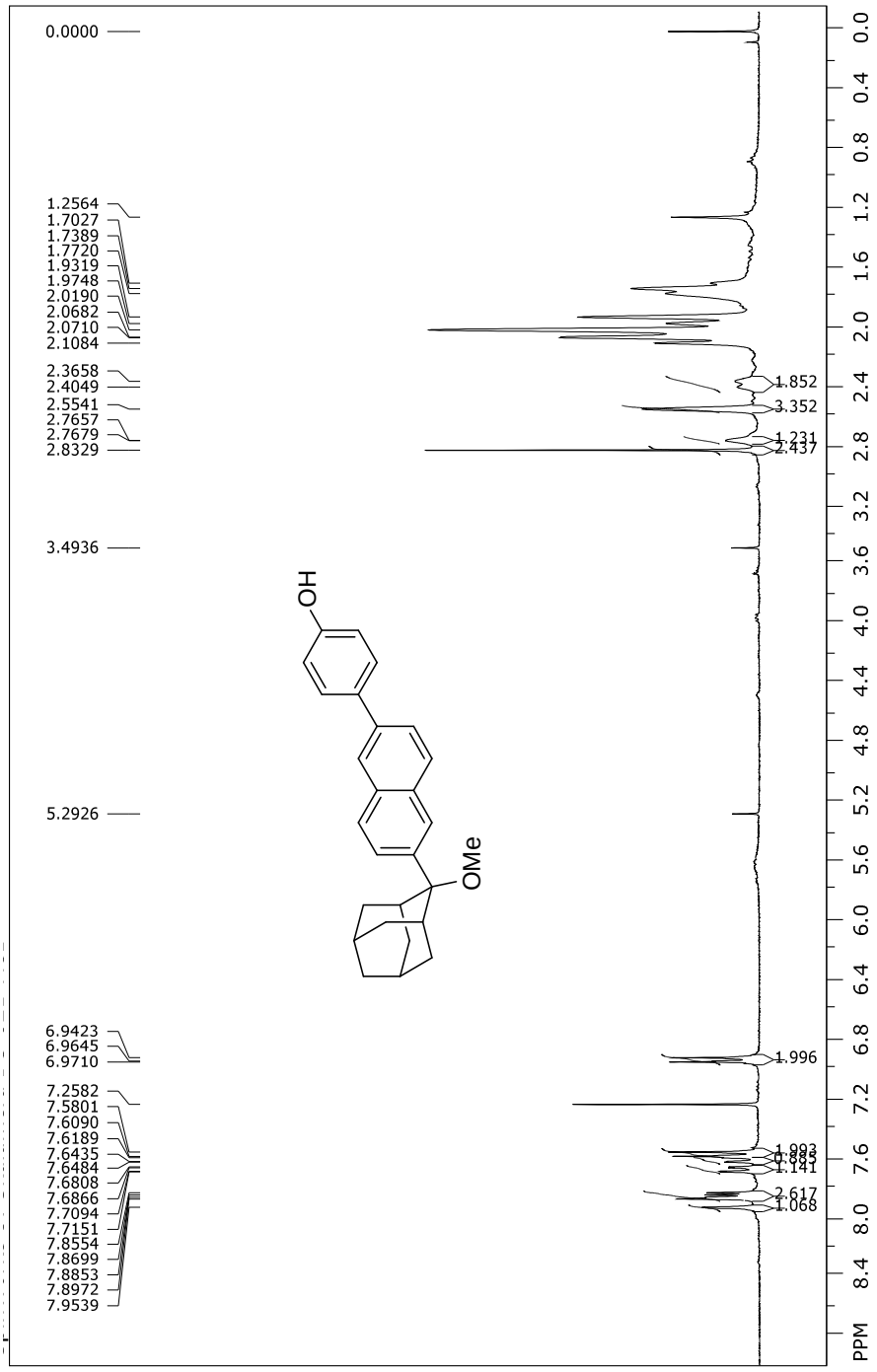

^{13}C NMR (75 MHz, $CDCl_3$) of compound **24**.

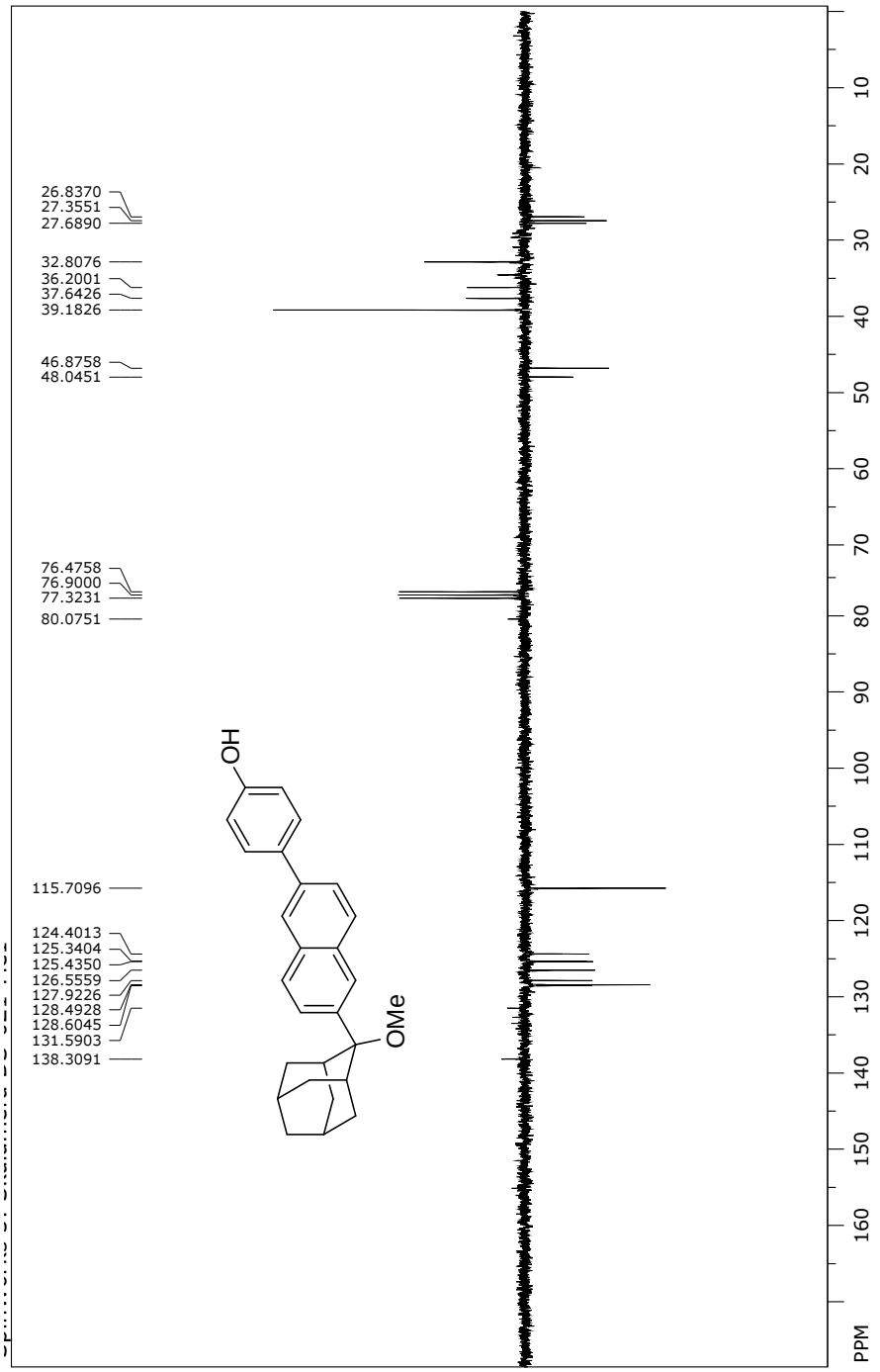

^{1}H NMR (300 MHz, $CDCl_3$) of compound **25**.

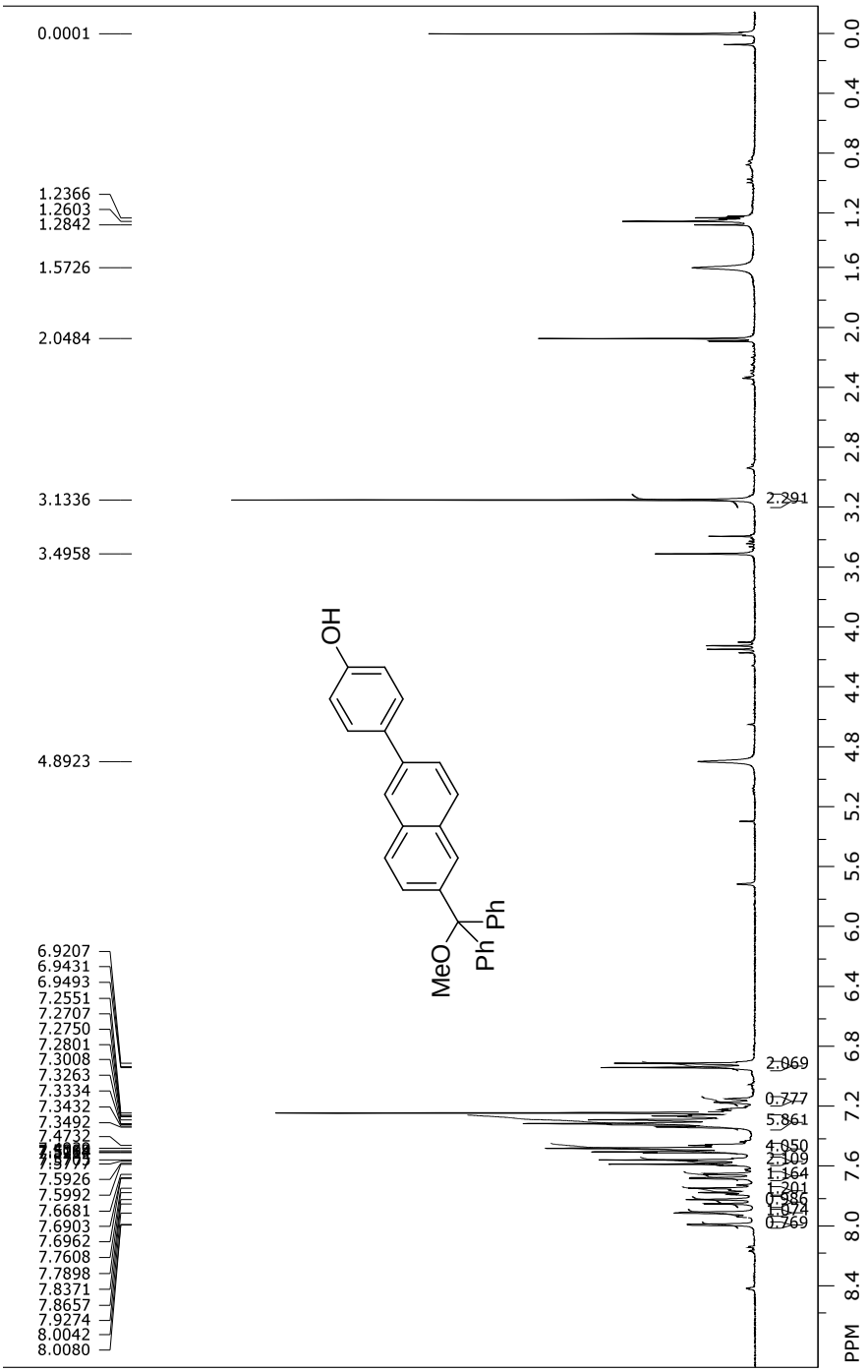

^{13}C NMR (300 MHz, $CDCl_3$) of compound **25**.

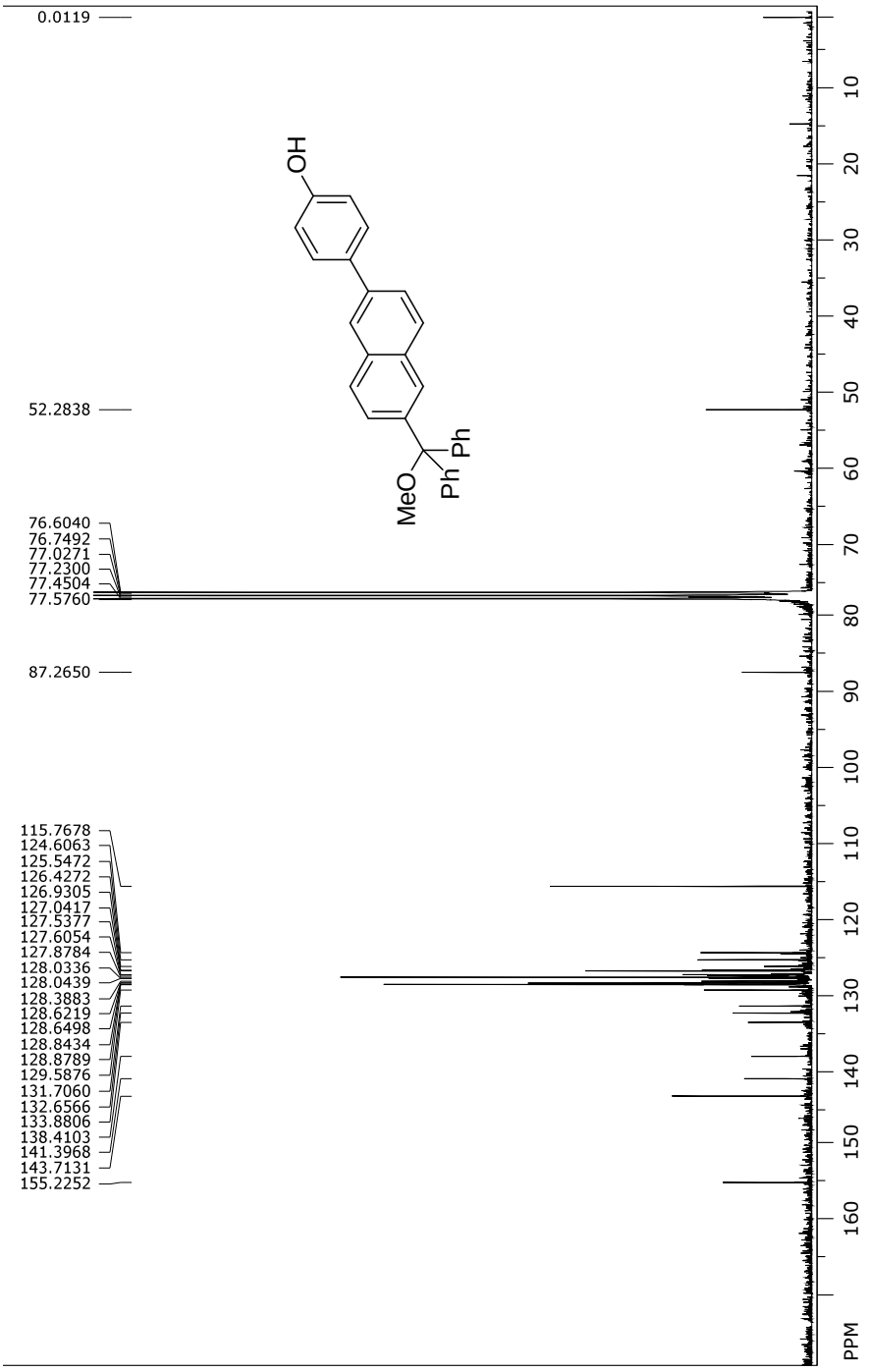

^{1}H NMR (300 MHz, $CDCl_3$) of compound **26**.

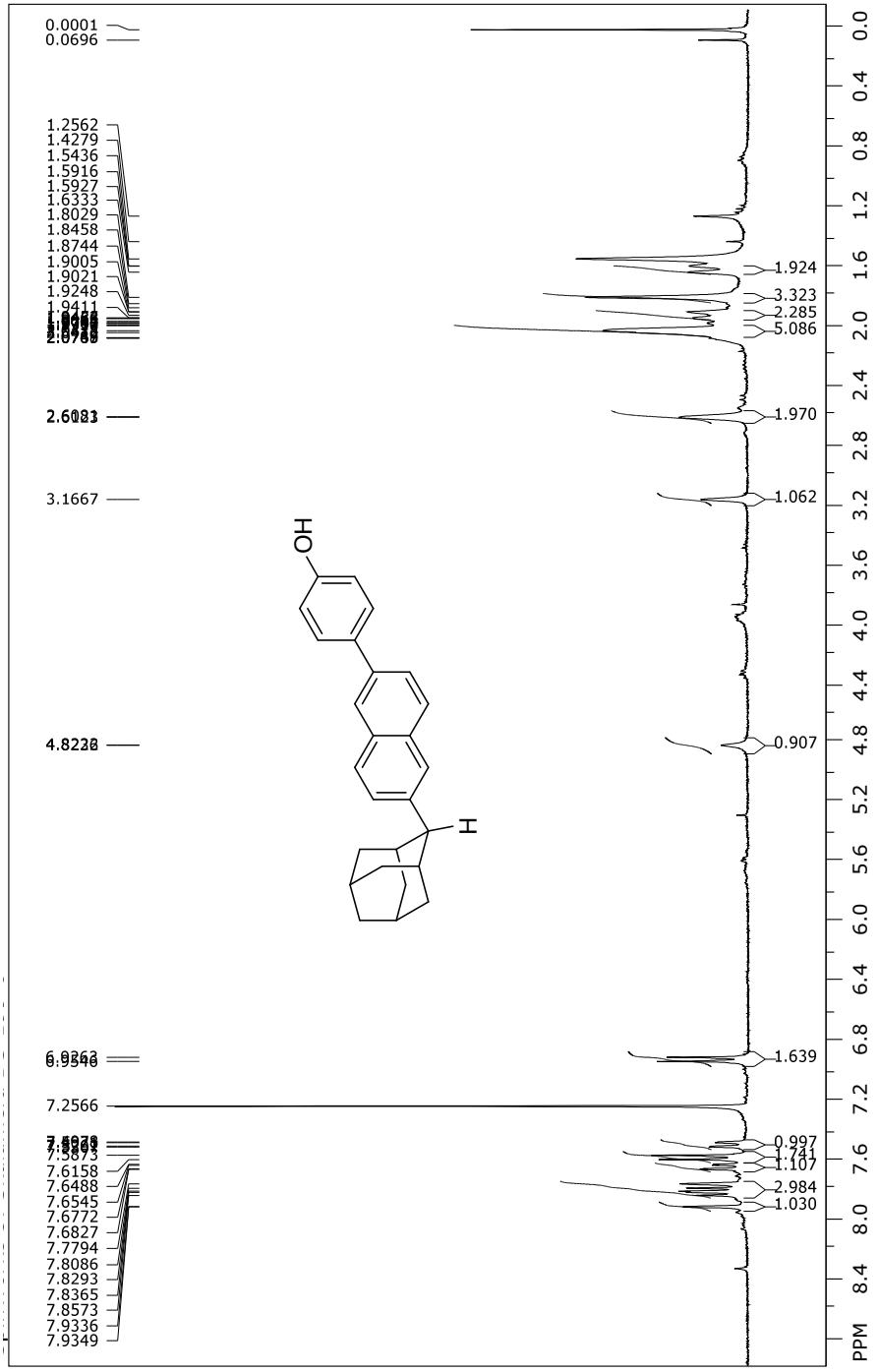

^{13}C NMR (300 MHz, $CDCl_3$) of compound **26**.